A FUZZY LOGIC APPROACH FOR REGULATION IN FLUX BALANCE ANALYSIS

by

Aris Tepeli

B.S. in Ch.E., Boğaziçi University, 2002

Submitted to the Institute for Graduate Studies in
Science and Engineering in partial fulfillment of
the requirements for the degree of
Master Science

Graduate Program in Chemical Engineering

Boğaziçi University

2006

…dedicated to my father.

ACKNOWLEDGEMENTS

I am deeply indebted to my supervisor Prof. Amable Hortaçsu whose help, stimulating suggestions and encouragement helped me in all the time of research and writing of this thesis. I would like to express my gratitude and my regards to her.

I would like to thank Prof. Uğur Akman and Assist. Prof. Berna Sarıyar Akbulut for their kind interest and for the time they have devoted to reading and commending on my thesis.

I am grateful to Prof. Öner Hortaçsu, Defne Kayrak Talay, Sinan Üzer, Seda Keskin and Nilay İnoğlu for their help and friendship in the supercritical fluid technology laboratory. Moreover, I would like to thank Selçuk Talay for his friendship either in or out of the laboratory.

Also, I would thank all other staff in the Department of Chemical Engineering for giving me satisfaction of being an academic member.

A special acknowledgement goes to one of my best friends, Can Kemal Ertan. He has been a true friend ever since we met each other in primary school. He shared my enthusiasm during the completion of my thesis. He has contributed intellectually, technically, and emotionally more than I can put into words in my life.

Basic laboratory and financial supports provided by the Department of Chemical Engineering, and Boğaziçi University Reasearch Fund (BAP, Project no: 03HA501) are gratefully acknowledged.

Finally, I would like to thank my loved family whom I owe my success. Especially, I would like to give my special thanks to my mother, Lusin Tepeli, whose patient love enabled me to complete this work.

ABSTRACT

A FUZZY LOGIC APPROACH FOR REGULATION IN FLUX BALANCE ANALYSIS

Technological advances in experimental observations give the ability to examine complex biological systems and the chance to forecast the bacterial behaviour *in silico*. In this thesis, the experimentally observed behavior by which bacteria are able to establish a time hierarchy of sugar utilization is examined and simulated. The optimal growth of bacteria on defined carbon sources are now easily predicted from the solutions of constraint-based metabolic models. However, these methods are unable to predict the sequence of carbon utilization and changes in cellular behavior of growth in mixed substrates. In this work a regulatory structure describing transcriptional regulation of catabolic genes or operons expressed in Fuzzy Logic Formalism is combined with dynamic Flux Balance Analysis (FBA). Since the transcription of operons is regulated by specific promoters and inducers that evolve from substrate usage, this regulatory structure is a natural part of any model of carbon source utilization. The Fuzzy Logic Formalism is a good alternative to differential equation models that require kinetic parameter values and superior to Boolean Formalism which automatically sets regulation as “on” or “off” rules.

The FBA/Fuzzy Logic combination was successfully used to simulate aerobic growth of *Escherichia coli* in mixed double (glucose-lactose) or triple (glucose-lactose-galactose, glucose-sorbitol-glycerol) substrates and anaerobic growth of *Lactococcus lactis* in a triple substrate (glucose-lactose-galactose). When well-defined data are available, the computed results are in good agreement with the data. The method also allows for the prediction of growth lag periods upon substrate substitution and changes in growth pattern and substrate utilization upon pulse injection of substrates in existing growth media.

ÖZET

AKI DENGE ANALİZİ İÇERİSİNDEKİ DÜZENLEME İÇİN FUZZY LOJİK YAKLAŞIMI

Deneysel olarak yapılan çalışmalarda teknolojik gelişmeler hem karışık biyolojik sistemlerin incelenmesine hem de bilgisayar ortamında bakteriyel davranışların tahmin edilmesine olanak sağlamaktadır. Bu tez çalışması kapsamında, deneysel olarak incelenen bakterilerin, zaman içerisinde değişik şeker kullanımına karşı uyumu modellendi ve benzetimi yapıldı. Bakterilerin farklı karbon kaynaklarında en uygun çoğalmaları, sınırlı ortamda metabolik modeller ile çözümü kolaylıkla tahmin edilmektedir. Fakat, bu metodlar karbon kullanım sıralarını ve böylelikle çoklu substrat ortamında büyüme sürecini kestirememektedir. Bu çalışmayla, karbon kullanımını düzenleyen genlerin transkripsiyonel düzenleyici yapısı veya operon, Fuzzy Lojik Biçimselliği içinde tanımlanarak dinamik Akı Denge Analizi (Flux Balance Analysis-FBA) ile birleştirildi. Operonların transkripsiyonu substrat kullanımından doğan spesifik destekleyiciler ve endükleyiciler tarafından düzenlenmektedir. Bu düzenleyici yapı karbon kullanımının doğal şeklidir. Fuzzy Lojik Biçimselliği kinetik parametrelere gereksinim duyan diferansiyel denklem modellerine alternatif ve "on"/"off" hükümlerine bağlı Boolean Lojik Biçimselliğinden daha iyi bir yöntemdir.

FBA/Fuzzy lojik birleşimi çoklu ortamlarda (glikoz-laktoz, glikoz-laktoz-galaktoz ve glikoz-sorbitol-gliserol) *Escherichia coli'nin (Koli basili)* oksijenli ortamda büyümesi benzetimini ve *Lactococcus lactis'in (süt ürünlerinde kullanılan bir tür bakteri)* oksijensiz ortamda büyümesi benzetimini çok iyi yapılabilmektedir. Hesaplanan sonuçlar elimizde bulunan iyi tanımlanmış deneysel veriler ile uyumlu olarak eşleşmektedir. Buna ilave olarak, bu metod bir substratın diğerinin yerine geçmesi ile oluşan lag fazındaki büyümeyi veya açıkça büyüme değişikliğini ve uyarı enjeksiyonu ile oluşan substrat kullanımını var olan ortamlarda tanımlayabilmektedir.

TABLE OF CONTENTS

LIST OF FIGURES

LIST OF TABLES

LIST OF SYMBOLS/ABBREVIATIONS

A_i	Fuzzy set
A^C	Complement of fuzzy set
$\boldsymbol{b}$	Vector of metabolic uptake
c	Mass fractions of the intracellular metabolites
p	Terminal extracellular or intracellular product
s	Extracellular substrate
$\boldsymbol{S}$	Stoichiometric matrix
S_c	Substrate concentration
S_{c0}	Initial substrate concentration
S_u	Substrate uptake rate
X	Cell density
α_i	Lower bound of flux constraint
β_i	Upper bound of flux constraint
μ	Growth rate
μ_A	Membership function of fuzzy set
$\boldsymbol{v}$	Vector of metabolic flux
$\boldsymbol{v_p}$	Vector of the specific accumulation rates for intracellular products
$\boldsymbol{v_s}$	Vector of the specific uptake rate
Arc	Anoxic Redox Control
ArcA	Cytosolic response regulator

ArcB	Transmembrane histidine kinase
CAP	Catabolite Activator Protein
CDA	Calcium Dependent Antibiotic
FBA	Flux Balance Analysis
FNR	Furmarate and Nitrate Reduction
H	High
L	Low
ME	Medium
MFA	Metabolic Flux Analysis
MOMA	Minimization of Metabolic Adjustment
PTS	Phosphotransferase System
rFBA	Regulatory Flux Balance Analysis
ROOM	Regulatory on/off Minimization
TCA	Tricarboxylic Acid
VH	Very High
VL	Very Low

1. INTRODUCTION

Technological advances in data collection give biologist the ability to study complex systems. Based on experimental observations, a biological model can be developed to predict the organism behaviour *in silico.* To model a biological pathway for a cellular process, chemical reaction network and regulatory structure must be combined. Transcriptional regulatory events as time dependent constraints on a metabolic network would be necessary to simulate bacterial growth on various environmental conditions.

In this work, flux balance analysis (FBA) and fuzzy logic formalism are used to find optimal solutions to selected metabolic networks and for the regulation of the structure, respectively. Mathematical modeling of a large system is hard to handle if parameter values are necesssary. Flux Balance Analysis (FBA) which is a type of Metabolic Flux Analysis (MFA), is explained in detail in the second chapter. The analysis does not deal with the parameters. It gives an optimal flux distribution upon substrate uptake rate. The dynamic behavior in the medium outside the cell provides a time course of by-product secretion, and biomass growth.

Fuzzy logic is a tool that describes human reasoning. It uses the whole interval between 0 (*False*) and 1 (*True*) of the logical statement. Fundamentals and applications of fuzzy logic are explained in Chapter 4. Fuzzy IF-THEN rules are incorporated for the analysis of complex biological systems. In principle, a crisp set of input is converted into fuzzy quantities to have a decision in human knowledge. Then, the conclusion is defuzzified to have a discrete result.

The utilization of carbon sources by organisms are described by central metabolism pathways. Substrate uptake mechanism through the cell membrane and ways to utilize multiple carbon source mixtures may be different for different microorganisms. A series of genes called operons regulate the sequence of utilization. *Lac* operon, *gal* operon, *gut* operon, *glp* operon in *E. coli* and gal operon in *L. lactis* are described in Chapter 5. The responses of biological operon structures and sugar uptake transport systems to environmental conditions are described in terms of fuzzy logic formalism.

The computational algorithm described in Chapter 6 is performed in Matlab. The algorithm contains two separate modules, which are constantly interacting with each other. The algorithm consists of a regulatory module and a metabolic network module. Dynamical flux balance analysis is performed to determine metabolic transients in response to regulatory signals in each time step of an interval.

Available experimental data found in literature are included in the results for the validation of simulations. Metabolic network maps containing the flux distribution at some chosen time intervals are also included in the results and discussion section. The differences between the main pathways for the utilization of substrates and different growth regimes are examined in *E. coli* for aerobic growth and in *L. lactis* for anaerobic growth.

The conclusion chapter enumerates the advantages of using Fuzzy Logic over Boolean formalism as a regulatory tool for regulatory metabolic flux analysis.

2. METABOLIC FLUX ANALYSIS

Genome sequencing and bioinformatics are producing detailed lists of the molecular components contained in many prokaryotic organisms. By the help of this information, *in silico* representations of integrated metabolic functions can be constructed and analyzed. Kinetic information on the dynamics and regulation of metabolic reactions are usually accompanied with problems concerning availability and in *vivo*/in *vitro* discrepancies. Metabolic Flux Analysis (MFA) is a method based on the fundamental physicochemical constraints on metabolic networks which can be used successfully instead of the ones using kinetic parameters of enzymes. Stoichiometry of metabolic pathways and metabolic demands are required for the analysis. Moreover, additional information can be incorporated in terms of imposing regulation on the growth performance.

In general, MFA is useful for analyzing specific flux distribution but is not able to characterize the complete admissible steady state solution space. By applying metabolic flux analysis (MFA), one tries to shrink the possible solution space of (Eq. 1) by measuring some of the reaction rates (such as uptake or excretion rates) in a certain steady state experiment. The stiochiometric matrix represents the central equation for MFA and characterizes a flux scenario. The ideal case where only one unique and exact solution exists occurs, if $\boldsymbol{S}$ is a square matrix and invertible, because then all unknown rates in $\boldsymbol{\nu}$ can be determined. If a scenario is underdetermined, then only some or even none of the unknown rates can be determined. In redundant systems, a consistency check can be performed, which is useful for detecting gross measurement or modeling errors. In larger networks, despite a number of measurements, all rates in the system often remain completely unobservable. However, for the general case, depending on the rank of $\boldsymbol{S}$, a scenario must be classified with respect to determinacy (determined or underdetermined) and redundancy (redundant or non-redundant).

Flux Balance Analysis (FBA) is the same as Metabolic Flux Analysis (MFA). However, the characteristic assumption of FBA is the optimal function of the network. In most cases, the linear objective function is maximizing growth, sometimes; maximizing product yield. The

three constraints, quasi-steady state, reaction capacities and optimal function form the linear optimization problem.

FBA enables one to predict production capabilities of a micro-organism such as predicting optimal yield and optimal behavior. Another very useful application of FBA is to investigate whether a certain function can be performed *at all* in a network, especially after removal of network elements by simulating gene deletions. It means that, if a reaction is removed in the network, then one may optimize the network again. If the optimal value, e.g. for the growth rate, now becomes zero, then one definitely knows that this function (growth) is not possible anymore.

The significance of whole-cell computational modeling is to combine detailed biochemical information with biological insight to produce testable predictions. The biochemical information and growth performance on prokaryotes such as *Escherichia coli (E. coli)* is known quiet well that FBA can predict metabolic flux distribution at steady state by using linear programming. It also gives an interpretation of experimental data, provides a guide to metabolic engineering, enables optimal medium formulation, and provides a method for bioprocess optimization.

2.1. Steady-State Methods

2.1.1. Flux Balance Analysis (FBA)

The first step in FBA is the construction of the metabolic network containing the most important metabolites and reactions between them. The central metabolism pathway reactions (glycolysis, pentose phosphate pathway, TCA cycle, electron transport system, etc.) are used to identify the growth and end products on sugar utilization. A metabolic steady state is assumed on the metabolism, meaning that, the metabolic pathway flux leading to the formation of the metabolite and that leading to the degradation of a metabolite must balance. This generates the flux balance equation.

$$\boldsymbol{S} \cdot \boldsymbol{v} = \boldsymbol{b} \qquad (1)$$

where $\boldsymbol{S}$ is a matrix comprising the stoichiometry of the catabolite reactions, $\boldsymbol{v}$ is a vector of metabolic fluxes, and $\boldsymbol{b}$ is a vector containing the net metabolic uptake by the cell. The number of metabolic reaction rates (also called; fluxes) normally exceeds the number of metabolites. Therefore, there is a plurality of solutions. A particular solution may be found by using linear optimization by stating an objective and searching its maximal value within stoichiometrically defined domain. In other words, optimization of the growth rate will determine the specific metabolic pathway utilization in the organism (Varma & Palsson, 1994a, b).

Upon this approach, certain constraints can be imposed to the biochemical reaction network to limit cellular possible behaviors. These *physicochemical constraints* are used to define a closed solution space within which the steady-state solution to the flux vector must lie (Palsson, 2000). The constraints can be coming from thermodynamic limitations (e.g. effective irreversibility of a given reaction due to an extremely high equilibrium constant), capacity limitations (e.g. maximum uptake rate for a given transport protein), or experimental data.

$$\alpha_i \leq v_i \leq \beta_i \qquad (2)$$

α_i or β_i may be set to zero or to another finite value to constrain the direction or magnitude of a flux.

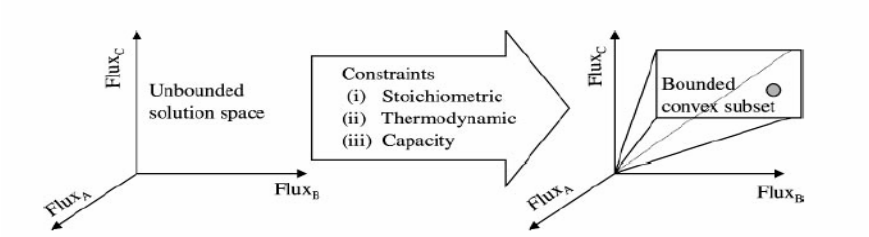

Figure 2.1. Constraints-based analysis of metabolic networks in geometrical term (Covert *et al.,* 2001)

Figure 2.1 depicts metabolic network in geometrical terms. By imposing the constraints, the solution space is bounded to a convex subset.

Some representative works on either metabolic flux analysis or flux balance analysis are given in Table 2.1 and 2.2. The metabolic system, aim of the work, constraints and auxiliary variables are tabulated for comparison.

Table 2.1. Representative studies in MFA and FBA

MAJEWSKI and DOMACH, 1990	14 metabolic reactions, 4 load fluxes. Optimal production of high-energy phosphate bonds on ATP and GTP. Enzymatic capacity constraints and electron transport chain constraints. The onset of acetate overflow and the rate of acetate production.	FBA
NEIDHARDT, 1987-1990	Reconstruction of *E. coli* metabolic network contained both anabolic and catabolite reactions (53 catabolic reactions and 94 biosynthetic reactions). Optimal production of cofactors (ATP, NADPH, NADH), optimal production of metabolic precursors (Pryuvate or Succinate). Energy, redox or stoichiometric constraints. Maximal theoretical yields for amino acid and nucleic acid, optimal flux distributions for biomass constituents.	FBA
NISSEN, 1997	37 pathway reactions involving 43 compounds. Anaerobic metabolism of *Saccharomyces cerevisiae*. Intracellular fluxes based on measurements of the uptake of substrates from the medium, secretion of products from the cells, and of the rate of biomass formation are calculated. Production rates of malate and fumarate are calculated.	MFA
PRAMANIK and KEASLING, 1997-1998	317 reactions and 305 metabolites. Optimal growth rate. Equations relate growth rate to biomass requirments. The biomass composition varies with the carbon source. Aerobic growth on acetate plus glucose.	FBA
GULIK, 1999	Growth and penicillin-G production in *Penicillium Chrysogenum*. Potential bottlenecks nodes for increased productivity. Stoichiometric model for yeast (Cytosol, mitochondrion, peroxisome;Van Gulik and Heijnen, 1995).	MFA
EDWARDS and PLASSON, 1999	Metabolic capabilities of *Haemophilus influenzae.* 488 metabolic reactions operating on 343 metabolites. Six different optimal metabolic phenotypes are obtained on different constraining features. Redundant functions under defined functions are also studied.	FBA
RAMKRISHNA and PALSSON, 1999	Mitochondrial energy metabolism. Systemic stoichiometric constraints. Optimal flux distributions for maximal ATP production in the mitochondrion are characterized. Metabolic behaviour due to genetic deletions at the metabolic level is characterized. Glycolytic pathways, TCA cycle, and the electron transport system (ETS) are modeled for mitochondria.	FBA

Table 2.2. Representative studies in MFA and FBA (Cont'd)

EDWARD and PALSSON, 2000	720 reactions and 436 metabolites (Glycolysis, TCA cycle, pentose phosphate pathway, respiration, anaplerotic reactions, fermentative reactions, amino acid biosynthesis and degradation, nucleotide biosynthesis and interconversions, fatty acid biosynthesis and degradation phospholipid biosynthesis cofactor biosynthesis and metabolite transport). In *silico* gene deletions and growth characteristics of a series of *E. coli* mutants on several different carbon sources.	FBA
EDWARDS and IBARRA, 2001	*E. coli* MG1655 metabolic network is used to obtain quantitative genotype-phenotype relationship. Reconstruction of complete metabolic network from annotated genome sequence. Optimal performance of a metabolic network under a range of growth conditions.	FBA
COVERT and PALSSON, 2002	113 metabolic reactions (45 of which are regulated by 16 regulatory proteins), 149 genes. Transcriptional regulation incorporated. The genes can be either on or off (Boolean Logic).	rFBA
KIM and MAVITUNA, 2004	400 reactions for the primary and secondary metabolism of *Streptomyces coelicolor*. Some of the factors affecting growth and production of calcium dependent antibiotic (CDA) investigated. Optimal (maximized) specific growth rates for different growth phases of the batch. Maximization of the specific CDA production rate. Experimental specific growth and glucose uptake rates are constraints.	MFA/ FBA

2.1.2. Minimization of Metabolic Adjustment (MOMA)

Minimization of Metabolic Adjustment (MOMA) is a method for the prediction of phenotypes of knocked-out (mutant) organisms (Segre *et al.,* 2002). Metabolic Flux Analysis looks for the flux distribution that maximizes the growth rate. However, MOMA searches for the distribution that is closest to wild-type strain one. It uses the same stoichiometric constraints as MFA, but it does not find the optimal growth flux for gene deletions.

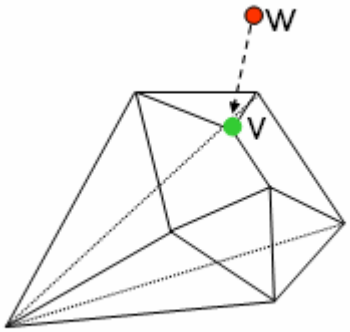

Figure 2.2. Optimal solution of wild-type strain and MOMA result (Segre *et al.,* 2002)

The size of the feasible solution space will be reduced (Figure 2.2) because the reactions associated with the knocked-out gene are constrained to zero. The flux distribution of the wild-type organism (denoted w) will reside outside the feasible solution space. MOMA employs quadratic programming to identify a point in flux space, which is closest to the wild-type point (denoted v), compatibly with the gene deletion constraint. In MOMA, in contrast to FBA, the objective function does not explicitly depend on biomass production. The goal is to find the vector $\boldsymbol{v}$ such that the Euclidean distance is minimized as shown in Eq. (3).

$$D(w,x) = \sqrt{\sum_{i-1}^{N} (w_i - x_i)^2} \qquad (3)$$

If a solution for the wild-type FBA problem w exists, and if the solution space of the knocked-out type is not empty (i.e., knocked-out genes constraints set to zero is compatible with the other constraints), then a solution to this problem always exists.

The prediction of essential genes in *E. coli* central carbon metabolism, comparison with measured growth performance of insertional mutants and comparison with experimental flux

measurements of an *E. coli* pyruvate kinase knockout (Segre *et al.,* 2002) have been examined by Minimization of Metabolic Adjustment method.

2.1.3. Regulatory on/off Minimization (ROOM)

Regulatory On-Off Minimization (ROOM) is a constraint-based algorithm for predicting the behavior of metabolic networks in response to gene knockouts (Ruppin *et al.,* 2005). It aims to minimize the number of significant flux changes (hence on/off) with respect to the wild type. The regulatory system governs a series of transient metabolic changes that converge to a steady-state condition. ROOM also shows its ability to correctly identify alternative pathways for reactions associated with the knocked-out genes, thus strengthening its biological plausibility. ROOM outperforms MOMA in predicting intracellular fluxes and gene knockout lethality in mutated *E. coli* and the *S. cerevisiae* strains, respectively.

ROOM has been tested to predict metabolic fluxes for five different *E. coli* knockouts: pyruvate kinase (*pyk*), phosphoglucose isomeras (*pgi*), glucose 6-phosphate 1-dehydrogenase (*zwf*), 6-phosphogluconate dehydrogenase (*gnd*), and phosphoenolpyruvate carboxylase (*ppc*) under growth conditions (Ruppin *et al.,* 2005). It was aimed to compare the results with the experimental findings and with the predictions of FBA and MOMA. ROOM's flux predictions are either equal to or more accurate than its contemporaries.

2.2. Dynamic Metabolic Modeling Method

MFA can be used in dynamic modeling even though it is based on a steady-state assumption. The biomass growth is performed in a batch culture. Because the time constants which describe metabolic transients and metabolic reactions are fast (on the order of milli-seconds to seconds) as compared to the time constants associated with cell growth (on the order of hours to days) and regulation (on the order of tens of minutes), the system may be treated by only considering the steady state behavior inside the cell and the dynamic behavior in the medium outside of the cell (quasi-steady state assumption).

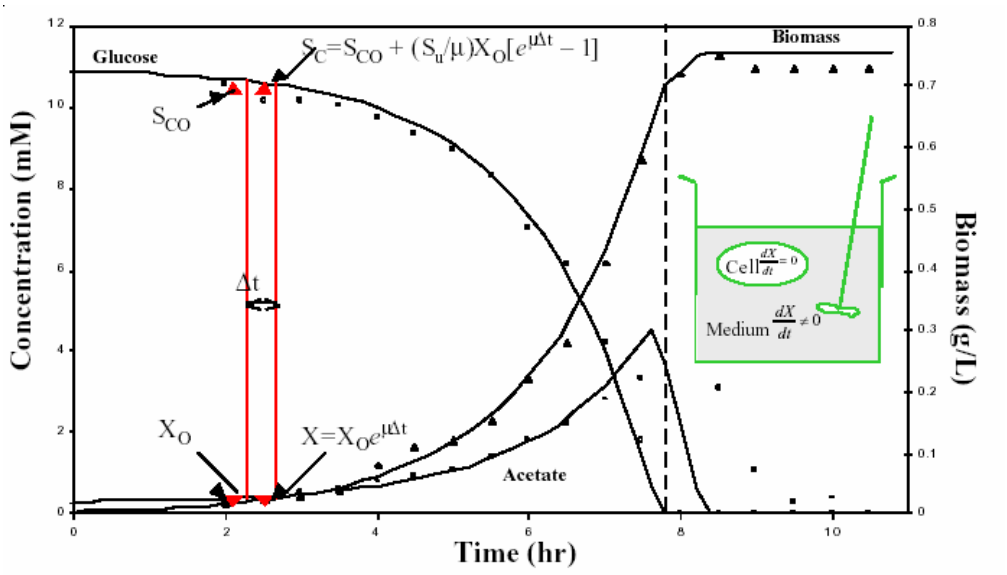

Figure 2.3. Time courses of aerobic growth on glucose and acetate reuptake (Covert, 2002)

The experimental time is divided into several small time steps. MFA is used to determine the steady state metabolic flux distribution for the given time interval. Then, substrate uptake, by-product secretion, and biomass growth are determined by solving the relevant differential equations. The new conditions of the system are the FBA inputs for the next time step (Varma, 1994a,b). The relevant differential equations to determine concentrations for each time step are;

$$\frac{dX}{dt} = \mu X \rightarrow X = X_0 \cdot e^{\mu\Delta t} \qquad (4)$$

$$\frac{\partial S_c}{\partial t} = -S_u \cdot X \rightarrow S_c = S_{c0} + \frac{S_u}{\mu} X_0 (1 - e^{\mu\Delta t}) \qquad (5)$$

Where X is the cell density, μ is the growth rate, S_u is the substrate uptake rate, S_c is the substrate concentration and S_{c0} is the previous step substrate concentration.

Sugar substrates and by-products are all considered as substrates that can be used by cells. As a result of implementing the above set of equations, the solution yields time profiles of biomass, substrate and extracellular products such as shown in Figure 2.3.

In another dynamic modeling study (Provost *et al.,* 2004), the metabolic network is divided into two groups of nodes; boundary nodes, extracellular metabolite, and internal nodes, intracellular metabolite. Boundary nodes can be further separated into initial and terminal nodes. Initial nodes correspond to the external substrates that are consumed but not produced. Terminal nodes correspond either to extracellular products released in the culture medium or intracellular products which form the cellular material during the growth.

The main purpose in the dynamical modeling is to combine macroscopic dynamical model with metabolic flux analysis. The elementary flux modes are computed and translated into a set of macro-reactions connecting the extracellular substrates and products (boundary and internal nodes). Then, a dynamical model, which is compatible with the underlying metabolic network, is build on the basis of these macro-reactions (Provost and Bastin, 2004). During the growth of the cells, the internal metabolites are supposed to be at quasi-steady state. Mass balance equations related to a fictional metabolic network, depicted in Figure 2.4 were written as follows;

$$\frac{dX}{dt} = \mu X \tag{6}$$

$$\frac{ds}{dt} = -\nu_s X \tag{7}$$

$$\frac{d(cX)}{dt} = N \cdot \nu \cdot X \tag{8}$$

$$\frac{dp}{dt} = \nu_p X \tag{9}$$

where

c denotes mass fractions of the intracellular metabolites inside the cells.

N denotes corresponding stoichiometric matrix.

p denotes terminal extracellular or intracellular product.

s denotes extracellular substrate.

X denotes cell density.

μ denotes specific growth rate.

$\boldsymbol{\nu_p}$ denotes vector of the specific accumulation rates for intracellular products or excretion rates for extracellular products.

$\boldsymbol{\nu_s}$ denotes vector of the specific uptake rate.

From the experimental data, the specific uptake and excretion rates ($\boldsymbol{\nu_s}$ and $\boldsymbol{\nu_p}$) are computed by linear regression during the growth phase. The steady state flux balance equations at the internal nodes of the network are expressed as $\mathbf{N.v = 0}$. By eliminating the internal metabolites between the reactions, the set of fundamental *macro-reactions* that connect the extracellular substrates and the end-products is obtained. Coupled with the steady state flux balance equations, the set of mass balance equations are solved. A simple fictional metabolic network is given in Figure 2.4. C denotes intracellular metabolite, S denotes extracellular substrate and P denotes terminal extracellular or intracellular product.

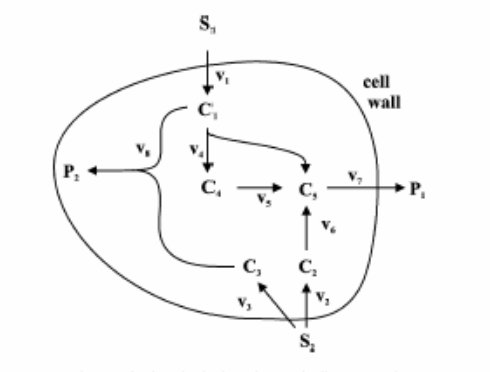

Figure 2.4. A simple fictional metabolic network (Provost and Bastin, 2004)

The proposed approach had been illustrated with the example of Chinese Hamster Ovary (CHO) cell metabolism. This has been proposed to provide a firm basis for the design of online monitoring and optimization of cell culture processes (Provost and Bastin, 2004). In particular, the underlying metabolic basis of the model could be helpful in determining how to alter the culture environment so as to achieve robust control and maintain optimal conditions.

2.3. Regulatory Metabolic Flux Analysis Using Boolean Logic

Metabolic flux balance analysis does not include transcriptional regulation meaning that all gene products in the metabolic reaction network are assumed to be available to contribute to an optimal solution. These regulations, which are biological in origin, are self-imposed regulatory constraints by the organism and the high level transcriptional regulation can have a significant effect on the cell behavior. The transcriptional regulatory structure and its resulting transcribed protein or enzyme has been described using Boolean logic equations (Covert. et al., 2002). This approach involves restricting expression of a transcription unit (meaning; transcribed enzyme or regulatory protein) to the value 1 if the transcription unit is transcribed and 0 if it is not. Similarly, the presence of certain conditions inside or outside of the cell may be expressed as 1 if a certain condition is present and 0 if it is not.

In geometrical term, regulation imposes temporary, adjustable constraints on the solution space.

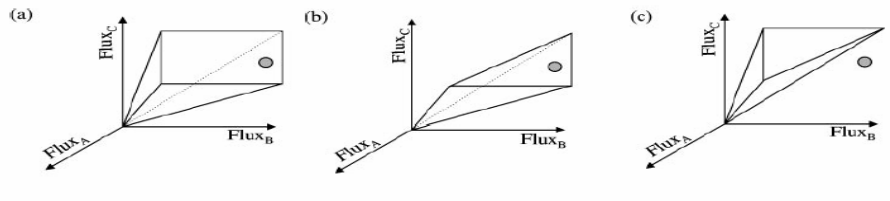

Figure 2.5. Regulatory constraint-based geometrical analysis of metabolic networks (Covert *et al.,* 2001)

Regulatory constraints change the shape of the solution space. Figure 2.5 (a) shows constraint based analysis of MFA with non-adjustable constraint. The flux through a certain reaction may be constrained by a transcriptional regulatory event. Therefore, the size of the solution space is reduced. In this case, the optimal solution may either be in the reduced solution space (Figure 2.5 (b)) or may not be (Figure 2.5 (c)) where new solution will be determined that is, new behavior will be searched by the cell.

As an example, the formalism of the Boolean logic has been applied to carbon uptake/catabolic repression in an organism. The organism can prefer one sugar source to another. The presence of one sugar source in the extracellular medium can inhibit the transport of the other through the cell membrane (diauxie on two carbon sources). Therefore, the resulting undesirable transport flux will be zero in FBA.

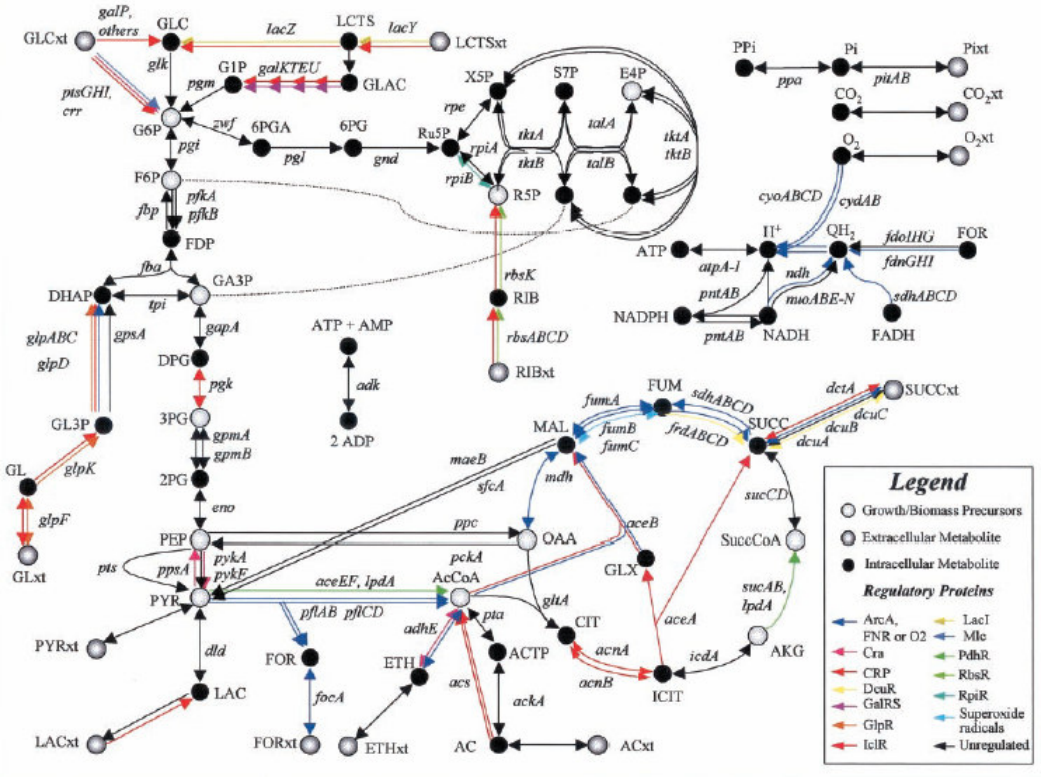

Figure 2.6. Metabolic network for central metabolism in *Escherichia coli* used in the calculations (Covert, 2002)

A regulatory metabolic network having 149 genes, the products of which include 16 regulatory proteins and 73 enzymes, which catalyze 113 reactions was studied to determine the ability of the model to make accurate phenotypic predictions (Covert, 2002). The analysis of the combined metabolic/regulatory network using Flux Balance Analysis may be called regulatory flux-balance analysis (rFBA). In the model, the synthesis of 43 of the enzymes is controlled by transcriptional regulation and as a result 45 of the reactions to the system is controlled by a logic statement. As an application of this model, the dynamic simulation of growth under three environmental conditions, aerobic growth on glucose with acetate reutilization, glucose fermentation, and a mixed aerobic glucose-lactose batch culture, are described.

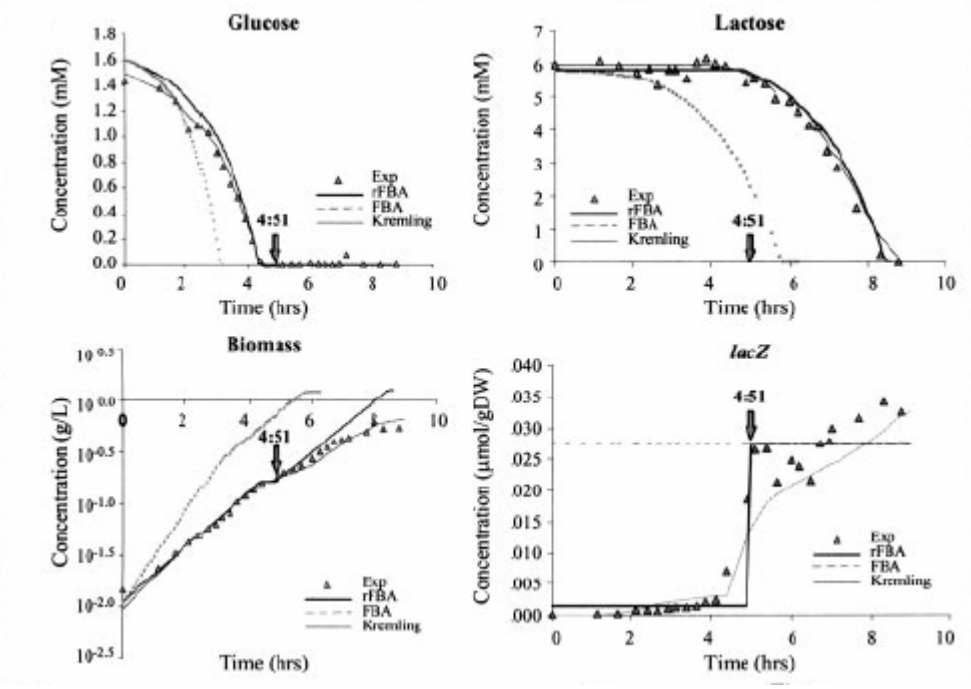

Figure 2.7. Aerobic growth on glucose and lactose in *Escherichia coli* (Covert, 2002)

The results for aerobic growth of *E. coli* on glucose and lactose are given in Figure 2.7. Experimental mixed batch culture, detailed kinetic model (Kremling *et al.,* 2001), metabolic flux balance analysis (FBA) model with/without regulation are all given together for comparison. Regulatory FBA model predictions are in good agreement with the data, comparable with the predictions made by the Kremling model, and far better than the predictions of the stand-alone FBA model. Due to the concurrent uptake of glucose and lactose, FBA predictions are far apart from the experimental data. Also, there is a much more rapid depletion of the substrates and a higher growth rate. Interestingly, because of the larger flux of carbon source uptake, the FBA model predicts that *E. coli* growth should be oxygen-limited rather than carbon-limited. The time 4:51 designates the shift in gene expression point. Lactose is utilized as a carbon source once the glucose in the medium has been depleted.

2.4. Genetically Constrained Metabolic Flux Analysis

Existing metabolic databases can be used to estimate metabolic fluxes. By adding or removing the corresponding pathway(s), one can analyze the behavior of organism due to the transcriptional regulation on the substrate uptake. A new framework on the regulation is modeled that utilizes genomic and metabolic databases, including available genetic/regulatory network structures and gene chip expression data, to constrain metabolic flux analysis. The genetic network consisting of the sensing/regulatory circuits activate or deactivate a specific set of genes in response to external stimulus. The activation and/or repression of this set of genes result in different gene expression levels that change the structure of the metabolic map. The adaptation to the external stimulus can be driven to the sub network from the pool of feasible reactions. The *Escherichia coli* oxygen and redox sensing/regulatory system has been modeled for metabolic pathways controlling of glycolysis and the TCA cycle (Cox *et al.,* 2005).

The analysis scheme is an extension of the traditional regulatory FBA. It includes the regulatory network shown in Figure 2.8. Two new components, ‘‘genetic network’’ and ‘‘expression pattern’’ shown inside dashed box, which were designed to capture any changes in the metabolic pathways in response to environmental variation, were included (San *et al.,* 2003).

The critical genetic network component was constructed from existing gene regulation knowledge in the literature and was supplemented with gene expression patterns from gene chip expression analysis experiments. The metabolic map was generated by the existing pathway data bases (KEGG Metabolic Pathways).

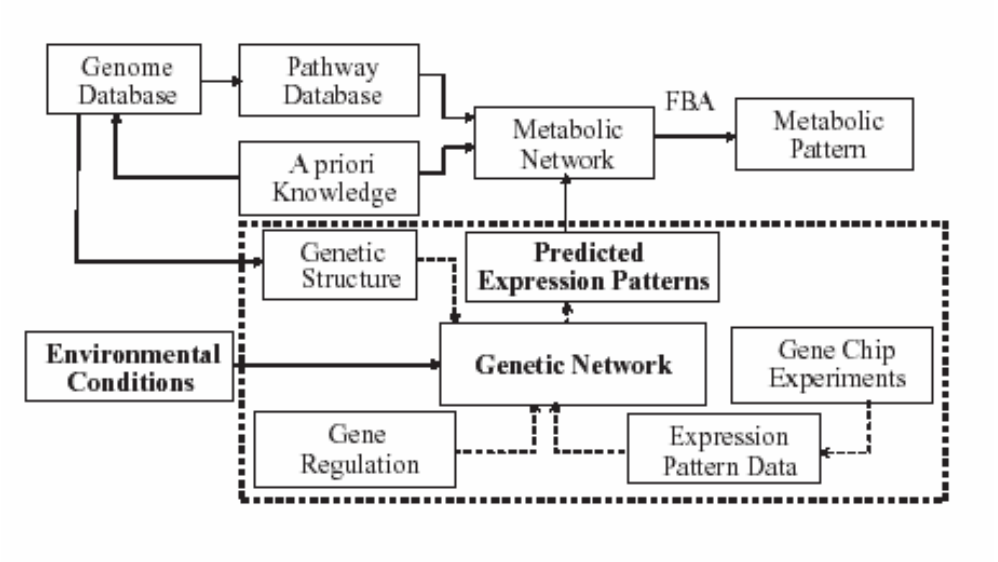

Figure 2.8. Schematic of genetic network assisted flux balance analysis (Cox *et al.*, 2005)

The central metabolism network pathways were included that are active in either aerobic and anaerobic conditions. The environment (via O_2) was perturbed in the gene network by FNR and ArcA/B. The regulatory impact of the transcription factors, FNR and ArcA/B was illustrated on extreme cases of either purely aerobic or anaerobic. In these two conditions, related genes are either "on" or "off" so, gene activity was modeled by Boolean variables. In particular, ArcA and FNR are "on" in the absence of oxygen. A small network was formed with two enzymes directing the flow of 7 metabolites.

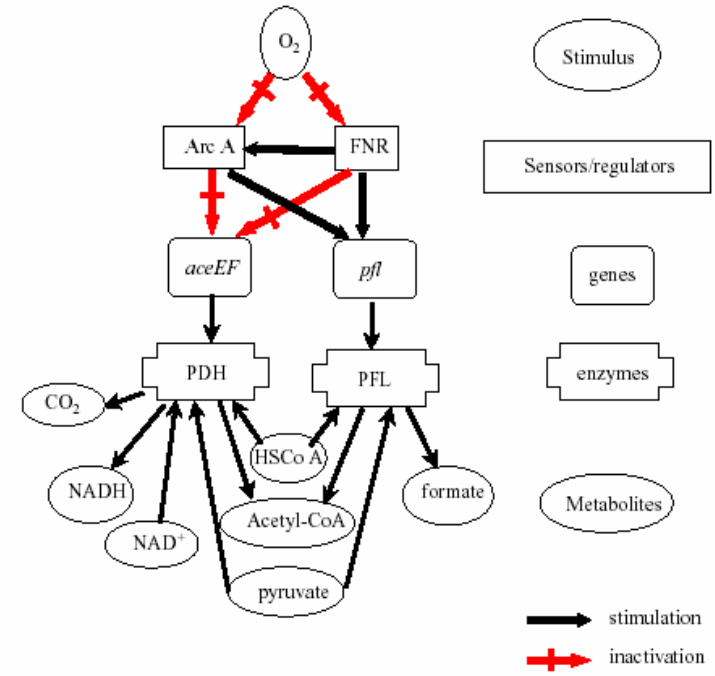

Figure 2.9. A small sub-network demonstrating cause and effect of the aerobic/anaerobic switch (Cox *et al.,* 2005)

The master stoichiometric matrix encodes 25 possible reactions between 16 potential intermediates. When this underdetermined system was solved by FBA, the original 25 variable problem was reduced to a 10 variable problem. The environment, acting through the gene net, placed further constraints on metabolism. Namely, in the absence of oxygen some reactions were inactivated. The dimension of the stoichiometric matrix has been changed by the activation and deactivation of the gene expression.

3. DIFFERENTIAL EQUATION MODELS

3.1. Signal-Oriented Approach in Using Differential Equation Models

A global signal transduction system has been used to describe carbon catabolite repression in *E. coli* is given in the below figure (Kremling *et al.*, 2001). As shown in this figure, the system includes the phosphoenolpyruvate (PEP)-dependent glucose phosphotransferase system (Glc-PTS), the synthesis of name cAMP, and the interaction of the name cAMP.CrpA complex with the specific DNA binding sites.

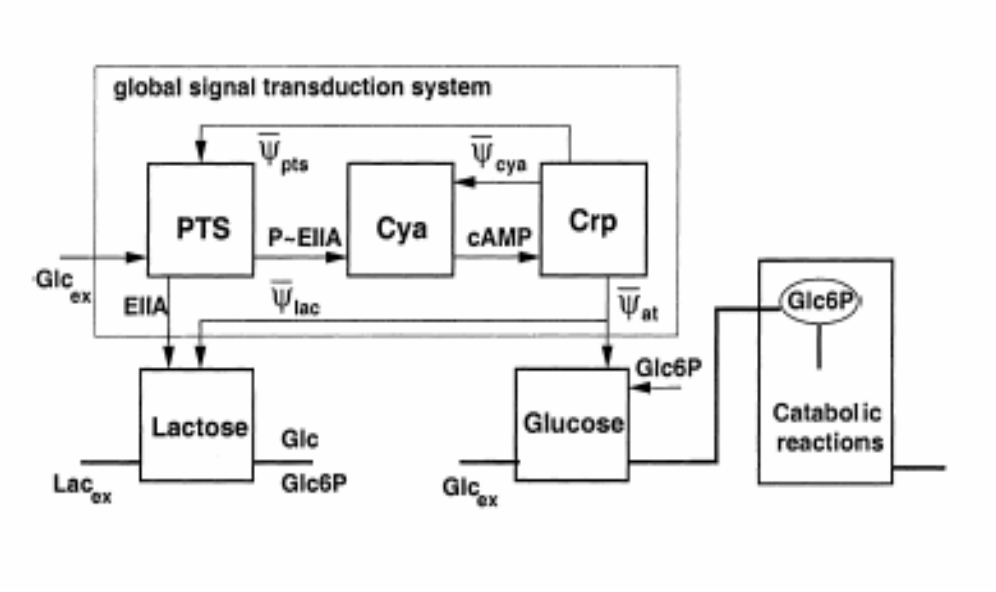

Figure 3.1. The elements of the crpA-modulon (Kremling *et al.,* 2001)

The model is aggregated from two functional units describing glucose and lactose transport and degradation. Both units are members of the *crp* modulon and are under the control of a global signal transduction system which calculates the signals that turn on or off gene expression for the specific enzymes.

In this contribution a mathematical model describing glucose and lactose uptake and metabolism was introduced by the current biological knowledge about the systems under

consideration. A subset of parameters related to glucose and lactose transport was estimated based on the measurements of biomass, extracellular glucose and lactose, and LacZ activity. A dynamic model was used to predict the growth behavior as well as the induction of genes and enzymatic activities very well. The model presented was used to simulate time courses of some variables that are difficult to measure but nevertheless essential toward an understanding of the system function. Influence of preculture on glucose-lactose diauxie was also investigated.

Although the preculture greatly influences the induction status of the genes of interest, there was no effect on the production of biomass and on the usage of carbohydrates (Kremling *et al.*, 2001). No matter which carbohydrate is present in the preculture (glucose or lactose) and regardless of preinduction of the *lac* operon, glucose is preferred in mixed cultures with glucose and lactose. As shown in Figures 3.2 and 3.3, the sugar consumption and biomass production are nearly identical.

Calculated EIIA, P~EIIA, cAMP, intracellular lactose, allolactose, and Glc6P, in addition to the measured data which was taken for the glucose preculture medium are given in Figure 3.2. As expected for the glucose phase, protein EIIA is mainly unphosphorylated. The lactose phase exhibits an interesting dynamics. Since intracellular glucose is also phosphorylated by the PTS, EIIA becomes again more and more unphosphorylated after a very quick drop in EIIA. The quick drop in EIIA phosphorylation state can be explained by the run out of glucose. The relatively slow rise of the phosphorylation state afterward reflects induction of the *lac* operon which leads to increased uptake of lactose and thereby to increased production of intracellular glucose 6 phosphates. The concentration of cAMP rises very fast, reflecting the drop in P~EIIA, and due to the high value of the degradation parameter, it drops down afterward. With increasing concentration of P~EIIA in the end of the growth phase, cAMP rises again. a low level of allolactose is synthesized from the beginning which leads to a small increase of LacZ in the glucose phase.

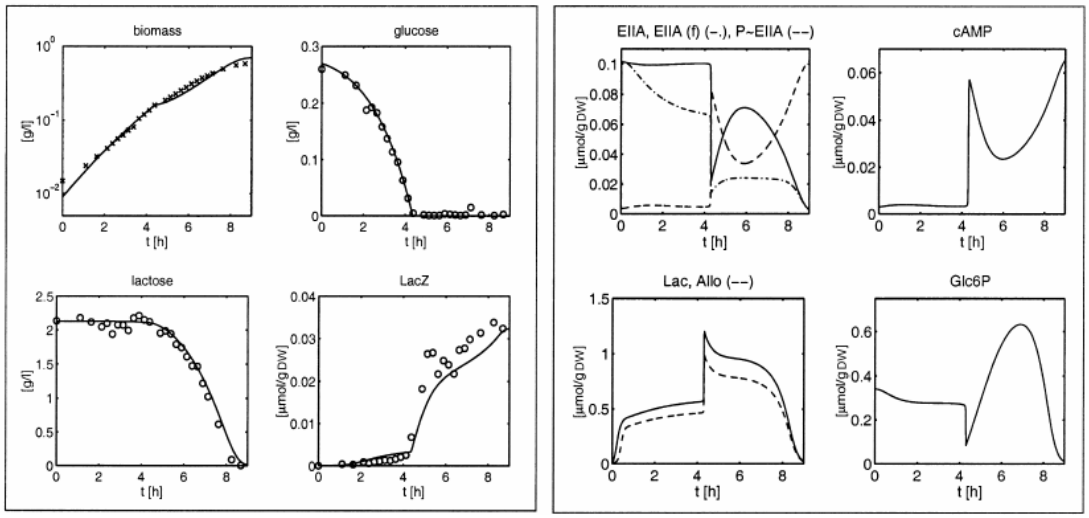

Figure 3.2. Diauxic growth of glucose and lactose with glucose preculture in *Escherichia coli* (Kremling *et al.*, 2001)

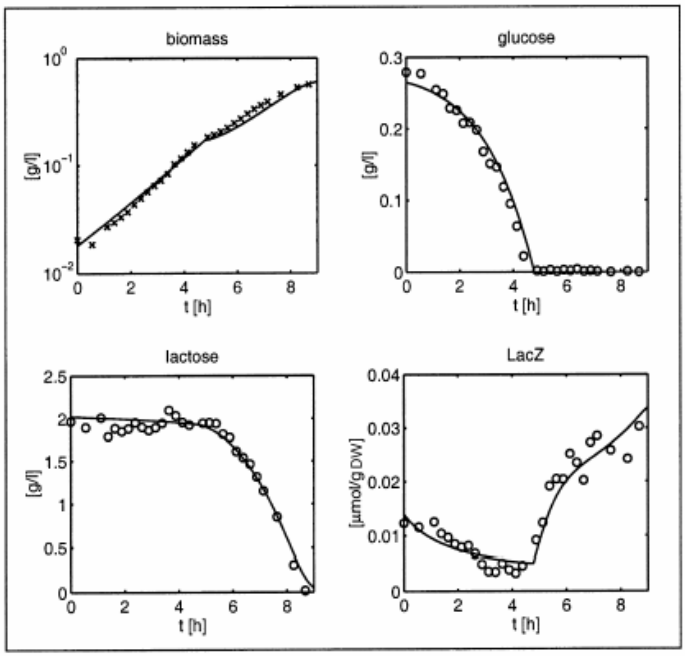

Figure 3.3. Diauxic growth of glucose and lactose with lactose preculture in *Escherichia coli* (Kremling *et al.*, 2001)

3.2. Simple Ordinary Differential Equation (ODE) Model

In studying biological behavior of an organism, regulatory structure plays an important role for its identification. In order to understand the metabolic regulation requires quantitative information about the concentrations of enzymes, metabolites, nucleotides and cofactors. The quantitative knowledge in combination with the known network of metabolic pathways allows the construction of mathematical models that describe the dynamic changes in metabolite concentrations over time. The constructed models will be high-dimensional systems of ordinary, non-linear differential equations. The main problems of the approach are the formation of the equations that describe the metabolic pathways in the form of kinetic rate equations and the parameter identification of the system parameters. It is hard to find a solution due to these model equations. A variety of pathway modeling software has been developed for the model construction and analysis.

A model was defined for the regulation of induction and repression of *lac* operon in *E. coli* (Wong *et al.,* 1997). The model contained twelve ordinary differential equations describing glucose transport through the cell, catabolite repression, induction and repression of the *lac* operon, lactose transport through the cell, degradation of lactose and cell growth. The parameters are collected from literature. The transient responses showed similar behavior to experimental data. Slow growth between glucose and lactose utilization is observed. Two possible models for the phosphorylation of internal glucose and catabolite repression were also investigated.

A mathematical model for the regulation of induction in the *Lac operon* in *E. coli* was also formulated (Yildirim and Mackey, 2003) to explain the dynamics of the permease facilitating the internalization of external lactose, internal lactose, β-galactosidase, glucose and galactose, the allolactose interactions with the *lac* repressor, and mRNA. The final model consists of five nonlinear differential delay equations with delays due to the transcription and translation process (dynamics of mRNA production, β-galactosidase, allolactose, permease productions and lactose). The parameters were determined from an extensive search of the existing literature. The model had been tested against the experimental data of β-galactosidase

activity versus time which gives changes after a step change from glucose to lactose growth for *E. coli* (Pestka *et al.,* 1984) and during periodic phosphate feeding which gives β-galactosidase concentration oscillations (Goodwin, 1969). Analytical and numerical studies had indicated that for physiologically realistic values of the external lactose and the bacterial growth rate, a regime existed where there might be bistable steady-state behavior.

A mathematical modeling work to show classical paradigms (Mackey *et al.,* 2004) for repressible and inducible operons of the tryptophan and lactose operons was presented. The model described for lactose operon is more or less the same with their previous work (Yildirim and Mackey, 2003). Some dilution rates and degradation terms of metabolites are added to the set of equations and better results than the previous one are obtained. The tryptophan operon is defined on a set of four nonlinear differential equations with delay for *mRNA* polymerase, *trp mRNA* molecules with free *TrpE* related ribosome binding sites, the enzyme anthranilate synthase, tryptophan concentrations. The model was solved numerically, and the results compared with the respective experiments performed (Yanofsky and Horn, 1994) on wild-type bacterial cultures as well as *trpL29* and *trpL75* mutant strains of *E. coli*. The model gave a reasonable qualitative agreement with the experimental results

4. FUZZY LOGIC

The fuzzy theory began in the 1960s and a paper explaining fuzzy sets was published in 1965 (Zadeh, 1965). The theory is the foundation for computing with words. The point of importance is the emphasis on precision in classical control theory. Therefore, the complex (biological) systems cannot be handled. Mathematics of fuzzy or cloudy quantities, which are not describable in terms of probability distributions, can define vague concepts. Using fuzzy theory, a new approach (Fuzzy IF-THEN rules) to the analysis of complex systems and decision processes was outlined for fuzzy control to formulate human knowledge (Zadeh, 1973).

In traditional set theory, membership of an object belonging to a set can only be one of two values: 0 or 1. An object either belongs to a set completely or it does not belong at all. No partial membership is allowed. However, there are countless vague concepts that humans can easily describe, understand, communicate with each other but that traditional mathematics, including the set theory, fails to handle in a rational way. The concept “young” is an example. For any specific person, his or her age is precise. However, relating a particular age to “young” involves fuzziness and is sometimes confusing and difficult. What age is young and what age is not? The nature of such questions is deterministic and has nothing to do with stochastic concepts such as probability and possibility (Yen and Langari, 1999).

4.1. Fundamentals of Fuzzy Logic

The introduction to fuzzy logic given in the following sections are summarized from the books, Yen & Langari and Ying.

4.1.1. Fuzzy Set

A fuzzy set generalizes 0 and 1 membership values of a traditional set to a membership function of a fuzzy set. Using the theory, one relates an age to “young” with a membership value ranging from 0 to 1; 0 means no association at all, and 1 indicates complete association.

One might think that age 10 is “young” with the membership value 1, age 30 with a membership value 0.75, age 50 with membership value 0.1, and so on. That is, every age/person is “young” to a certain degree. The fuzzy set (Figure 4.1) is called membership function of the fuzzy set “young”. Usually, the membership or characteristic function is denoted by the Greek lower-case letter μ.

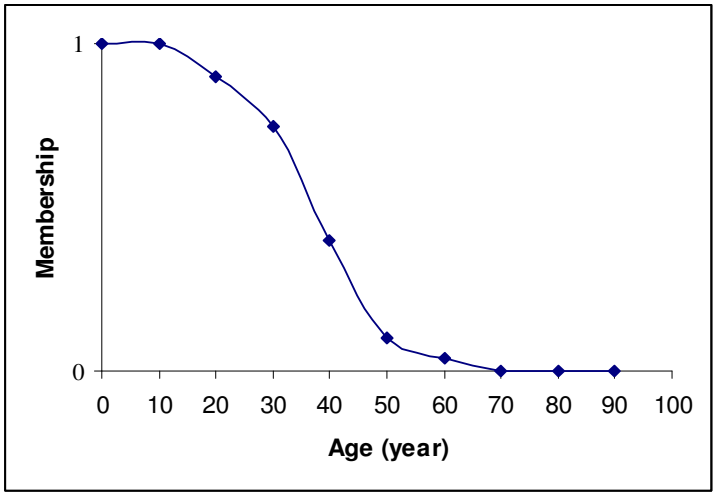

Figure 4.1. A possible description of the vague concept “young” by a fuzzy set

People have different views on the same (vague) concept. Fuzzy sets can be used to easily accommodate this reality. Some people might think age 50 is “young” with membership value as high as 0.9, whereas others might consider that 20 is ”young” with membership value merely 0.2. Different membership functions can be used to represent these different versions of “young”. Not only do people have different membership functions for the same concept, but even for the same person, the membership function for “young” can be different when the context in which age is addressed varies. A 40 year old president of the country would likely be regarded as young, whereas a 40 year athlete would not. Two different fuzzy sets “young” are needed to effectively deal with the two situations.

A fuzzy set can be defined in two ways: (1) by enumerating membership values of those elements in the set (completely or partially), or (2) by defining the membership function mathematically.

4.1.2. Designing Membership Functions

The crucial question is; “How would the exact shape of the membership function for a fuzzy set be determined?” The important thing about membership function is that it provides a *gradual transition* from regions completely outside a set to regions completely in the set.

A membership function can be designed in three ways: (1) Interview those who are familiar with the underlying concept and later adjust it based on a tuning strategy. (2) Construct it automatically from data; (3) learn it based on feedback from the system performance.

The parameterizable membership functions most commonly used in practice are the triangular membership function and trapezoid membership function. The former has three parameters and the latter has four parameters.

Simplicity is the main advantage of triangular and trapezoidal membership functions. A membership function is intended to *approximate* a smooth transition between two regions (the region outside the set and that inside the set).

To summarize, the following guidelines for the membership function design is used.

1. Always use parameterizable membership functions. Do not define a membership function point by point.
2. Use a triangular or trapezoidal membership function, unless there is a good reason to do otherwise.
3. If you want to learn the membership function using neural network learning techniques, choose a differentiable (or even continuous differentiable) membership function (e.g., Gaussian)

The membership functions of an input variable’s fuzzy sets should usually be designed in a way such that the following two conditions are satisfied: (1) each membership function overlaps only with the closest neighboring membership functions; (2) for any possible input data, its membership values in all relevant fuzzy sets should sum to 1 (or nearly so). These conditions are usually represented as:

$$A_i \cap A_j = \varnothing \qquad \forall\ j \neq i,\ i+1, i-1 \qquad (10)$$

$$\sum_i \mu_{A_i}(x) \cong 1 \qquad (11)$$

The three fundamental operations in classical sets are union, intersection, and complement. The union of two sets A and B (denoted as A∪B) is the collection of those objects that belong to either A or B. the intersection of A and B (denoted as A∩B) is the collection of those objects that belong to both A and B. The complement of a set A (denoted as A^C and $\overline{A}$) is the collection of objects that belonging to A.

4.1.3. Tools for Implementing Fuzzy Logic Applications

There are several companies that market hardware and software packages for developing fuzzy logic applications in the late 1980s and early 1990s. Even though these companies had some initial success, several did not survive through the mid- 1990s. This is partially due to the fact that vendors of conventional control design software such as MathWorks started introducing add-on toolboxes for designing fuzzy systems. The *Fuzzy Logic Toolbox* for MATLAB was introduced as an add-on component to MATLAB in 1994.

4.2. Basics of Fuzzy Rules

A fuzzy if-then rule is a knowledge representation scheme for capturing knowledge (typically human knowledge) that is imprecise and inexact by nature. This is achieved by using linguistic variables to describe elastic conditions (i.e., conditions that can be satisfied to a degree) in the "if part" of fuzzy rules.

The main feature of fuzzy rule-based inference is its capability to perform inference under partial matching. That is, it computes the degree the input data matches the condition of a rule.

4.2.1. Fuzzy Rule-Based Inference

The algorithm of fuzzy rule-based inference consists of three basic steps and an additional optional step.

1. **Fuzzy Matching:** Calculate the degree to which the input data match the condition of the fuzzy rules.
2. **Inference:** Calculate the rule's conclusion based on its matching degree.
3. **Combination:** Combine the conclusion inferred by all fuzzy rules into a conclusion.
4. **(Optional) Defuzzification:** for applications that need a traditional output (e.g., in control systems), an additional step is used to convert a fuzzy conclusion into a discrete one.

Fuzzy Matching can be explained in terms of an example discussed below.

The degree to which the input target variables (*V*) satisfies the condition of rule *R3* "target temperature is Low" is the same as the degree to which the input target variable belongs to the fuzzy set Low.

$$MatchingDegree(V, R3)=\mu_{Low}$$

where"=" represents assignment (not equality test)

$$MatchingDegree(V, R3)=\mu_{High}$$

The variable *V* is 0.2 Low (μ_{Low}) and 0.8 High (μ_{High}) at the value of 60 as shown in Figure 4.2. The sum of two membership functions at the value 60 is equal to unity (Eq. 10) and the two membership functions do not overlap on the other (Eq. 11). When an input is entered to fuzzy inference system, it is matched to a degree of any fuzzy set, initially. There are two fuzzy sets in this example (i.e., Low and High).

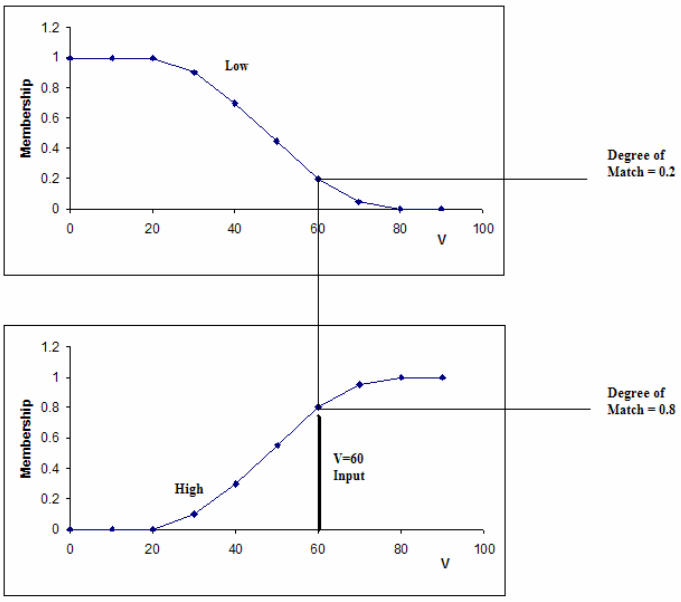

Figure 4.2. Fuzzy matching for simple conditions of variable V

When a rule has multiple conditions combined using AND (conjunction), a fuzzy conjunction operator to combine the matching degree of each condition is used. The most commonly used fuzzy conjunction operators is the min operator or the product (i.e., multiplication) operator.

After the functional mapping relationship between inputs and outputs has been performed, a fuzzy inference step is invoked for each of the relevant rules to produce **a conclusion** based on their matching degree. How should the conclusion be produced? There are two methods: (1) the clipping method and (2) the scaling method. Both methods generate an inferred conclusion by suppressing the membership function of the consequent. The extent to which they suppress the membership function depends on the degree to which the rule is matched. The lower the matching degree, the more severe the suppression of membership function will be.

The clipping and scaling methods produce their inferred conclusion by suppressing the membership function of the consequent differently. The clipping method cuts off the top of the membership function whose value is higher than the matching degree. The scaling method scales down the membership function in proportion to the matching degree.

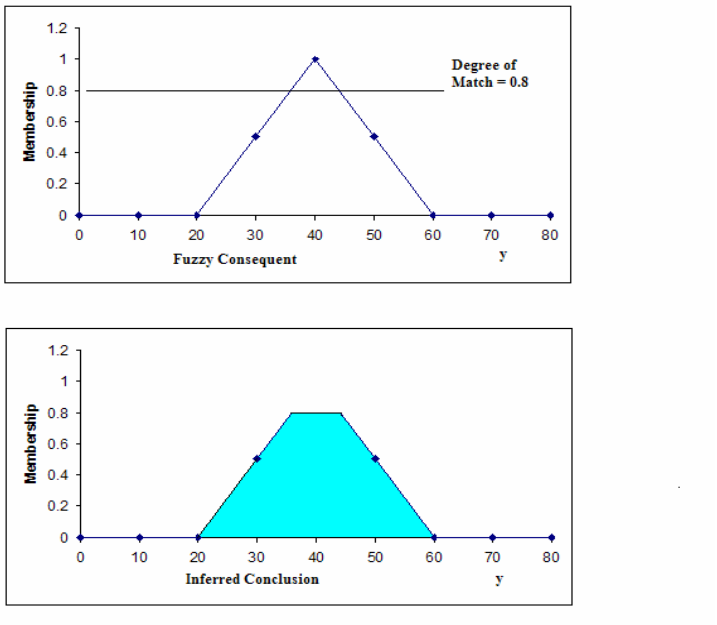

Figure 4.3. The clipping method for fuzzy inference

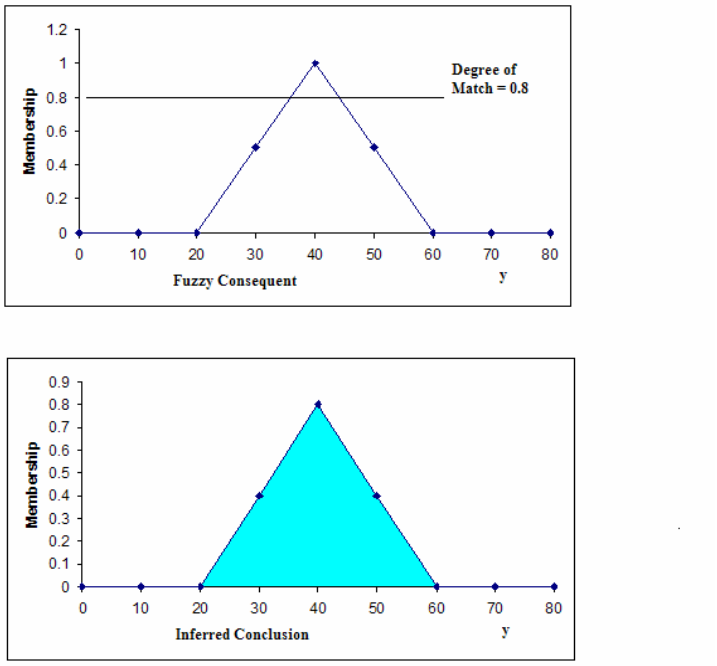

Figure 4.4. The scaling method for fuzzy inference

The fuzzy inference is exemplified in Figure 4.3 and 4.4. The matching degree of the input 60 is 0.8 High. After the mapping between inputs and outputs has been performed, the

conclusion (output) is a membership function belonging to a fuzzy set. The difference of fuzzy inference to a conclusion between scaling and clipping methods can be seen easily. The clipping method of inference is used for the calculation in this work.

The two steps in fuzzy inference described so far enable each fuzzy rule to infer a fuzzy statement about the value of the consequent variable. Because a fuzzy rule-based system consists of a set of fuzzy rules with partially overlapping conditions, a particular input to the system often "triggers" multiple fuzzy rules (i.e., more than one rule will match the input to a nonzero degree). Therefore, a third step is needed to combine the inference results of these rules. This is accomplished typically by superimposing all fuzzy conclusion about a variable.

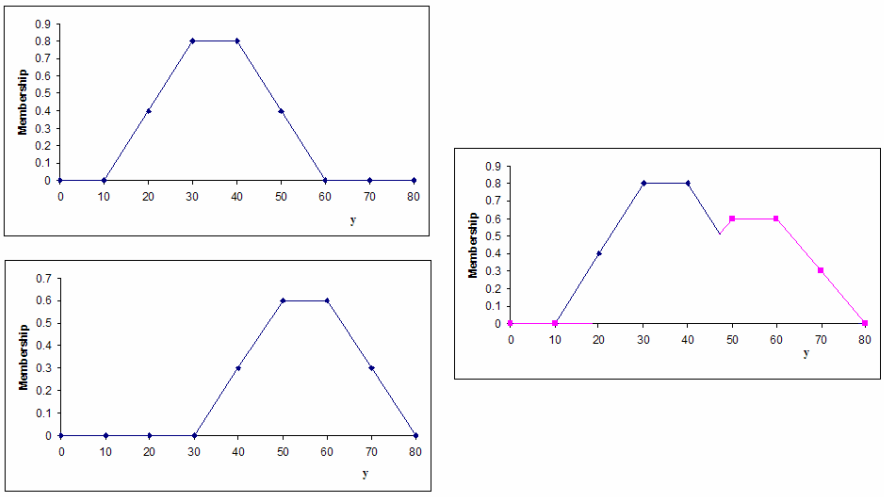

Figure 4.5. Combining fuzzy conclusions inferred by the clipping method

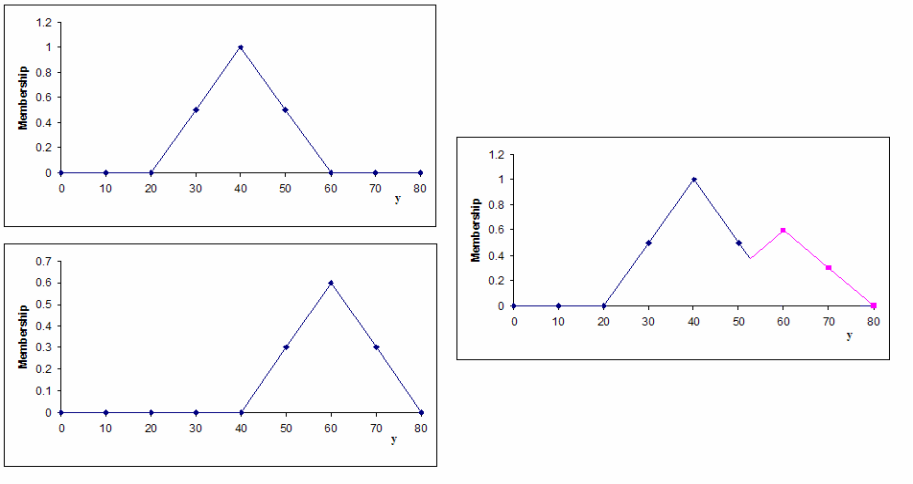

Figure 4.6. Combining fuzzy conclusions inferred by the scaling method

Combining fuzzy conclusions through superimposition is based on applying the max fuzzy disjunction operator to multiple possibility distributions of the output variable.

In Figures 4.5 and 4.6, combining fuzzy inference conclusions by scaling and clipping methods are explained. Every fuzzy set for an input is mapped to a conclusion of an output. In order to evaluate the result, all fuzzy conclusions must be combined through superimposition.

For a fuzzy system whose final output needs to be a crisp (nonfuzzy) form, a fourth step is needed to convert the final combined fuzzy conclusion into a crisp one. This step is called the *defuzzification.*

There are two major defuzzification techniques: (1) the Mean of Maximum (MOM) method and (2) the Center of Area (COA) or the centroid method. The mean of maximum defuzzification calculates the average of all variable values with maximum membership degrees. However, center of area defuzzification calculates the center of the whole shape formed after the superimposition of all conclusions.

The crisp output is formed either MOM or COA as shown in Figures 4.7 and 4.8. The center of area is used in this work to have a conclusion in nonfuzzy form.

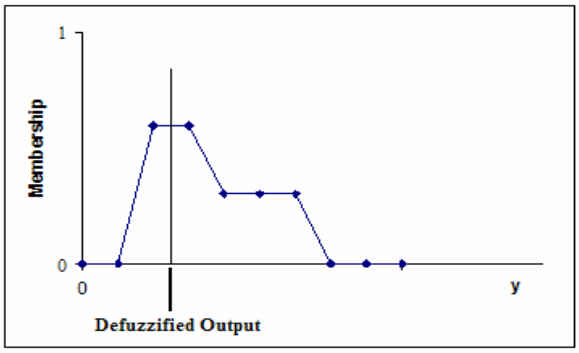

Figure 4.7. An example of MOM defuzzification

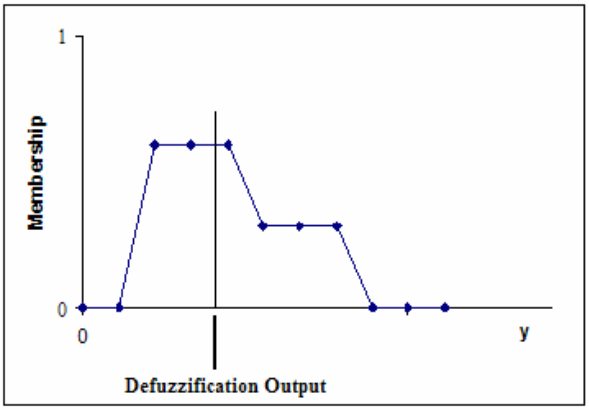

Figure 4.8. An example of COA defuzzification

4.2.2. Types of Fuzzy Rules

There are two types of fuzzy rules: 1) fuzzy mapping rules, and 2) fuzzy implication rules. A fuzzy mapping rule describes a functional mapping relationship between inputs and an output using linguistic terms, while a fuzzy implication rule describes a generalized logic implication relationship between two logic formulas involving linguistic variables and imprecise linguistic terms. The types of fuzzy rules are related to different disciplines. Fuzzy mapping rules are related to functional approximation techniques in system identification and artificial neural networks, whereas fuzzy implication rules are related to classical two-valued logic and multi-valued logic.

Fuzzy Mapping Rules

In many real-world problems, one is interested in finding the functional relationship between a set of observable parameters and one or multiple parameters whose values are not known. Indeed, fuzzy logic tools use rules of this type to approximate a mapping (typically nonlinear) from the observed state to a desired control or regulatory action. The needs to approximate a function of interest are often due to one or more of the following reasons. First, the mathematical structure of the function is not precisely known, but the structure is known. One could use various parameter identification techniques to find the parameters. Second, the function is so complex that finding its precise mathematical form is either impossible or practically unfeasible due to its high cost. Third, even if finding the function is not impractical, implementing the function in its precise mathematical form in a product or service may be too costly.

The entire function is approximated by a set of fuzzy mapping rules. The inference (i.e., mapping) for this type of rule is always in forward direction. The main difference between fuzzy rules and non-fuzzy rules for function approximation lies in their "interpolative reasoning" capability, which allows the output of multiple fuzzy rules to be fused for a given input. Function approximation technique is classified in three categories: global techniques, superimposition techniques, and partition based techniques. The global techniques approximate a function globally using one mathematical structure (e.g., linear, second order polynomial). The issue of the technique lies in finding the suitable model structure for a given problem. The superimposition techniques approximate a function by superimposing a function of a given form (e.g., Taylor expansion). The partition-based approximate techniques approximate the function by partitioning the input space of the function and approximate the function in each partitioned region separately (e.g., piecewise linear approximation).

Fuzzy Implication Rules

Fuzzy implication rules are a generalization of "implication" in two-value logic. Their aim is to mimic human reasoning in its ability to reason with ideas or statements that are imprecise by nature. Even though it is obvious that human beings perform certain kinds of

approximate reasoning, it is unclear how one can characterize such a reasoning process due to our present limited understanding of the human reasoning process to date. Consequently, there has not been imagined a unique set of desired properties for fuzzy implication rules. Rather, several sets of desired properties have been developed. Even though, the set of desired properties are not unique, they are useful for comparing different reasoning schemes using fuzzy implication rules. It is important to point out this "non uniqueness" aspect of fuzzy implication, because it is in sharp contrast with many other techniques in science and engineering that were built on a set of well defined axioms, properties, or principles.

The inference of fuzzy implications generalizes two kinds of logic inference using the implications in classical logic: modus ponens and modus tollens. As an example;

IF a person's IQ is high THEN the person is smart.

Modus ponens, "Jack's IQ is high", is a given implication or fact and enables us to infer modus tollens "Jack is smart". Also, the implication and fact "Jack is not smart" can be given to infer "Jack's IQ is not high".

These if-then rule statements are used to formulate the conditional statements that comprise fuzzy logic. Another example can be given as;

IF *service* is good THEN *tip* is average.

Good is represented as a number between 0 and 1, and so the modus ponens is an interpretation that returns a single number between 0 and 1. In general, the input to an if-then rule is the current value for the input variable (in this case, *service*) and the output is an entire fuzzy set (in this case, *average*). This set will later be *defuzzified,* assigning one value to the output. Interpreting an if-then rule involves distinct parts: first evaluating the modus ponens (which involves *fuzzifying* the input and applying any necessary *fuzzy operators*) and second applying that result to the consequent (known as *implication*).

The modus ponens of a rule can have multiple parts.

IF *sky* is gray and *wind* is strong and *barometer* is falling, THEN…

All parts of the antecedent are calculated simultaneously and resolved to a single number using the logical operators (AND, OR etc.).

The consequent (modus tollen) of a rule can also have multiple parts. All consequents are affected equally by the result of the modus ponen.

IF *temperature* is cold THEN *hot water valve* is open AND *cold water valve* is shut.

The degree of support is used for the entire rule to shape the output fuzzy set. The consequent of a fuzzy rule assigns an entire fuzzy set to the output. This fuzzy set is represented by a membership function that is chosen to indicate the qualities of the consequent. If the antecedent is only partially true, (i.e., is assigned a value less than 1), then the output fuzzy set is truncated according to the implication method.

4.3. Fuzzy Logic Applications in Biological Systems

Recent technological advances in huge data collection give biologist the ability to study complex systems. To develop and test biological models based on experimental observations and predict the effect of perturbations of the network, a biological pathway can be modeled in two general categories; a logical network and chemical reaction network. Boolean logic models cannot represent necessary biological details. Chemical kinetics simulations require large numbers of parameters that are very difficult to accurately measure.

Fuzzy Logic has been successfully used in some mathematical modeling of biological systems. One of these is the enzyme kinetic modeling (Lee *et al*., 1999) which is the one that accounts for metabolite effects that contribute significantly to the regulation of enzyme activity. In order to incorporate the effect of metabolite effector to the three enzyme kinetic equations of *E. coli* central metabolisms (phosphoenolpyruvate carboxylase, phosphoenolpyruvate carboxykinase, and pyruvate kinase I), a strategy using fuzzy logic-based factor was used. The use of fuzzy logic in phosphoenolpyruvate carboxylase metabolism was described as follows;

E. coli phosphoenolpyruvate carboxylase (PPC) catalyzes the carboxylation of phosphoenolpyruvate (PEP) to form oxaloacetate (OAA). The reaction rate of PPC is formulated as:

$$V_{ppc} = \alpha_{ppc} V_m \frac{[PEP]}{K_m + [PEP]} \qquad (12)$$

The rate constant V_m is modulated by the two activators; acetyl-CoA (ACoA) and fructose 1,6-diphosphate (FDP). K_m is the parameter and [ ] is the concentration. α_{ppc} captures the various activation effects of ACoA and FDP by the following fuzzy rules.

If [ACoA] is LOW and [FDP] is LOW, then $\alpha_{ppc} = c_1$

If [ACoA] is LOW and [FDP] is HIGH, then $\alpha_{ppc} = c_2$

If [ACoA] is HIGH and [FDP] is LOW, then $\alpha_{ppc} = c_3$

If [ACoA] is HIGH and [FDP] is LOW, then $\alpha_{ppc} = c_4$

c_1, c_2, c_3, and c_4 are parameters to be optimized with respect to experimental data.

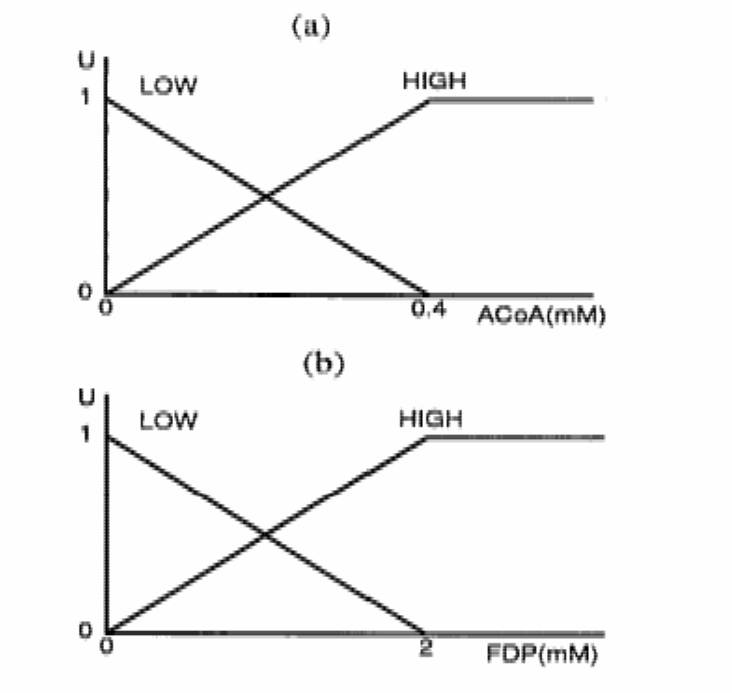

Figure 4.9. Membership functions of the fuzzy sets for PPC modeling (Lee *et al*., 1999)

The membership functions of the fuzzy sets (i.e., LOW and HIGH), shown in Figure 4.9, were chosen based on experimental data. The fuzzy logic IF-THEN rules stated above are conceptually clear and can be readily generalized. By setting the rules, the parameters $c_{1\text{-}4}$ can be obtained from the rules and their respective membership function.

Another modeling and simulation of gene regulation was studied on *lac* operon of *E. coli* (Sokhansanj and Fitch, 2001).

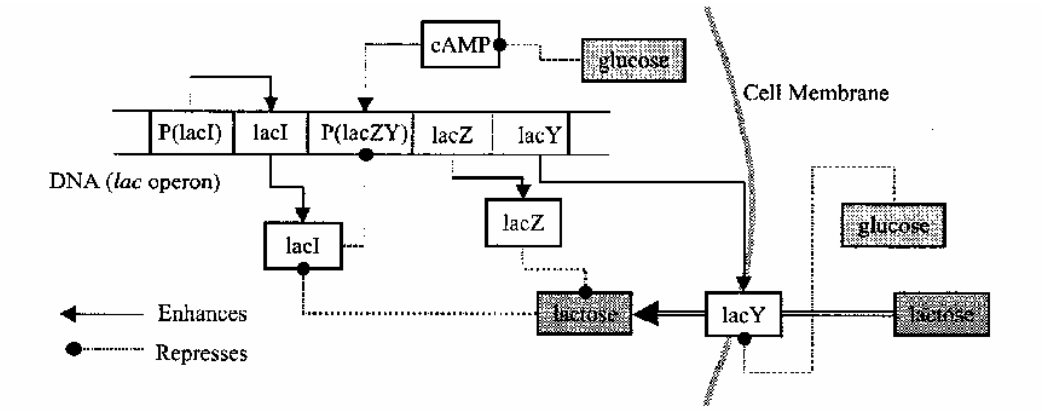

Figure 4.10. Model of lac operon regulation (Sokhansanj, 2001)

Union Rule Configuration (URC) in the fuzzy rule base was utilized to describe the system. In the linear (URC) fuzzy logic scheme, there are distinct fuzzy rules for each individual input to a given output. Then, the fuzzy rules are combined with the logical statement of "OR". The system consists of four genes and a number of protein binding sites clustered near each other in *E. coli* chromosome. The genes and their protein products are lacI (lac repressor), lacZ (β-galactoside permease) and lacA (not involved in lactose regulation). When RNA polymerase (RNAP) binds to the promoter of the gene (P(*lacI*) and P(*lacZY*)), it catalyzes its transcription. Promoters have different binding strengths. The rule IF (promoter strength) THEN (protein production) refers to the absolute promoter strength independent of any other regulatory activity.

The model for *lac* operon in *E. coli* is the prototype for most genetic regulatory systems in bacteria. It involves a group of genes regulated together by one or two stimuli. Lactose is used secondly as a carbon source after glucose is depleted. The proteins and sugars are all fuzzified on different domains and URC fuzzy rule base for the *lac* operon was constructed given in Table 4.1. However, a clear result indicating the effectiveness of the model was not described in this paper.

Table 4.1. Table of URC fuzzy rule base for *lac* operon (Sokhansanj, 2001)

IF	**VL**	**LO**	**ME**	**HI**	**VH**
	lacI production				
P(lacl) strength	VL	LO	ME	HI	VH
	lacl activity				
lacl production	VL	LO	ME	HI	VH
lactose (in cell)	VH	ME	LO	LO	VL
protease	VH	HI	HI	LO	VL
	cAMP activity				
glucose	VH	HI	ME	LO	VL
	lacY, lacZ production				
P(lacZY) strength	VL	LO	ME	HI	VH
lacl activity	VH	HI	LO	LO	VL
cAMP activity	VL	LO	HI	HI	VH
	lacY activity				
lacy production	VL	LO	ME	HI	VH
glucose	VH	HI	ME	LO	LO
protease	VH	HI	HI	LO	VL
	lacZ activity				
lacZ production	VL	LO	ME	HI	VH
peotease	VH	HI	HI	LO	VL
	lactose (in cell)				
lactose (outside cell)	VL	LO	ME	HI	VH
lacy activity	VL	LO	ME	HI	VH
lacZ activity	VH	HI	ME	LO	VL

The genes and their protein products are modeled by IF-THEN rule based fuzzy logic. The list can be read as;

(IF lactose (outside cell) is very low THEN lactose in the cell is very low) OR (lacY activity is very low THEN lactose in the cell is very low) OR (lacZ activity is very high THEN lactose in the cell is very low)

A novel algorithm using fuzzy logic for analyzing gene expression data was developed. A model to find activators, repressors, and targets in a yeast gene expression data set was designed (Woolf and Wang, 2000). The algorithm can assist in determining the function of uncharacterized proteins and is able to detect a substantially larger number of transcription factors than could be found at random. In analyzing genetic expression data, the data was transformed from crisp values to fuzzy values. Data was fuzzified by first normalizing the data from 0 to 1, then the normalized value was broken up into various membership classes.

The three fuzzy sets used in this algorithm, “HI,” “MED,” and “LO” as a function of the normalized value is given in Figure 4.11. The three fuzzy sets HI, MED, and LO were chosen after manually examining expression data and finding that the abundance of most transcripts was high, medium or low.

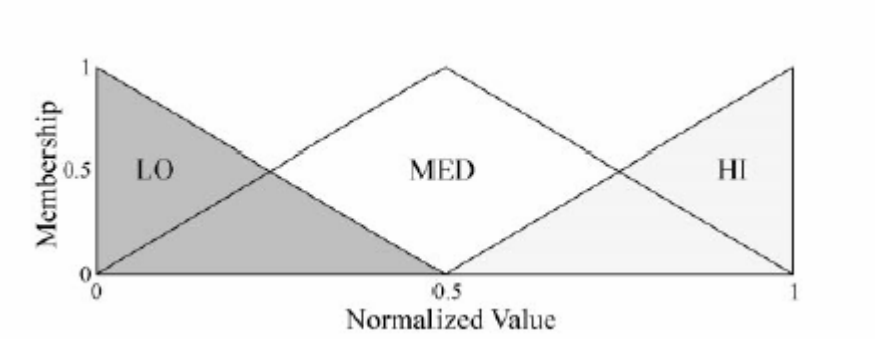

Figure 4.11. Fuzzy membership as a function of a normalized expression data (Woolf and Wang, 2000)

Triplets of data were compared using a set of heuristic rules in the form of a decision matrix given in Figure 4.12. Triplets were defined as the expression values of three different proteins (A, B, and C) all taken at the same time point in the yeast growth cycle time series. Fuzzified values of A and B are entered into this matrix, and at points where their predictions overlap, a score is generated as the fuzzified value of predicted C. A fuzzy value for C can be defuzzified back into a crisp number. The predicted expression values of C for each time point in the time series were calculated.

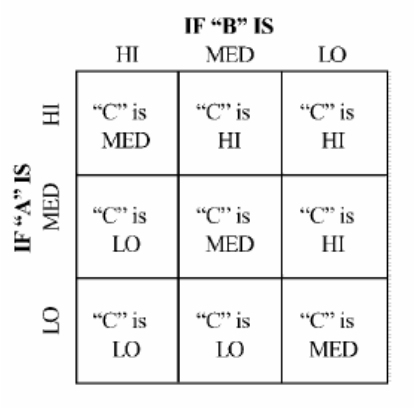

Figure 4.12. Decision matrix describing an activator (A) and a repressor (B) acting on a target (Woolf and Wang, 2000)

5. SUGAR UPTAKE REGULATION IN MICROORGANISMS

Every organism has a large number of genes and it is important to express them in the right circumstances and in the right amount. Models of gene regulation in prokaryotic cells lead to a better understanding of gene regulation in more complex eukaryotic cells. Generally, prokaryotes need to regulate their gene expression temporally to accommodate for changing environments. Microbial growth on mixtures of substrates is a classical problem of gene regulation. Indeed, the molecular basis of gene regulation was discovered by studying the *diauxic* phenomenon observed during growth of *E. coli* on a mixture of glucose and lactose.

An operon is a cluster of bacterial genes along with an adjacent promoter that controls the transcription of the genes. The genes to be controlled coordinately are next to each other on the DNA. The linked genes are transcribed as a unit to give one single mRNA. One mRNA is made per operon, because all the genes in a cluster share a single promotor. Regulation is at the level of transcription. The level of translation is controlled by regulating the synthesis of mRNA. This is the usual method for regulation of protein synthesis in prokaryotes.

Repressible system and inducible system are the two major types of regulations. When the end product of the system increases, it will shut off transcription of the coding region in repressible system. In inducible system, the expression of genes depends on the presence or absence of certain substances. In carbon catabolite repression (CCR), the expression of genes required for the utilization of secondary sources of carbon is prevented by the presence of the preferred substrate (Hillen, 1999). Actually, it enables the organism to increase its fitness by optimizing growth rate in natural environments.

5.1. *Lac* Operon in *Esherichia coli*

The *lac* operon describes the regulation of lactose uptake in bacterium. The schematic diagram of this operon is shown in Figure 5.1. Lactose is broken down into glucose and galactose. There are very few molecules of the enzyme β-galactosidase (coded for by *lacZ* gene) in normal cells of *E. coli* when no lactose is present. When lactose is added to the

medium, the concentration of this enzyme increases rapidly. Also, two other enzymes increase: β-galactoside permease (coded for by the *lacY* gene), β-galactoside acetyltransferase (coded for by *lacA*). These three are the proteins involved in lactose metabolism in the *E. coli* cell. Actually, β-galactosidase converts lactose into glucose and galactose, and the permease is involved in transport of lactose across the membrane whereas, the function of β-galactoside transacetylase is unknown. The three genes are all transcribed together by the same mRNA. However, there is a regulatory molecule, the repressor (coded for by the *lacI* gene), which interferes with the transcription of genes involved in lactose metabolism. It is also located adjacent to the other three but its regulation is totally independent of the other lac genes.

Bacteria (*E. coli*) adapt to changes in their surroundings by using regulatory proteins to turn groups of genes on and off in response to various environmental signals. Whenever glucose is present, *E. coli* metabolizes it before using alternative energy sources such as lactose, arabinose, galactose, and maltose. Lactose is not the preferred carbohydrate source for *E. coli*. If lactose and glucose are present, the cell will use all of the glucose before the *lac* operon is turned on. This is a type of regulation, called catabolite repression.

There are two binding sites for the promoter of the *lac* operon to be turned on. One site is the location where RNA polymerase binds. The second location is the binding site for a complex between the **catabolite activator protein (CAP)** and **cyclic AMP (cAMP)**. To prevent lactose metabolism, the binding of RNA polymerase and the complex must be hindered.

The LacI protein is a REPRESSOR that binds to the lacO sequence, which lies close to the promoter. This prevents RNA polymerase accessing the promoter to transcribe the operon. Inducer molecules can bind to the repressor and this causes a change in conformation so that it no longer binds DNA. In *E. coli*, allolactose is an inducer molecule, which is produced from lactose as a side reaction of β-galactosidase in the conversion. Then, the RNA polymerase can transcribe the operon and LacY, LacZ proteins are produced. Thus, presence of inducer switches on the operon.

Another control of the *lac* operon mediated by glucose is the binding of the CAP-cAMP complex. If glucose is present the *lac* operon gets expressed to less than 5% of its level in the absence of glucose. This turns out to be mediated by an intracellular signal of cAMP. The presence of this complex is closely associated with the presence of glucose in the

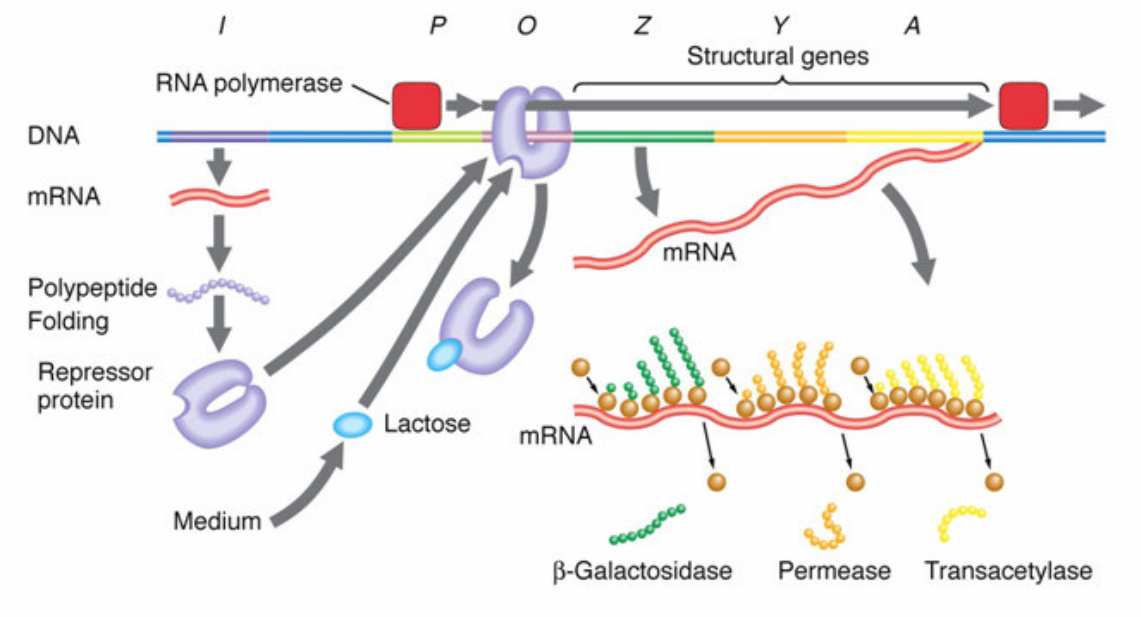

Figure 5.1. The scheme of *lac* Operon

cell. When the concentration of glucose increases in the medium, the amount of cAMP will decrease. As the cAMP decreases, the amount of complex decreases. This decrease in the complex inactivates the promoter, and the *lac* operon is turned off. The CAP-cAMP exerts a **positive control** over the expression of the *lac* operon.

cAMP is synthesized from ATP by the membrane-bound enzyme adenylate cyclase. Glucose is transported into the cell by a system that phosphorylates the glucose during transport and has several membrane components. These react with adenylate cyclase and stop its activity during glucose transport. Thus, when glucose is present there are low levels of cAMP in the cell and the level rises when glucose is not present. The lac-promoter is actually a very weak promoter when only RNA polymerase is present. However, catabolite activator protein bounded by cAMP is strong promoter and stimulates a better transcription. Thus, there is only good expression when there is no glucose present.

5.2. Glucose Phosphotransferase System (PTS) in *Escherichia coli*

The purpose of the bacterial phosphotransferase system, is the specific uptake of sugars into the cells, the sugars are transported uphill a concentration gradient with concomitant phosphorylation. The phosphate donor is the 'energy rich' phosphoenolpyruvate (PEP). As shown in Figure 5.2, the phosphate is transferred via the soluble (and non sugar specific) enzymes EI and HPr to the enzyme complex EII. EII is made up of the components A, B and C, which according to sugar specificity and bacterium involved may be domains of composite proteins. Component/domain C is the permease and anchored to the cytoplasmic membrane. In the glucose PTS EIIA is a soluble protein, EIIB/C is membrane bound.

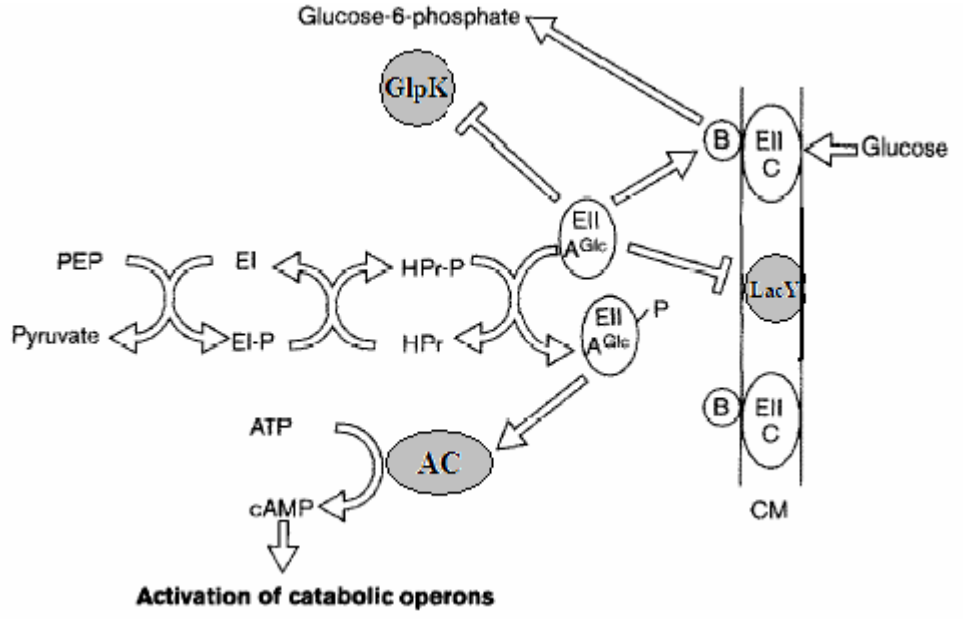

Figure 5.2. Glucose Phosphotransferase System in *Escherichia coli* (Postma *et al.,* 1993)

The amount of phosphorylation of the enzymes influences other regulatory mechanisms in the cells (eg., catabolite repression). Carbon catabolite repression in *E. coli* is mainly mediated by the glucose-specific EIIA of the PTS. As shown in Figure 5.2, in the presence of glucose, $EIIA^{Glc}$ binds and inactivates the lactose permease (LacY) and glycerol kinase (GlpK). In the absence of sugars, phosphorylated $EIIA^{Glc}$ activates adenylate cyclase (AC) to result in Crp-mediated transcriptional activation of catabolic operons (Postma *et al.,* 1993).

5.3. Galactose (Gal) Operon in *Escherichia coli*

An example of negative regulation is the galactose (*gal*) operon in *E. coli*. Galactose enters central metabolism by a rather indirect route. The regulation is accomplished by the gal operon having two promoters, two operators and two repressors. The structure of galactose operon is shown in Figure 5.3.

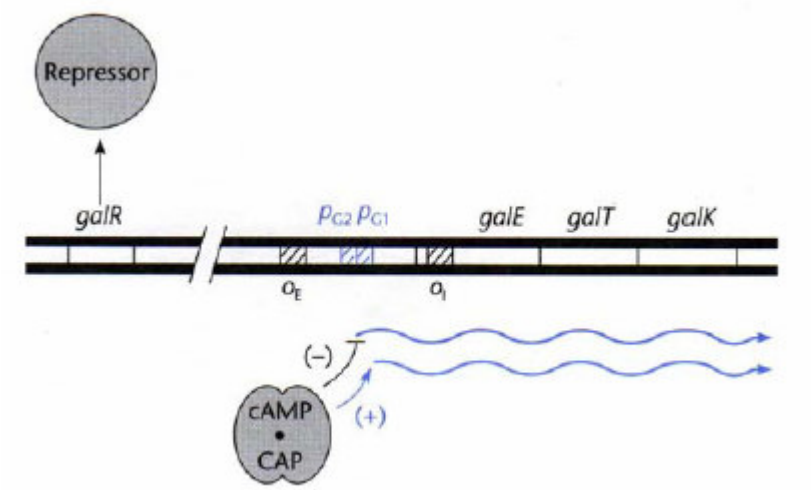

Figure 5.3. Structure of *gal* operon in *Escherichia coli* (Snyder, 1997)

The *galE*, *galT*, and *galK* genes are transcribed from two promoters, p_{G1} and p_{G2}. The CAP protein with cyclic AMP (cAMP) bound turns on p_{G1} and turns off p_{G2}. There are also two operators, gal_{OE} and gal_{OI}. The repressor genes are some distance away, as indicated by the broken line but, the GaIR repressor gene is shown. It negatively controls the transcription initiation of the *galETKM* operon and *galS* gene in the absence of galactose. The other pair of repressor GalS selectively represses the downstream promoter, p_{G1} of the *gal* operon and slightly activates the promoter, p_{G2}. It strongly interacts with other operator *mgl* operator (Adhya, 1997).

The biological interconversion of galactose to glucose is the galactose degradation pathway (Leloir pathway). The three enzymes; galactokinase (Frey *et al.,* 1996), galactose-1-phosphate uridylyltransferase, and UDP-galactose 4-epimerase (Neiderhart *et al.,* 1996) are coded from galK, galT, galE, are required for the degradation.

A model for the regulation of the galactose operon is structured in such a way that the absence of galactose results in the bending of the DNA and disruption of promoter activity.

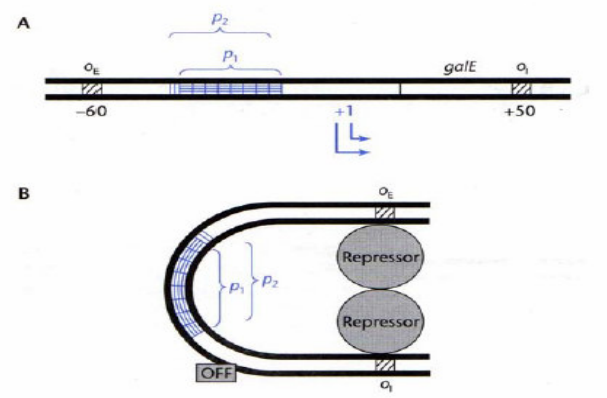

Figure 5.4. Regulatory model for *gal* operon in *Escherichia coli* (Snyder, 1997)

In the presence of galactose, the repressor is not bound to the operators, and the operon is on. In the absence of galactose, a dimer repressor molecule binds simultaneously to both operators, bending the DNA and preventing binding of the RNA polymerase to the promoter region, and the operon is off (Snyder, 1997).

5.4. Gut Operon in *Escherichia coli*

The enzymes and proteins responsible for glucitol (sorbitol) catabolism are coded within the gut operon in *E. coli*. Expression of the glucitol (gut) operon is regulated by an unusual, complex system which consists of an activator (encoded by the gutM gene) and a repressor (encoded by the gutR gene) in addition to the cAMP-CRP complex (CRP, cAMP receptor protein). The GutM protein encoded by gutM gene, is a positive DNA-binding transcriptional regulator for glucitol utilization. GutR protein is required for the repression of the expression of the srlAEBD-gutM-srlR-gutQ genes. The gut operon consists of at least five structural genes and has the following gene order: gutOPABDMR (Yamada, 1988).

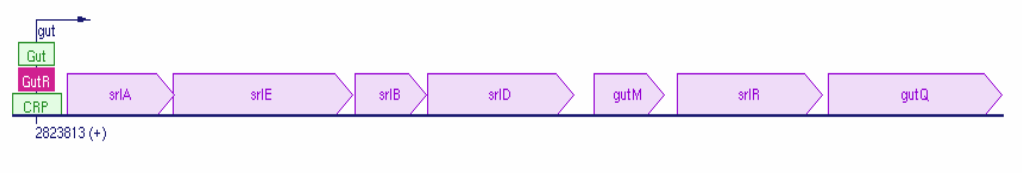

Figure 5.5. *Gut* operon gene expression sequence in *Escherichia coli* (biocyc.org)

Synthesis of the mRNA, which initiates at the promoter specific to the gutR gene, occurs within the gutM gene. Expressional control of the gut operon appears to occur as a consequence of the antagonistic action of the products of the spontaneously regulated gutM and gutR genes (Yamada, 1988).

There are two open frames downstream from gutD, which are termed gutM and gutR. The physiological function of the GutM protein is activation of gut operon transcription. It unusually invokes participation of both a glucitol-specific repressor and a glucitol-specfic activator in addition to the general activator, the cAMP-CRP complex. On the other hand, the physiological function of *gutR* gene product is to bind the inducer presumed to be glucitol (Lengeler & Steinberger, 1978). Each of the two regulatory proteins exhibits an effect on gut operon expression in the absence of others, but normal regulation depends upon the structural integrity of both. The cAMP-CRP complex is indispensable for the expression of the operon and functions independently of the GutM and GutR protein (Yamada, 1988).

5.5. Glycerol Transport System (GlpK) in *Escherichia coli*

Unlike other carbonhydrates, glycerol enters the cytoplasm by facilitated diffusion across the cytoplasmic membrane. The facilitator protein provides a selective channel. Internal glycerol is trapped as G3P by the action of an ATP-dependent kinase (GlpK) that can also phosphorylate dihydroxyacetone.

$$Glycerol + ATP \xrightarrow[glpK]{} G3P$$

As a catabolic enzyme, the kinase has the unusual feature of being subject to noncompetitive allosteric inhibition by fructose 1,6-biphosphate and the nonphosphorylated

form of enzyme III^{Glc}, a feature which would account for the extreme effectiveness of glucose utilization in preventing glycerol consumption (Neidhardt, 1996).

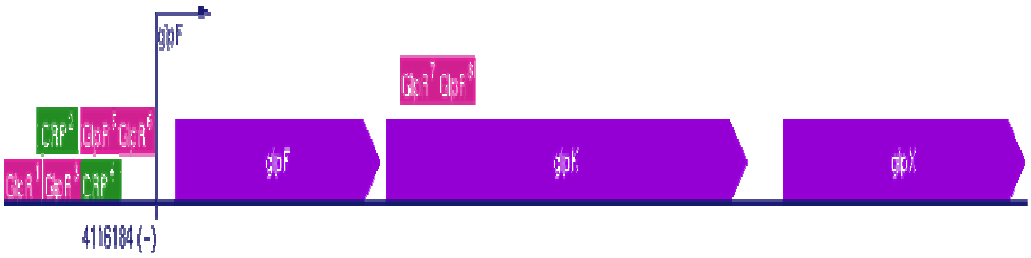

Figure 5.6. Transcriptional unit glpKF in *Escherichia coli* (biocyc.org)

In wild-type cells, both glycerol and G3P induce the *glp* regulon, but in mutants lacking glycerol kinase only G3P has this effect. The expression of the *glpKF* operon itself is also induced by G3P, rather than by glycerol, was demonstrated with a mutant that produces a glycerol kinase protein without catalytic activity. Thus, G3P seems to be the true inducer of the entire *glp* operon.

5.6. Glucose, Lactose, Galactose Transport System in *Lactococcus lactis*

Lactic acid bacteria and particularly *Lactococcus lactis* are widely used for the production of lactic acid in fermented foods as a starter in milk fermentation and cheese manufacture. Control of the catabolic rate in *L. lactis* is determinant for dairy product quality. Also, it remains unclear whether the catabolic rate is controlled at the level of transcription, translation or enzyme activity. However, low genetic information and metabolic studies concerning anaerobic sugar catabolism in *L. lactis* give clues on growth rate and lactic acid production.

Most sugars are taken up either by the phosphoenolpyruvate (PEP)-dependent phosphotransferase systems (PTS) or by permease systems in *L. lactis*. PTS involves coupled transport and phosphorylation of the sugar. In permease transport, sugar transport is followed by kinase-mediated phosphorylation of the free sugar within the cytosol (Yamada, 1987).

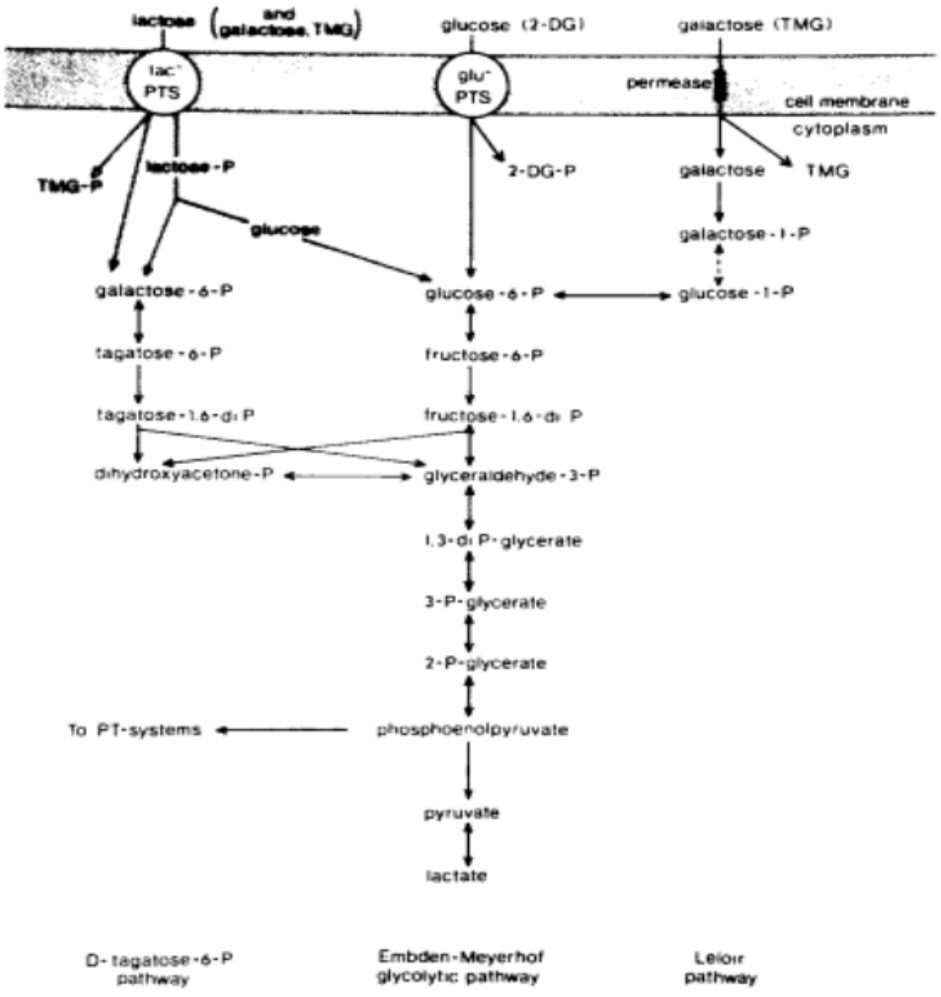

Figure 5.7. Major pathway for the transport and metabolism of sugars in galactose grown cells in *Streptococcus lactis* (Thompson, 1978)

In a medium containing a mixture of glucose, galactose, and lactose, the growth of *Lactococcus lactis (Streptococcus lactis)* is initially on the simultaneous metabolism of glucose and lactose. Galactose has been utilized only after the latter sugars have been exhausted from the medium (Thompson, 1978). Therefore, there is an inhibition of galactose utilization when glucose or lactose is added to medium. As shown in Figure 5.7, glucose and lactose are simultaneously taken up through the cell membrane on coupled PTS system, whereas galactose is transported via permease system. Lactose-P is broken down to glucose and galactose-P and the latter enters the EMP pathway by the D-tagatose 6-P pathway.

5.7. Galactose (Gal) Operon in *Lactococcus lactis*

Lactococcus lactis is a low GC gram-positive bacterium. The carbon catabolite repression of *L. lactis* is different than *E. coli* and other gram-negative bacteria. Catabolite Repression (CR) is mediated by a negative regulatory mechanism with a catabolite control protein CcpA (Hueck & Hillen, 1995). Catabolite-responsive element (*cre*) is present near the promoter of genes which is affected by CR. Increase/decrease in the CcpA protein will result in the same way with *cre*.

The binding of CcpA to *cre* sites is reported to be enhanced by elevated concentrations of early glycolytic intermediates such as glucose 6-P. Another signal involved in the activation of ccpA is the PTS phosphate carrier HPr. A metabolite activated kinase has been shown to phosphorylate HPr on residue series 46. This phosphorylated form of HPr interacts with CcpA which enhances the binding of CcpA to *cre* sites (Luecsink, 1998)

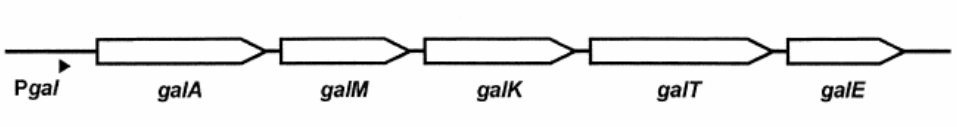

Figure 5.8. Schematic representation of the *Lactococcus lactis* gal operon (Kuipers, 1998)

The gal operon shown in Figure 5.8 consists of 5 genes with the order *galAMKTE* and encodes the promoter necessary for the uptake and conversion of galactose to glucose 1-P via the Leloir pathway. The presence of a putative *cre* site in the promoter region of the *L. lactis* gal genes suggested a possible involvement of CcpA in the regulation of the expression of these genes. No gal transcription could be detected in a wild-type strain grown on glucose, but when the cells were grown on galactose the transcription is increased. This observation could be attributed to negative regulation by CcpA promotion of the *gal* genes. The repression may result from either prevention of transcription initiation, a transcriptional block or interference with interaction between RNA polymerase and an activation (Stülke *et al.,* 1999).

6. COMPUTATIONAL STRATEGY FOR REGULATORY FBA

Regulation of gene transcription with constraints-based models of *prokaryotic* metabolism is under investigation in order to understand and predict the cellular behavior. Our goal is to develop a modeling and simulation approach that uses current advances in the knowledge of regulatory structures and genetic consequences. The computational algorithm performed in MatLab contains two separate, but constantly interacting modules: a regulatory module and a metabolic network module. The regulatory module uses fuzzy logic to quantify transcriptional regulation and enzyme activity. The latter uses dynamical flux balance analysis to determine metabolic transients in response to regulatory signals. The modeling framework is applied to carbon-source utilization, aerobic/anaerobic diauxic shifts in bacteria; *Escherichia coli* and *Lactococcus lactis*.

The utilization of carbon sources in *E. coli* and in any other bacteria are described by central metabolism pathways. Substrate uptake mechanism through the cell membrane may be different in many organisms. Also, the way to utilize multiple carbon source mixtures can be different; namely, sequential or simultaneous. The sequence of utilization of some substrates is regulated by a series of genes called operons.

The most studied operon in *E. coli, lac* operon, contains genes whose transcription is regulated by a repressor protein and by catabolic repression from glucose. Gene expression of enzymes necessary for lactose utilization is dependent on the concentrations of the regulatory substances. The activation or repression of these genes depends on the level of corresponding molecules in the cell. Rather than using a flux to be turned “on” or “off”, a gradual shift from totally turned on system to totally turned off one (or vice versa) is crucial to determine internal concentrations on the activation or repression of the operon. Therefore, knowing the mechanism of operon is not enough to construct the interaction between extracellular metabolite and regulatory protein or enzyme. The concentration profiles of each coming from experimental data or mathematical model plays important role (Wong, 1997; Kremling, 2001).

Fuzzy logic considers the level of high and low between two end points, so there will be smooth shift from glucose utilization to lactose.

Two separate, but constantly interacting modules are written in matlab/simulink: a regulatory module and a dynamic metabolic network module. Fuzzy Logic Controller network in Matlab/Simulink was used for various operon regulatory structures co-operating with membrane transport system. Dynamical structure of metabolic network module is constructed by Flux Balance Analysis of metabolites in Matlab. In every iteration of the FBA, the program developed calls for the regulatory module in Simulink to simulate the uptake rate of the corresponding substrate.

6.1. Model Formulation of Flux Balancing

Basic metabolic pathways of *E. coli* are used for the model formulation of flux balancing to generate maximal time courses of growth for the two model bacteria, *E. coli* and *L. lactis.* The basic pathways of catabolism in *E. coli* are shown in Figure 6.2 and a list of reaction list is provided in Appendix C. These pathways consist of glycolysis, pentose phosphate pathway, TCA cycle, electron transport system, and reactions that interconnect these. Especially, *E. coli* is chosen for the model because its physiological and biochemical structure has been well known for a long time. *E. coli* is a gram-negative bacteria. It is a prokaryote belonging to the family Enterobacteria.

Substrate uptake and by-product secretion uptake rates, the initial concentrations of carbon sources and oxygen amount in the media must be all set to a value in order to simulate flux balancing. Then, the simulation is run until the carbon sources have been completely exhausted. Glucose, lactose, galactose, glycerol, sorbitol are the main carbon sources that are involved in the catabolism of *E. coli* or *L. lactis*. In order to simulate, some data provided in the literature, initial concentrations of biomass, glucose and lactose as well as uptake rate constraints for the growth on glucose and lactose are the same as the parameters used by Covert *et al.*

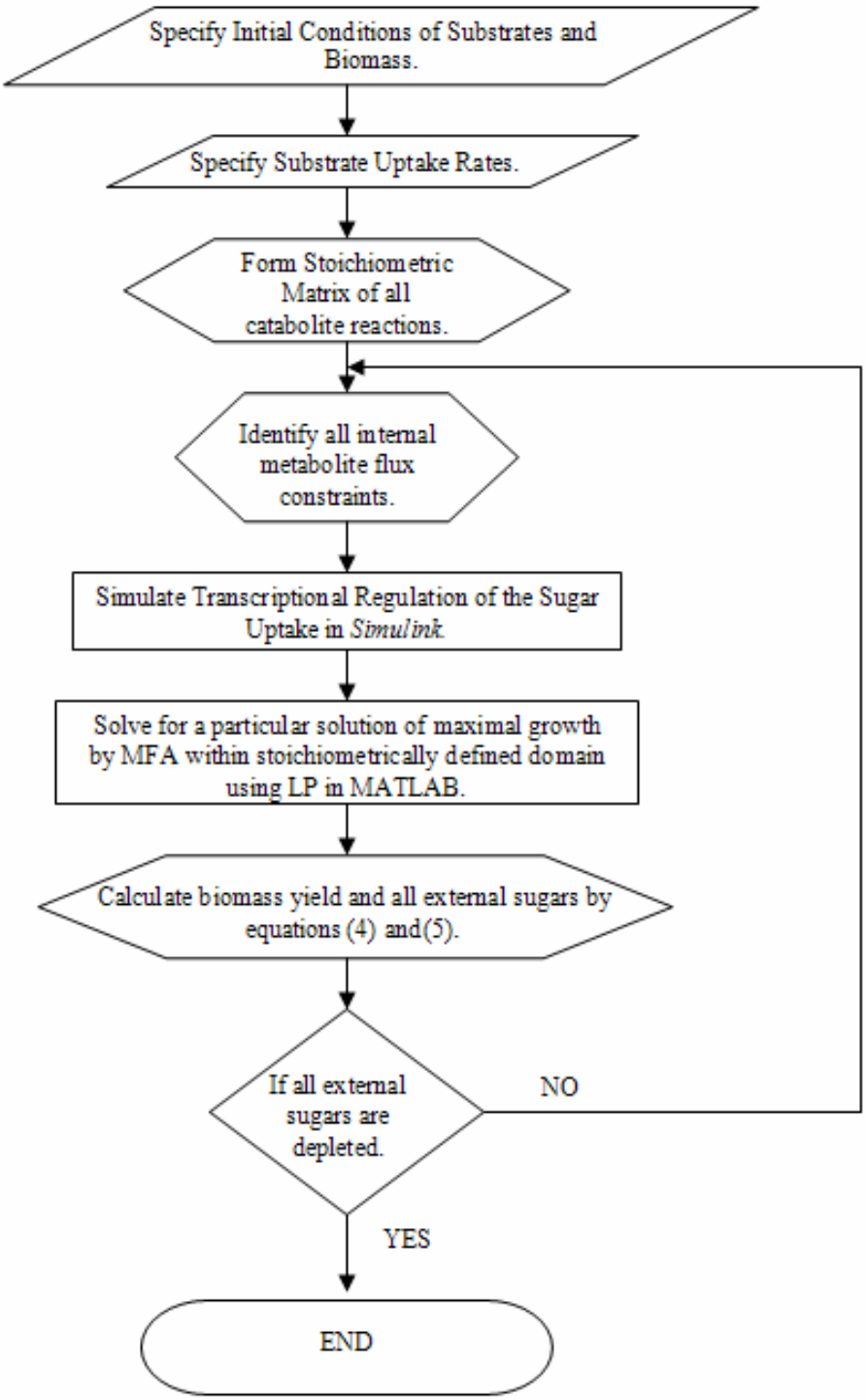

Figure 6.1. Computational Flow Diagram

The computational flow diagram as shown in Figure 6.1, gives the strategy to solve optimal time growth of a bacterium including transcriptional regulation. The regulatory module always interacts with metabolic network for the flux distributions in all iterations. By looking at the uptake rates of the substrate(s) the logical controlling mechanism permits the uptake of the others. The biomass yield and substrate concentrations are modeled for the exponential phase of growth at constant substrate uptake rates given in chapter 2. The stationary phase is not considered.

The metabolic network system of *E. coli* having 113 reactions is used as a model. As shown in Figure 6.2, the map for *E. coli* includes the basic pathways for the utilization of external substrates. A maintenance requirement for ATP per substrate is included. The substrate is processed by the glycolytic pentose phosphate pathway and the TCA cycle and for aerobic cultures the electron transport system. There are multiple arrows on the map that show fluxes from one metabolite to another. Each reaction is catalyzed by different enzymes that are synthesized from their respective genes.

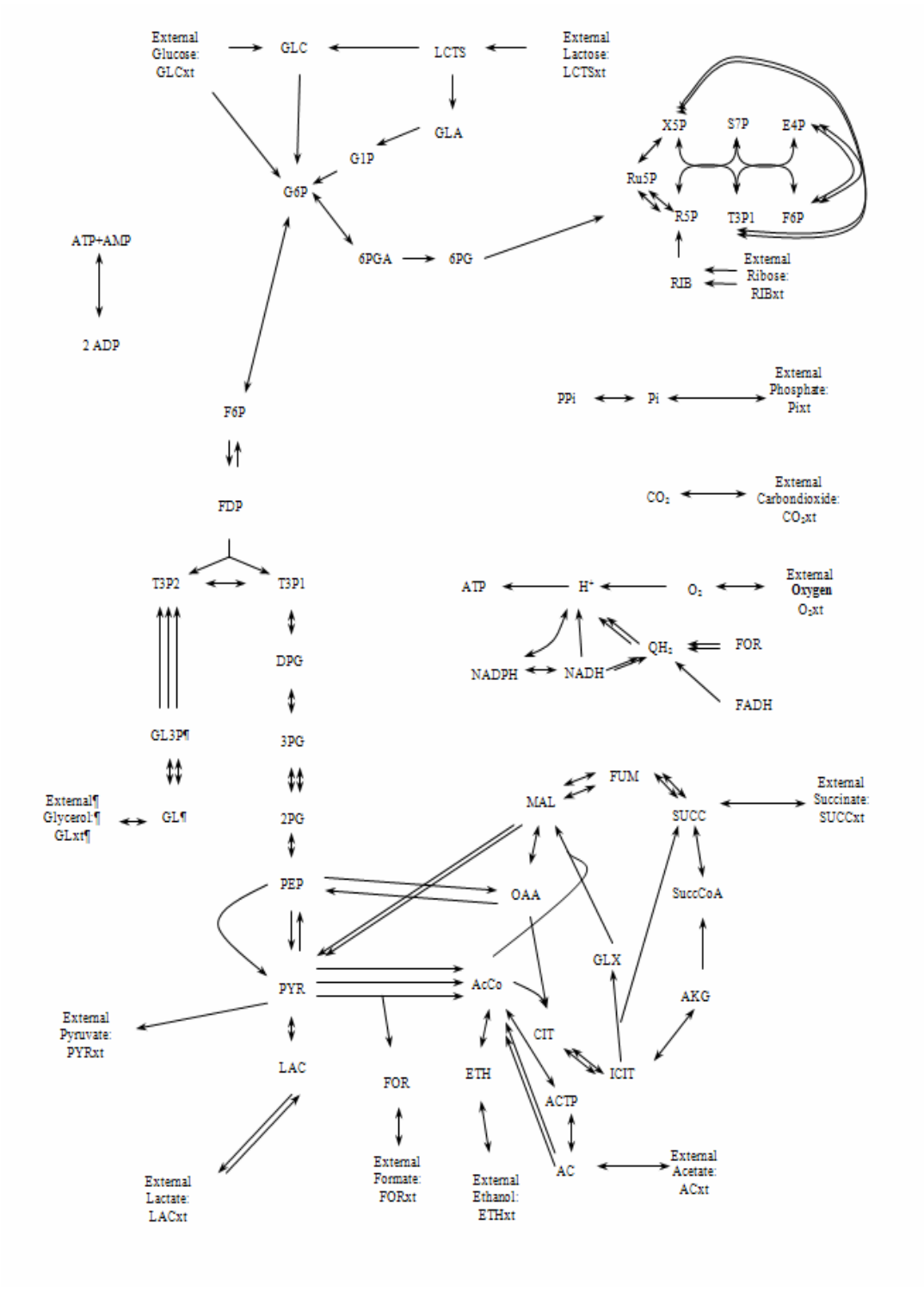

Figure 6.2. Model metabolic network map for *Escherichia coli*

As the first example, diauxic growth on glucose and lactose is investigated. As discussed in Chapter 5, the bacterium takes them sequentially. Lactose is only utilized in a very small proportion (less than 5% of that in the absence of glucose) as glucose is present in the medium. With a constant uptake rate of substrates, biomass concentration, glucose and lactose concentrations, O_2 uptake rate by the bacteria are computed from dynamic FBA while, cAMP level in the cell which is dependent on the glucose concentration, from the fuzzy logic module.

Table 6.1 shows the initial conditions and uptake rate constraints used for the diauxic growth on glucose and lactose in *E. coli.* These are just the estimated values and are taken from the previous works (Covert *et al.,* 2002).

Table 6.1. Initial conditions used and uptake rate constraints for the growth in glucose and lactose only

Initial Conditions	
Biomass (g/L)	0.011
Glucose (mmol/L)	1.6
Lactose (mmol/L)	5.8
Uptake Rate Constraints	
Glucose (mmol/(gDW hr))	6.5
Lactose (mmol/(gDW hr))	3
Oxygen (mmol/(gDW hr))	15

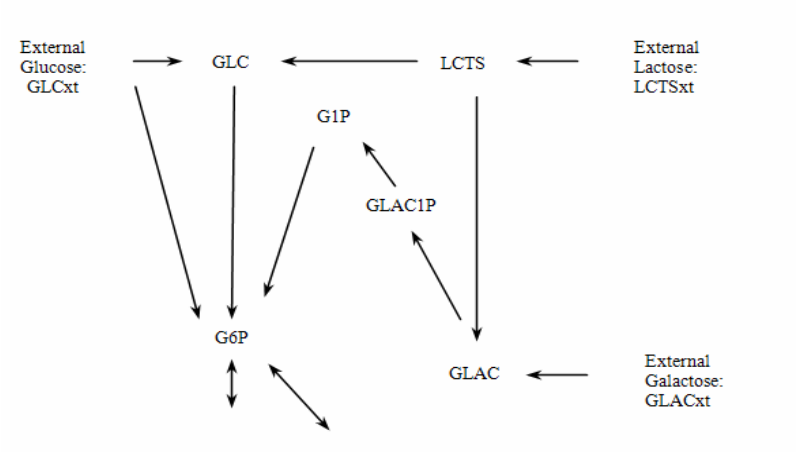

Figure 6.3. Uptake map of external glucose, lactose, and galactose in *Escherichia coli*

Based on the glucose-lactose diauxic growth, different scenarios are imposed on the growth condition in order to examine the operon working principles. Pulse injections of glucose only, or galactose only, and a mixture of glucose and galactose while lactose is the dominant substrate on the growth, are studied. Figure 6.3 shows the pathways before glycolysis for the uptake of glucose, lactose and galactose in *E. coli.* The reactions are given in Appendix C. The *lac operon* and *gal operon* in *E. coli* as discussed in Chapter 5 are tested and the Simulink structures are explained below.

The pulse injection of glucose will show how the concentration of CAP-cAMP complex will change and how the uptake rate of lactose to the cell will be effected because the presence of this complex is closely associated with the presence of glucose in the cell. When the concentration of glucose increases in the medium, the amount of cAMP will decrease. However, there will be molecules of the enzyme β-galactosidase and β-galactoside permease in the cell which are responsible for the catabolism and transport of the lactose. Therefore, lactose transport is expected to be in small amount during the utilization of injected glucose. The same initial concentrations of the biomass, glucose, and lactose will be used and 2.50 mmol/L glucose will be injected to the medium of the batch culture.

Galactose injection is expected to show how the *gal* operon in *E. coli* will work. Because the injection is held while lactose is being utilized by the bacterium, galactose will be present in the cell. Galactose is a self inducer that binds to the repressor molecule. Therefore, lactose and galactose all together will be taken up and utilized simultaneously. However, the situation will be different when a mixture of glucose and galactose are injected. 2.50 mmol/L glucose and 8.5 mmol/L galactose will be given to the medium of the batch culture immediately. Again, the amount of cAMP will decrease as glucose concentration of the medium increases. This means that, CAP-cAMP complex will not transcribe the corresponding promoter region to activate the *gal* operon. Table 6.2 shows the initial conditions and uptake rates used in the pulse simulations.

Table 6.2. Initial conditions and uptake rate constraints used for the growth in glucose, lactose, and galactose pulse

Initial Conditions	
Biomass (g/L)	0.011
Glucose (mmol/L)	1.6
Lactose (mmol/L)	5.8
Galactose (mmol/L)	0
Uptake Constraint Rates	
Glucose (mmol/(gDW hr))	6.5
Lactose (mmol/(gDW hr))	3
Galactose (mmol/(gDW hr))	6.5
Oxygen (mmol/(gDW hr))	15

In addition to the glucose, lactose and galactose pairs, growth on glucose, glucitol (sorbitol) and glycerol in *E. coli* will be investigated. *Gut* operon discussed in Chapter 4 is the crucial mechanism that controls the uptake of the sugar metabolisms of glucose and glucitol. Similar to growth on glucose and lactose, glucose has a repressive effect on the uptake of glucitol. Glucose and glucitol are taken up by both PTS system in the cell membrane. Like growth on glucose and lactose, the cAMP-CRP complex is the significant catabolite repressor in an unknown manner besides GutM protein in *E. coli.* Actually, both are consumed, but the rate of glucitol consumption is less in the presence of glucose than in the absence of it. On the other hand, the third component, glycerol, is transported directly through the cell membrane. But, there are inhibitory effects of non-phosphorylated form of EIIA belonging to both glucose and glucitol on the formation of Glycerol 3-Phosphate (G3P). G3P is formed from glycerol catalyzed by glpK kinase. Therefore, glucose and glucitol have both repressive effects on glycerol metabolism in *E. coli.*

In Figure 6.4, the uptake map of glucose, sorbitol and glycerol is given. Glucose and sorbitol are directly converted to 6-Phosphate forms, whereas glycerol is taken up by normal diffusion. Table 6.3 gives the initial conditionsy the PTS mechanism and uptake rate constraints for the growth on glucose, glucitol, and glycerol. These parameters are just the estimates which give satisfactory results with respect to experimental data (Kompala and Ramkrishna, 1984).

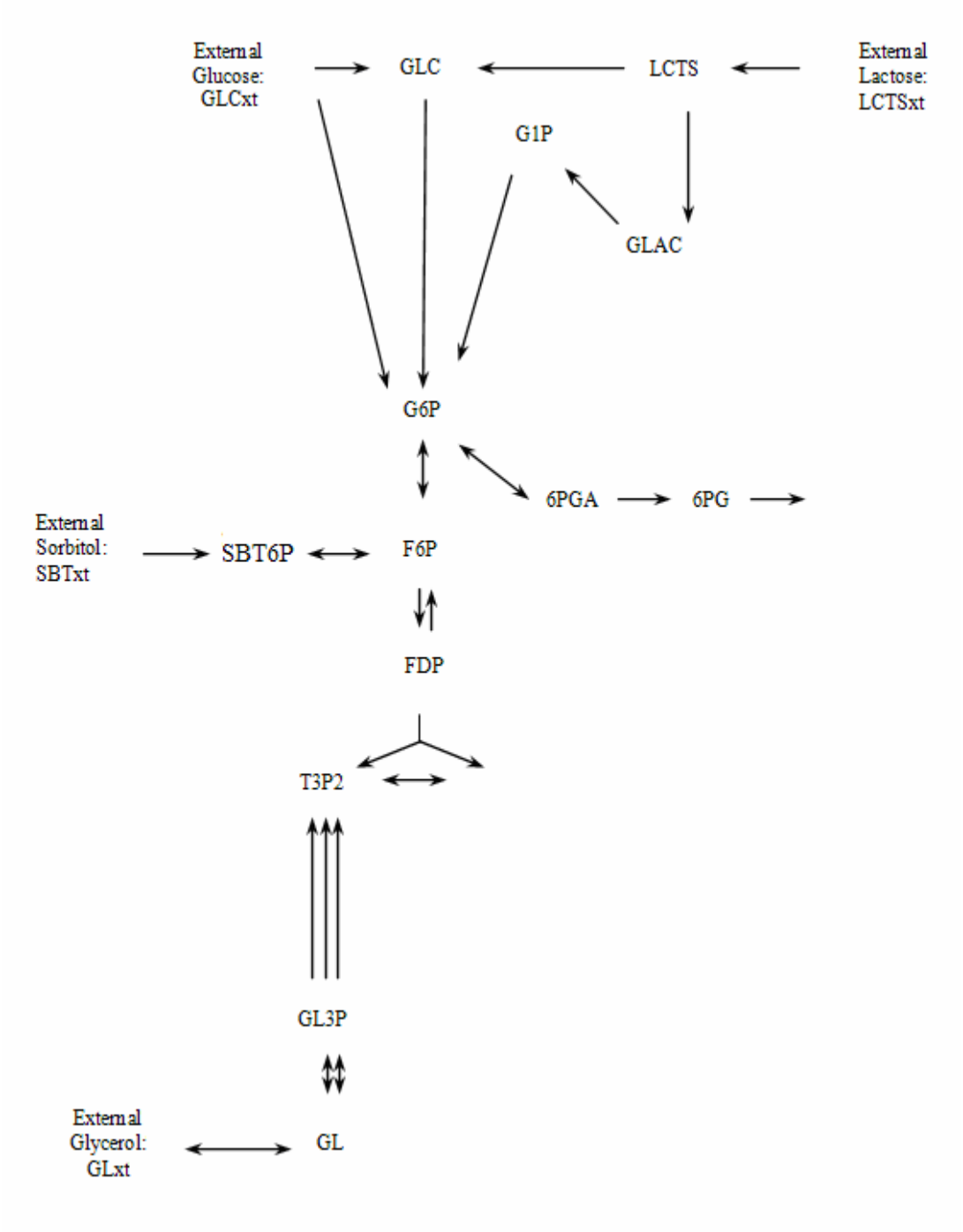

Figure 6.4. Uptake map of external glucose, sorbitol and glycerol in *Escherichia coli*

Table 6.3. Initial conditions and uptake rate constraints used for the growth in glucose, glucitol and glycerol

Initial Conditions	
Biomass (g/L)	0.008
Glucose (mmol/L)	1.2
Glucitol/Sorbitol (mmol/L)	1.1
Glycerol (mmol/L)	1.1
Uptake Rate Constraints	
Glucose (mmol/(gDW hr))	8.5
Glucitol/Sorbitol (mmol/(gDW hr))	4.5
Glycerol (mmol/gDW hr)	4.0
Oxygen (mmol/(gDW hr))	15

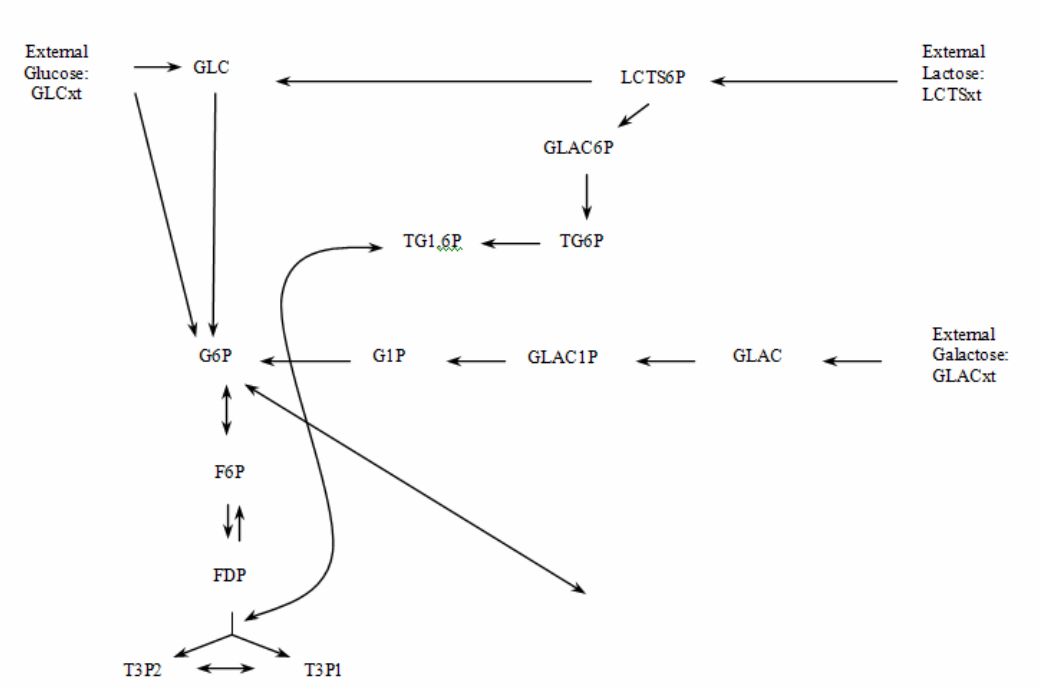

Figure 6.5. Uptake map of external glucose, lactose, and galactose in *Lactoccoccus lactis* including Tagatose 6-P and Leloir pathways

In addition to *E. coli* metabolic network, Tagatose 6-P pathway of lactose transport and Leloir pathway of galactose transport through the cell membrane are used to form the metabolic network of *L. lactis.*

L. lactis is a gram-positive bacteria and catabolic repression is mediated by a negative regulatory mechanism (Heuck and Hillen, 1995). *Gal* operon discussed in Chapter 5 in *L. lactis* is investigated to realize the repression of galactose by glucose and lactose. A mixture of glucose, lactose and galactose is assumed to be in the medium for the simulation. Initially, a simultaneous catabolism of glucose and lactose sugars is expected. Galactose utilization will start when glucose and lactose are depleted. Glucose and lactose are simultaneously taken up through the cell membrane on coupled PTS system, whereas galactose is transported via permease system. Gal operon controls the production of permease system which is a key factor of galactose uptake in the membrane. The metabolic pathway for the utilization of glucose, lactose and galactose in *L. lactis* is shown in Figure 6.5.

6.2. Model Formulation of Fuzzy Inference System and Fuzzy Contoller

A logic based on the two truth values *True* and *False* is sometimes inadequate when describing human reasoning. Fuzzy logic uses the whole interval between 0 (*False*) and 1 (*True*) to describe human reasoning. As a result, fuzzy logic is being applied in rule based automatic controllers.

In order to construct the fuzzy system, Matlab® *Fuzzy Toolbox* is used. *Toolbox* can easily make fuzzification interface, fuzzy inference, knowledge base (result), and defuzzification interface. *Toolbox* consists of two useful tools: FIS editor and Fuzzy Controller. FIS editor in combination with four other editors provides a powerful environment to define and modify Fuzzy Inference System (FIS) variable whereas, Fuzzy Controller is a block in Fuzzy Toolbox Library in Simulink environment. This admits FIS variable produced by FIS Editor and implements the desirable rules.

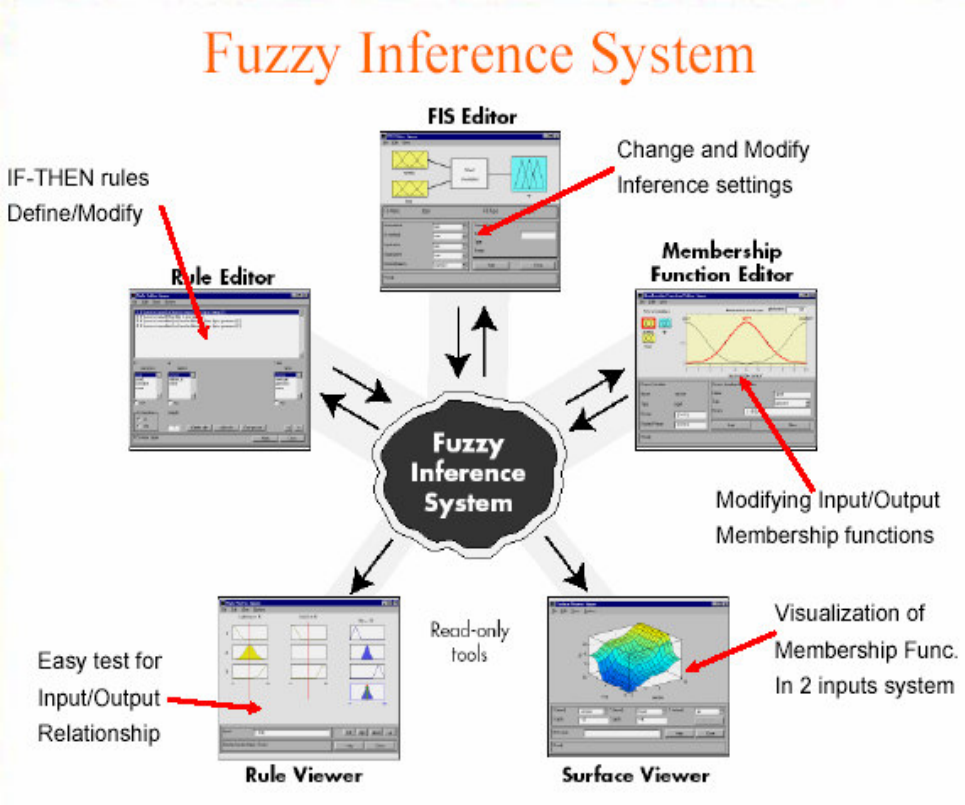

Figure 6.6. Fuzzy Inference System (FIS) in MATLAB fuzzy toolbox

MATLAB® *Simulink* can build the system that use fuzzy logic. By combining Fuzzy Logic Controller blocks, a controlling action is structured. The structure variable describing its Fuzzy Inference System must be entered to a Fuzzy Controller block and the variable must be located in the MATLAB workspace.

Modeling the *lac* operon is conceptualized in two parts, an inducible operon and catabolite repression. Therefore, simulink fuzzy control system of the *lac* operon in *Escherichia coli* is divided into two parts; one will implement the inducible part and the other will implement the catabolite repression due to glucose. In the inducible operon (part 1), the expression of the genes will increase by the presence of the inducer which is allolactose in *lac* operon. The main property of allolactose is to bind the repressor molecule attached on the way of transcription and to maintain mRNA translation on the DNA sequence. LacY, LacZ and LacA proteins are produced as a result and lactose can be taken up by the action of LacY permease.

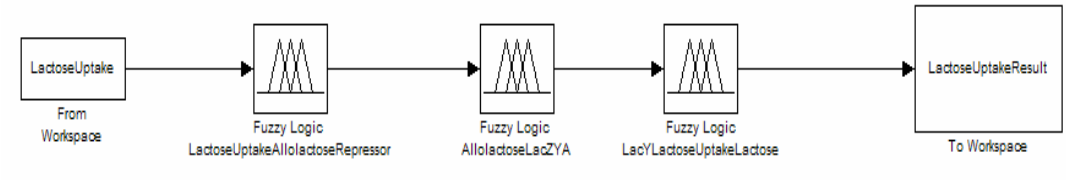

Figure 6.7. Simulink fuzzy controller system of *lac* operon in *Escherichia coli* (part 1)

Figure 6.7 and Table 6.4 give clues as to how the fuzzy controller system works. Lactose uptake rate value is taken from the workspace (MATLAB) which is fuzzified in the "LactoseUptakeAllolactoseRepressor" controller. Then, the rate is quantified with the values very low, low, medium, etc. The decision on the result between lactose uptake and allolactose repressor concentration in normalized form is judged based on the fuzzy rule bases stated in Table 6.4. The table can be read simply as , "If Lactose Uptake is *Very Low*, THEN Normalized form of Allolactose + Repressor Product is *Low*". A numerical result is taken from the controller after the defuzzification of a fuzzy result has been held. The same procedure is applied to other two controller to have a new numerical result of Lactose Uptake rate used for the calculations at the end.

Table 6.4. Fuzzy rule base configuration for *lac* operon in *Escherichia coli* (part 1)

IF	**VL**	**L**	**ME**	**H**	**VH**
	Allolactose + Repressor Product (Normalized)				
Lactose Uptake	L	L	L	H	H
	LacY, LacZ, LacY Production (Normalized)				
Allolactose	L	ME	ME	H	VH
	Lactose Uptake				
LacY Production	VL	VL	L	ME	H

Catabolite repression is the second part, glucose is the preferred energy substrate to lactose in *E. coli*. The cell will use glucose in preference to lactose, when both are present. Catabolite activator protein (CAP) is involved in the control of transcription of *lac* operon.

CAP must bind to cAMP molecule to promote the transcription in addition to inducible part. However, the concentratrion of cAMP is dependent on the glucose transport rate to the cell. When it is high, cAMP level will be low (or vice versa). The cAMP-CAP complex exerts a **positive control** over the expression of the *lac* operon. When this region of the promoter is bound, RNA polymerase has a greater ability to bind and produce transcripts. Again, LacY, LacZ and LacA proteins will be produced as a result. In these two parts, the lactose uptake rate through the cell will be much higher in catabolite repression part than the inducible part.

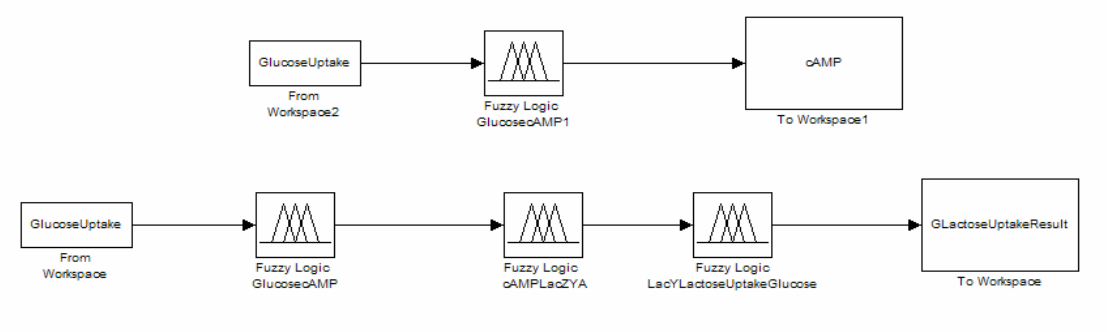

Figure 6.8. Simulink fuzzy controller system of *lac* operon in *Escherichia coli* (part 2)

Table 6.5 is the summary of fuzzy rule configurations used for Figure 6.8. Glucose repression is the second part of *lac* operon. Glucose uptake rate value is taken from the workspace and fuzzified in order to calculate normalized cAMP value. The first line of Table 6.5 can be read as such; If the glucose uptake is very low, the normalized cAMP will be very high or if the glucose uptake is low, the normalized cAMP will be high. In all time steps, cAMP concentration is collected to form a time profile which gives indication of the shift from glucose utilization to lactose utilization. The controllers for the calculation of cAMP concentration, Permease (LacY) concentration and lactose uptake rate are combined in sequence to determine lactose uptake through the cell membrane due to glucose repression.

Table 6.5. Fuzzy rule base configuration for *lac* operon in *Escherichia coli* (part 2)

IF	VL	L	ME	H	VH
	Normalized cAMP				
Glucose Uptake	VH	H	ME	L	VL
	LacY, LacZ, LacY Production (Normalized)				
Normalized cAMP	VL	VL	L	ME	H
	Lactose Uptake				
LacY Production	VL	L	ME	ME	H

The rule viewer of fuzzy inference system shown in Figure 6.9 for the calculation of normalized cAMP gives the details of input (Normalized Glucose Uptake Rate) and output (Normalized cAMP) relation. The scaling method is used to scale down the resulting membership functions. All result coming from each rules are combined to produce an inferred conclusion. The center of area (COA) is taken as a numerical result of all combined conclusions.

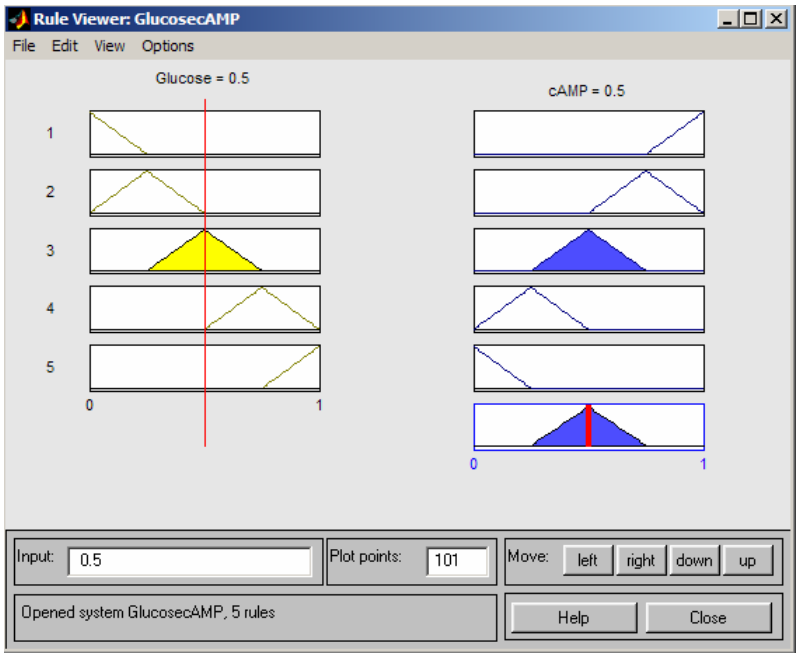

Figure 6.9. FIS rule viewer of glucose uptake to cAMP

In addition to the catabolite repression (part2), membrane transport phosphorylation is added in order to compare the results with part 2 shown in Figure 6.10. The phosphorylated form of glucose-specific EIIA of the PTS is important for cAMP production which affects the transcription in the same manner. Normally, EIIA-P results in both cAMP production and LacY repression. The signal of EIIA-P is connected with dashed line to the fuzzy controller of LacY because the pathway is not considered in this work.

The rules for the calculation of EIIA-P concentration (normalized), cAMP concentration (normalized), Permease (LacY) concentration (normalized) and lactose uptake rate are combined in sequence in Table 6.6 to determine lactose uptake through the cell membrane due to glucose repression.

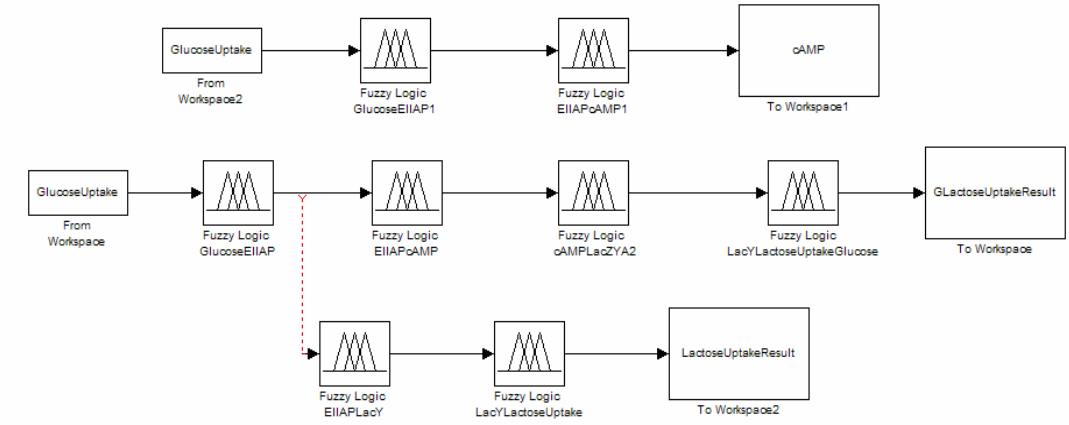

Figure 6.10. Simulink fuzzy controller system of *lac* operon in *Escherichia coli* (membrane transport phosphorylation is added)

Table 6.6. Fuzzy rule base configuration for *lac* operon in *Escherichia coli* (membrane transport phosphorylation is added)

IF	**VL**	**L**	**ME**	**H**	**VH**
	Normalized EIIA-P				
Glucose Uptake	VH	H	ME	L	VL
	Normalized cAMP				
EIIA-P	VL	L	H	H	VH
	LacY, LacZ, LacY Production (Normalized)				
Normalized cAMP	VL	L	ME	H	H
	Lactose Uptake				
LacY Production	VL	L	ME	ME	H

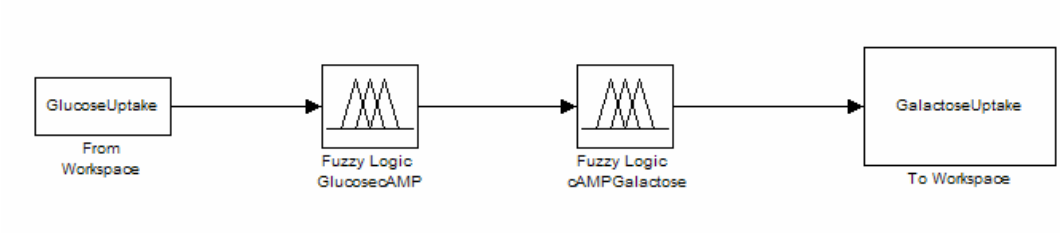

Figure 6.11. Simulink fuzzy controller system for *gal* operon in *E. coli*

The *gal* operon in *E. coli* has three important parts; promoter, operator and repressor parts as usual. The CAP protein with cyclic AMP activates the promoter of the *gal* operon. Because free cAMP is abundant in the absence of glucose, galactose uptake and glucose uptake are inversely related. As glucose concentration diminishes, galactose uptake level will increase with the activation of *gal* operon promoter site. The inducer of gal repressor is the galactose itself. The function of the other parts of the genome of the *gal* operon are not clear, hence only the promoter site is included in the modeling of Simulink fuzzy controller.

The rules that combine glucose uptake to normalized cAMP and finally to galactose uptake is given in the Table 6.7.

Table 6.7. Fuzzy rule base configuration for *gal* operon in *Escherichia coli*

IF	VL	L	ME	H	VH
	Normalized cAMP				
Glucose Uptake	VH	H	ME	L	VL
	Galactose Uptake (Normalized)				
Normalized cAMP	VL	L	ME	H	VH

Glucitol (gut) Operon is controlled by both positive and negative regulation. Expression of the glucitol (gut) operon is regulated by a complex system which consists of an activator (encoded by the gutM gene) and a repressor (encoded by the gutR gene) in addition to the cAMP-CRP complex (CRP, cAMP receptor protein). In simulink fuzzy controller system, CRP (cAMP receptor) is modeled as shown in Figure 6.12 for the repression of glucitol/sorbitol. The repression effect of GutR is lower than cAMP-CRP. Therefore, the main effect is controlled by cAMP-CRP. The physiological function of the GutM protein is activation of gut operon transcription. The physiological function of gutR gene product is to bind the inducer presumably to be glucitol. Normal regulation depends upon the structural integrity of both.

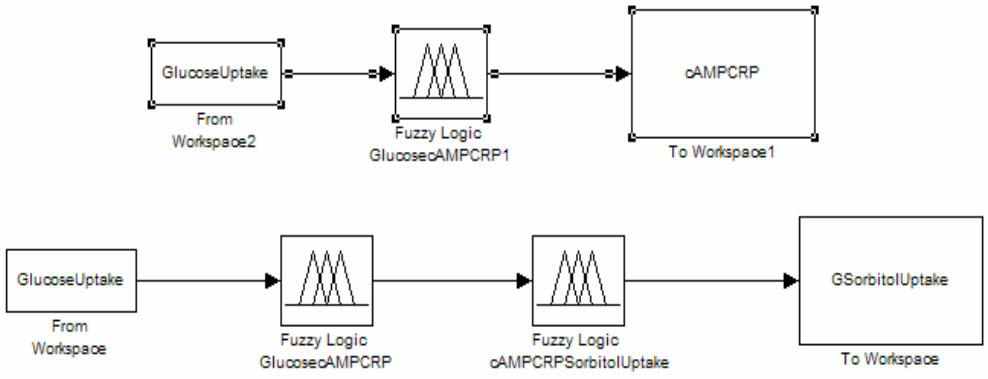

Figure 6.12. Simulink fuzzy controller system for *glucitol/sorbitol* operon in *Escherichia coli*

The rules that combine glucose uptake to normalized cAMP-CRP complex and finally to sorbitol uptake is given in the Table 6.8. As an example, first line of Table 6.8 can be read as such; If the normalized cAMP-CRP complex is very low, Sorbitol Uptake will be very low or if the normalized cAMP-CRP complex is low, Sorbitol Uptake will be very low.

Table 6.8. Fuzzy rule base configuration for *gut* operon in *Escherichia coli*

IF	**VL**	**L**	**ME**	**H**	**VH**
	Normalized cAMPCRP				
Glucose Uptake	VH	H	ME	L	VL
	Sorbitol Uptake (Normalized)				
Normalized cAMPCRP	VL	VL	L	ME	H

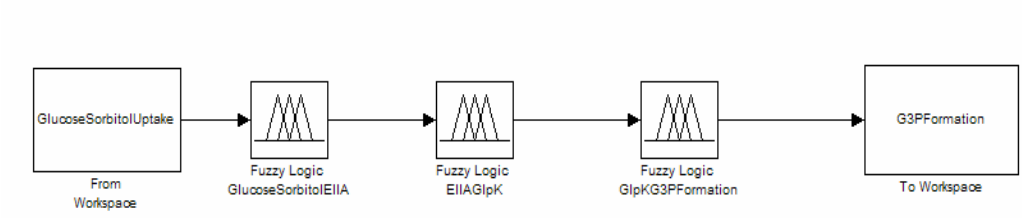

Figure 6.13. Simulink fuzzy controller system for *glpK* regulon in *Escherichia coli*

In wild-type cells, EIIA is for the inhibition of glycerol kinase (GlpK). EIIA is synthesized in the presence of glucose and sorbitol and GlpK protein is responsible for the phosphorlylation of glycerol by ATP. When the glycerol 3-phosphate is formed, the succeeding fluxes become active for the catabolism of glycerol. Thus, G3P is the true inducer of the entire *glp* operon. EIIA is high when both glucose and sorbitol are present. On the other hand, GlpK is low when EIIA is high because of its inhibitory effect. In Figure 6.13, simulink fuzzy controller is modeled as it is explained by the preceding relations. The fuzzy rule base configuration for the *glp* regulon in *E. coli* is cited in Table 6.9.

Table 6.9. Fuzzy rule base configuration for *glp* regulon in *Escherichia coli*

IF	VL	L	ME	H	VH
	Normalized EIIA				
Glucose/ Sorbitol Uptake	VL	L	ME	H	VH
	GlpK (Normalized)				
Normalized EIIA	VH	H	ME	L	VL
	G3P Formation (Normalized)				
Normalized GlpK	VL	L	ME	H	VH

Unlike in *E. coli*, glucose and lactose can be consumed simultaneously in *Lactococcus lactis*. The transport phenomena of both belong to the phosphotransferase system (PTS). However, galactose is transported by the permease system. Therefore, there is an operon system that controls the utilization and even transport through the cell membrane. CcpA protein and Galactokinase (GalK) are the key enzymes that play role in the Leloir pathway. CcpA protein is involved in the negative regulation, the level of CcpA will be low on glucose growth and will increase as glucose level decreases and galactose increases.

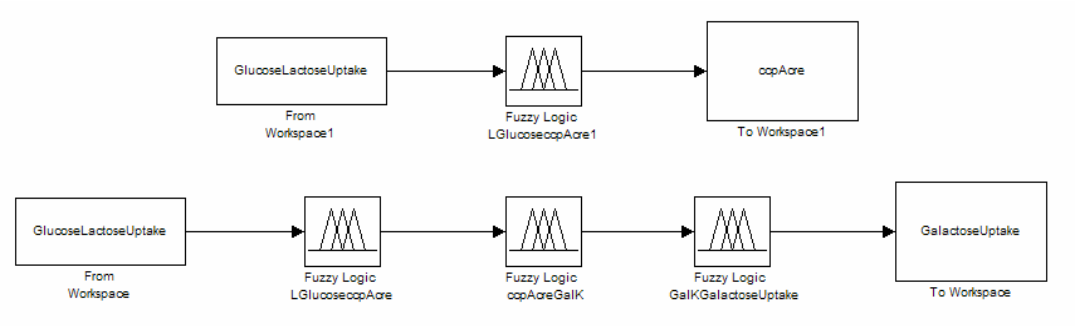

Figure 6.14. Simulink fuzzy controller system for *gal* operon in *Lactococcus lactis*

Table 6.10. Fuzzy rule base configuration for *gal* operon in *Lactococcus lactis*

IF	**VL**	**L**	**ME**	**H**	**VH**
	Normalized ccpAcre				
Glucose or Lactose Uptake	VH	H	ME	L	VL
	GalK Production (Normalized)				
Normalized ccpAcre	VL	L	ME	VH	VH
	Galactose Uptake				
GalK Production	VL	L	ME	H	VH

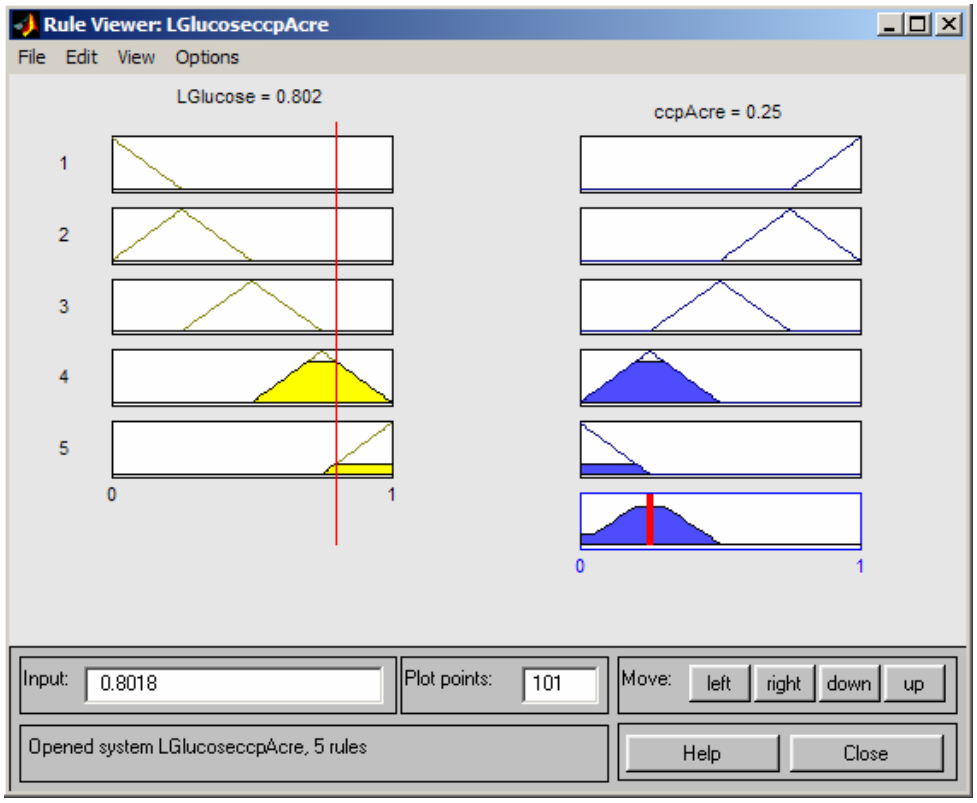

Figure 6.15. FIS rule viewer of lactose or glucose uptake to *ccpAcre*

The rule viewer of fuzzy inference system shown in Figure 6.15 for the calculation of normalized CcpAcre gives the details of input (Normalized Glucose and Lactose Uptake Rate) and output (Normalized CcpAcre) relation. The scaling method is used to scale down the resulting membership functions. All result coming from each rules are combined to produce an inferred conclusion. The center of area (COA) is taken as a numerical result of all combined conclusions. For instance, normalized value of glucose and lactose uptake of 0.8018 is given to the corresponding controller and a normalized value of 0.25 is taken out for the CcpAcre concentration.

7. RESULTS AND DISCUSSION

In this section, the computational results and discussions for the following systems are presented.

1. Single substrate of glucose or lactose is fed to *E. coli*.
2. Mixed substrates of glucose and lactose are fed to *E. coli*.
3. Mixed substrates of glucose and lactose are fed and a pulse of glucose is injected on lactose growth to *E. coli*.
4. Mixed substrates of glucose and lactose are fed and a pulse of galactose is injected on lactose growth to *E. coli*.
5. Mixed substrates of glucose and lactose are fed and a pulse of glucose and galactose mixture is injected on lactose growth to *E. coli*.
6. Mixed substrates of glucose, sorbitol (glucitol) and glycerol are fed to *E. coli*.
7. Mixed substrates of glucose, lactose and galactose are fed to *L. lactis.*

The sequence of utilization of the mixed substrates is controlled by transcriptional regulatory constraints of the relevant operons. Instead of using a logic based on the *True* and *False* values (Boolean Logic), fuzzy logic is used to explain the whole interval between these two values. Therefore, in all these constrained uptakes there is no sharp change of substrate utilization.

7.1. Dynamics of Single Substrate Uptake in *Escherichia coli*

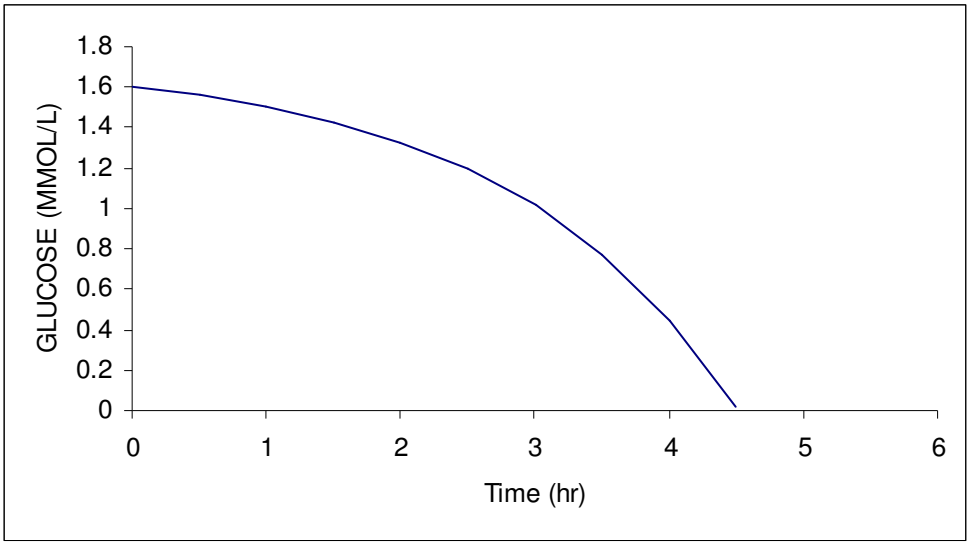

Figure 7.1. Glucose concentration profile during glucose uptake in *Escherichia coli*

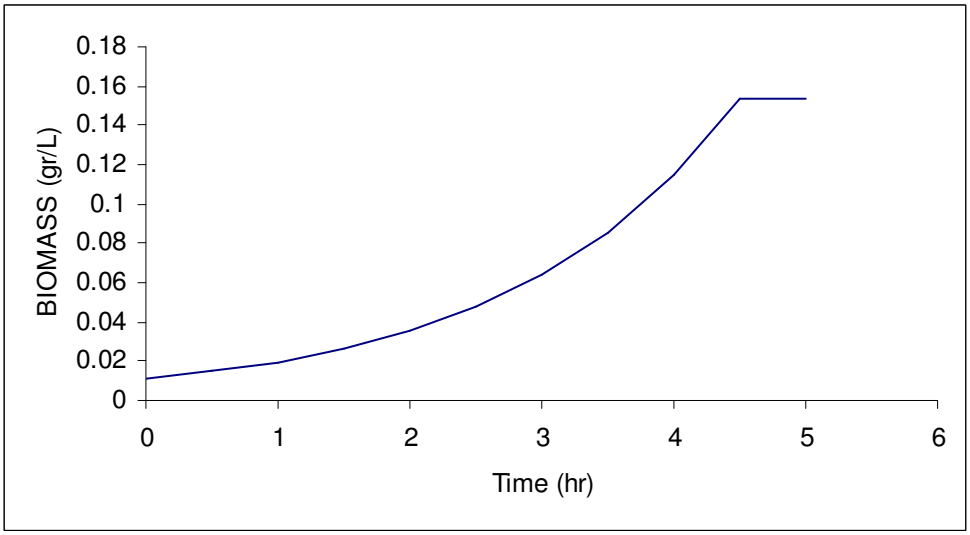

Figure 7.2. Biomass profile during glucose uptake in *Escherichia coli*

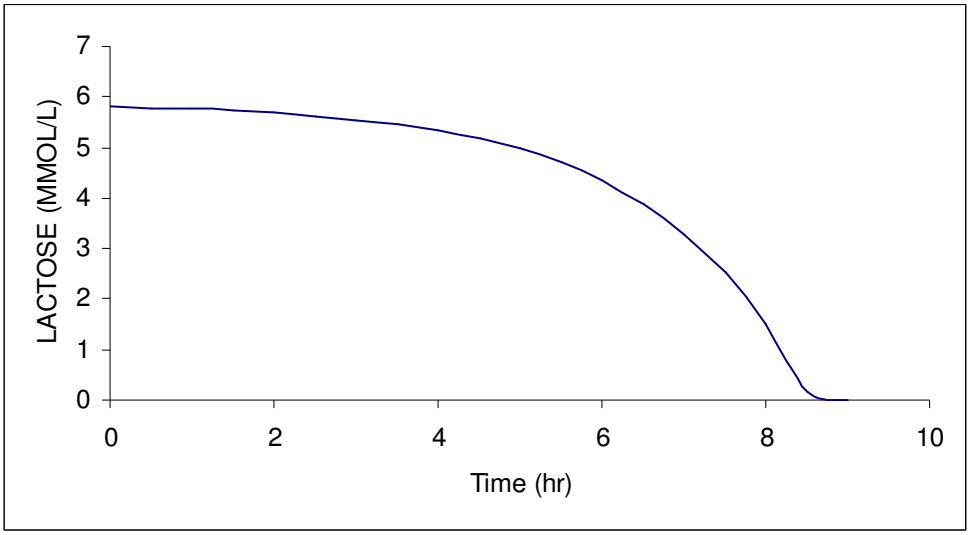

Figure 7.3. Lactose concentration profile during lactose uptake in *Escherichia coli*

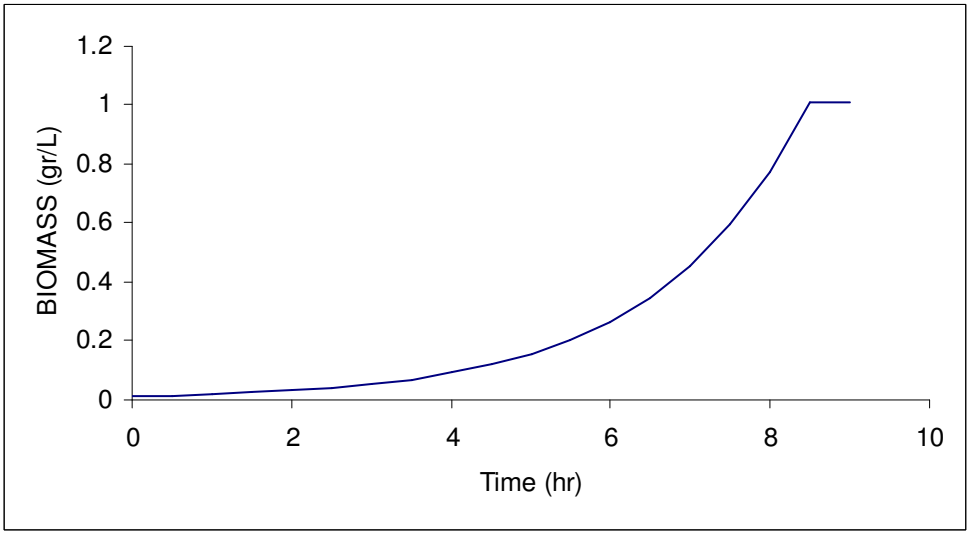

Figure 7.4. Biomass profile during lactose uptake in *Escherichia coli*

Figures 7.1 and 7.3 show the time courses of utilization of glucose and lactose, respectively. Correspondingly, biomass profiles are given in Figures 7.2 and 7.4. The initial substrate and biomass concentrations, and substrate uptake rates are given in Table 6.1. As it

can be seen for Figures 7.2 and 7.4, the maximum growth rate for glucose (μ_{glu}) is greater than that for lactose (μ_{lac}).

7.2. Dynamics of Mixed Substrates Uptakes; Glucose and Lactose, in *Escherichia coli*

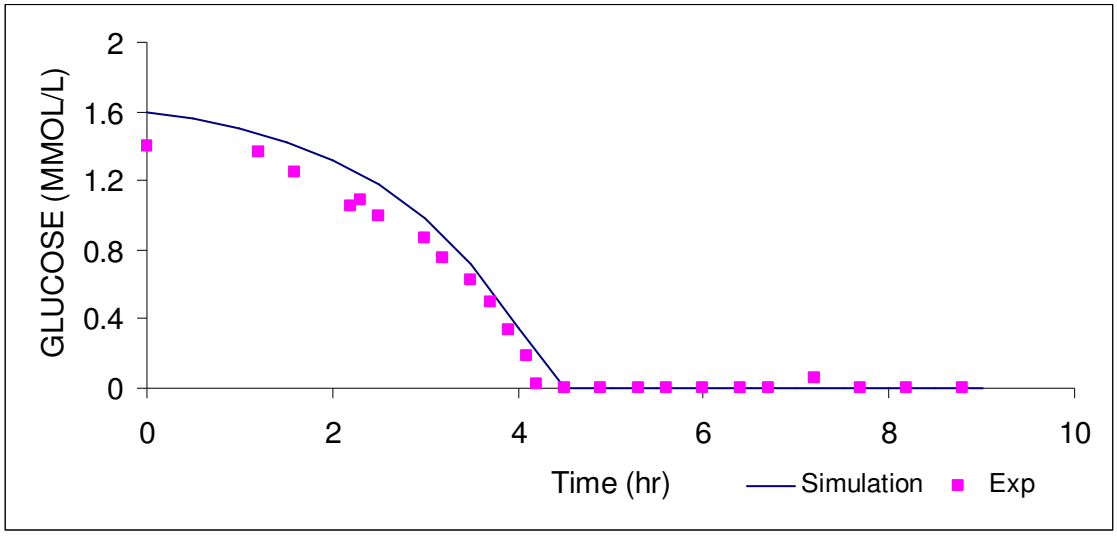

Figure 7.5. Experimental and calculated glucose concentration profile for mixed substrates; glucose and lactose in *Escherichia coli*

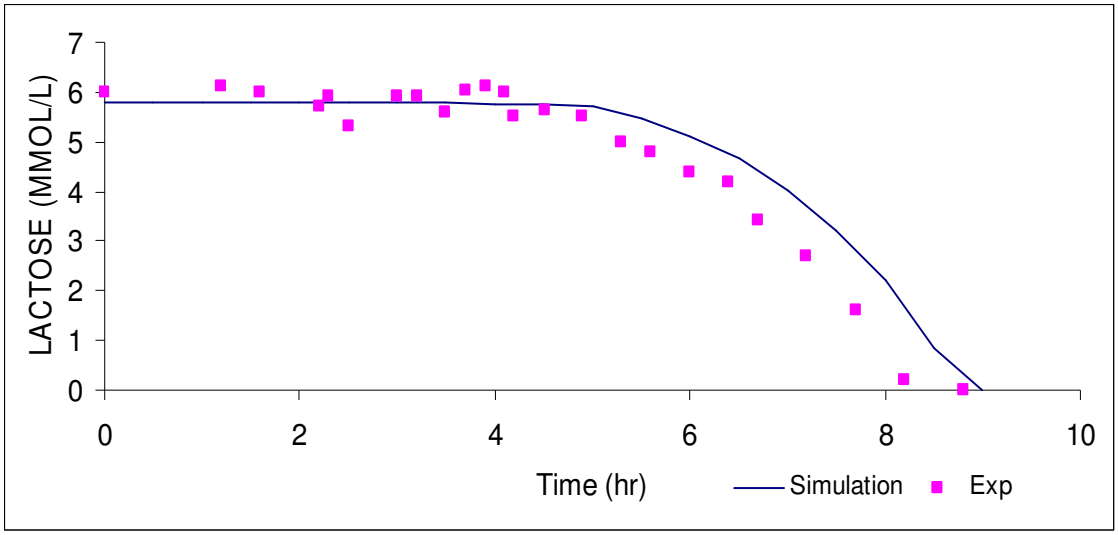

Figure 7.6. Experimental and calculated lactose concentration profile for mixed substrates; glucose and lactose in *Escherichia coli*

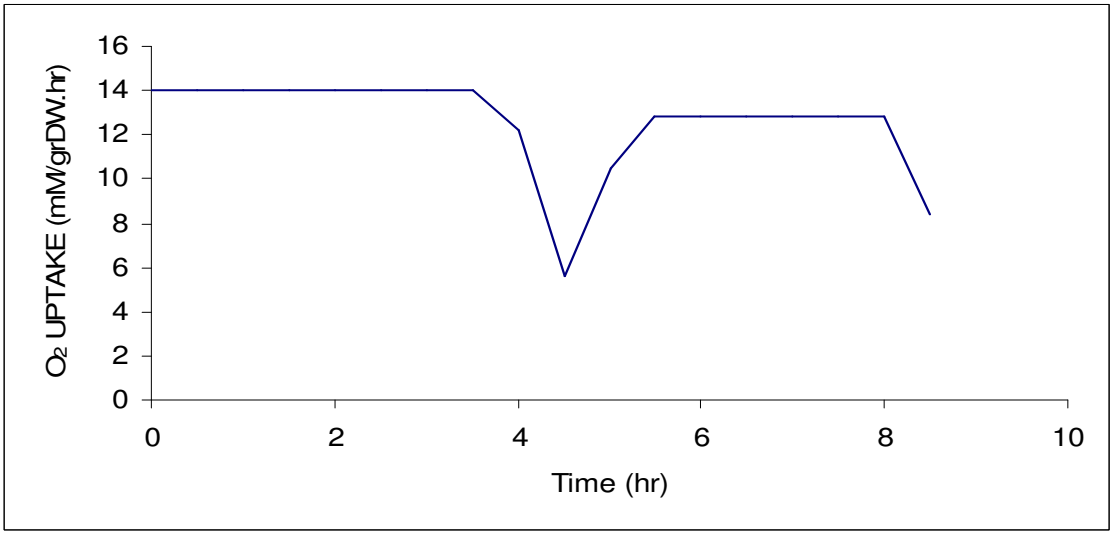

Figure 7.7. O_2 uptake rate for mixed substrates; glucose and lactose in *Escherichia coli*

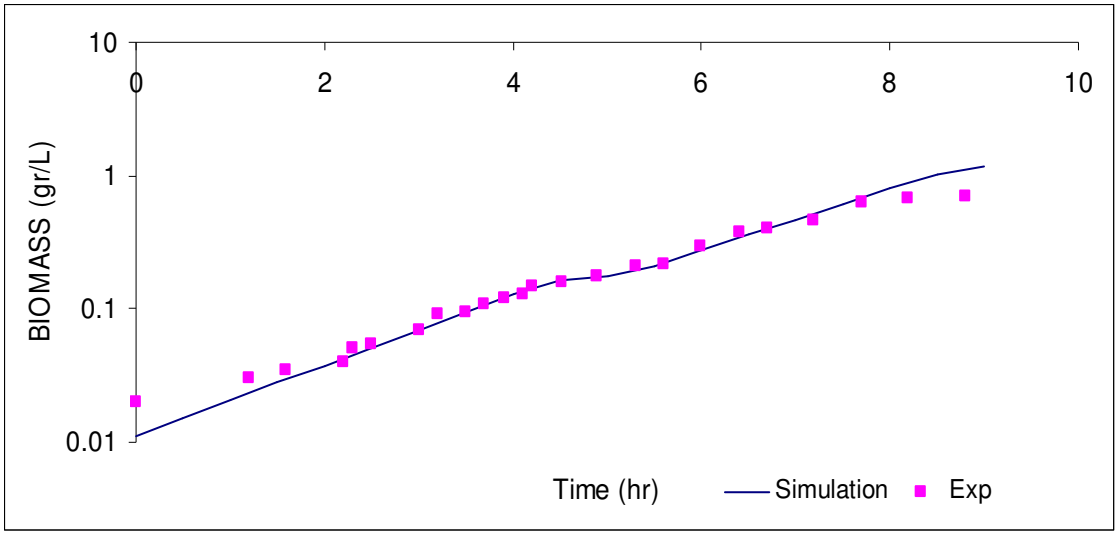

Figure 7.8. Experimental and calculated biomass production profile for mixed substrates; glucose and lactose in *Escherichia coli*

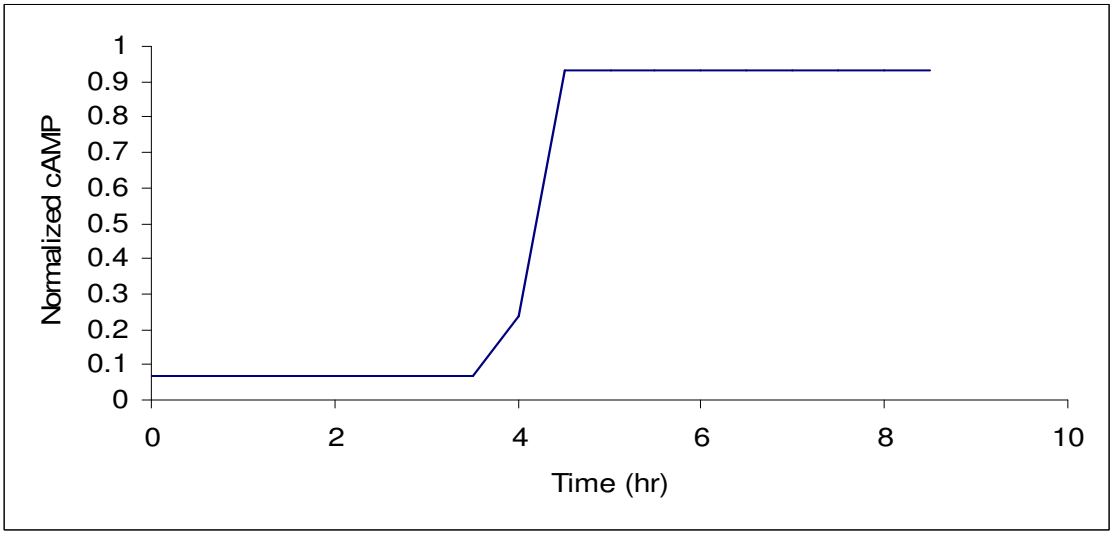

Figure 7.9. Normalized cAMP profile for mixed substrates; glucose and lactose in *Escherichia coli*

Figures (7.5 - 7.9) are the plots of dynamic glucose and lactose utilization profile in the mixed substrates, glucose and lactose. Experimental data taken from the literature (Covert, *et*

al., 2002) are indicated, to show the accuracy of the simulated results. For the starting point of FBA, initial conditions and substrate uptake rate constraints must be estimated in order to get an output of growth rate. These parameters are taken from the same reference. A best fit of biomass yield is obtained in the exponential phases of growth because the simulations are for constant uptake rates of relevant substrates. The preference of glucose over lactose results in sequential utilization of glucose, and then lactose. This is due to the catabolite repression of glucose over lactose. In Figure 7.8, it is clear that there is a lag phase between the two exponential growth phases. This lag phase results from both catabolite repression by glucose and induction of *lac* operon by lactose. Another crucial point about the lag phase is the gradual increase of lactose uptake to the cell. Namely, it does not mean that there is no growth at this stage. In general, a lag phase of *lac* operon in *E. coli* takes place in 10 to 30 minutes. If a Boolean formalism is held for the regulation of glucose and lactose utilization, the time of lag phase must be specified in the calculations. In the work of Covert *et al.* (2002), nearly half an hour was taken and inserted to the calculation to simulate a lag as the shift occurs in diauxic growth on glucose and lactose. In fuzzy logic formalism, the lag phase of about 30 minutes is the natural result of gradual shift of the lactose uptake from low to high level after glucose is depleted. Oxygen uptake rate shown in Figure 7.7 and normalized cAMP concentrations shown in Figure 7.9 are given to show the shift from glucose uptake to lactose uptake. cAMP concentration is directly related to the glucose concentration in the medium and helps to promote the *lac* operon by the CAP-cAMP complex. When glucose comes to exhaustion, cAMP level will give a shift from a low level to a high one. O_2 uptake rate level will decrease as the shifting occurs. It will increase and come to another level because of the new substrate uptake. In Figure 7.7, O_2 uptake rate level of lactose is lower than the glucose. It means that the growth rate on lactose is being low compared to glucose.

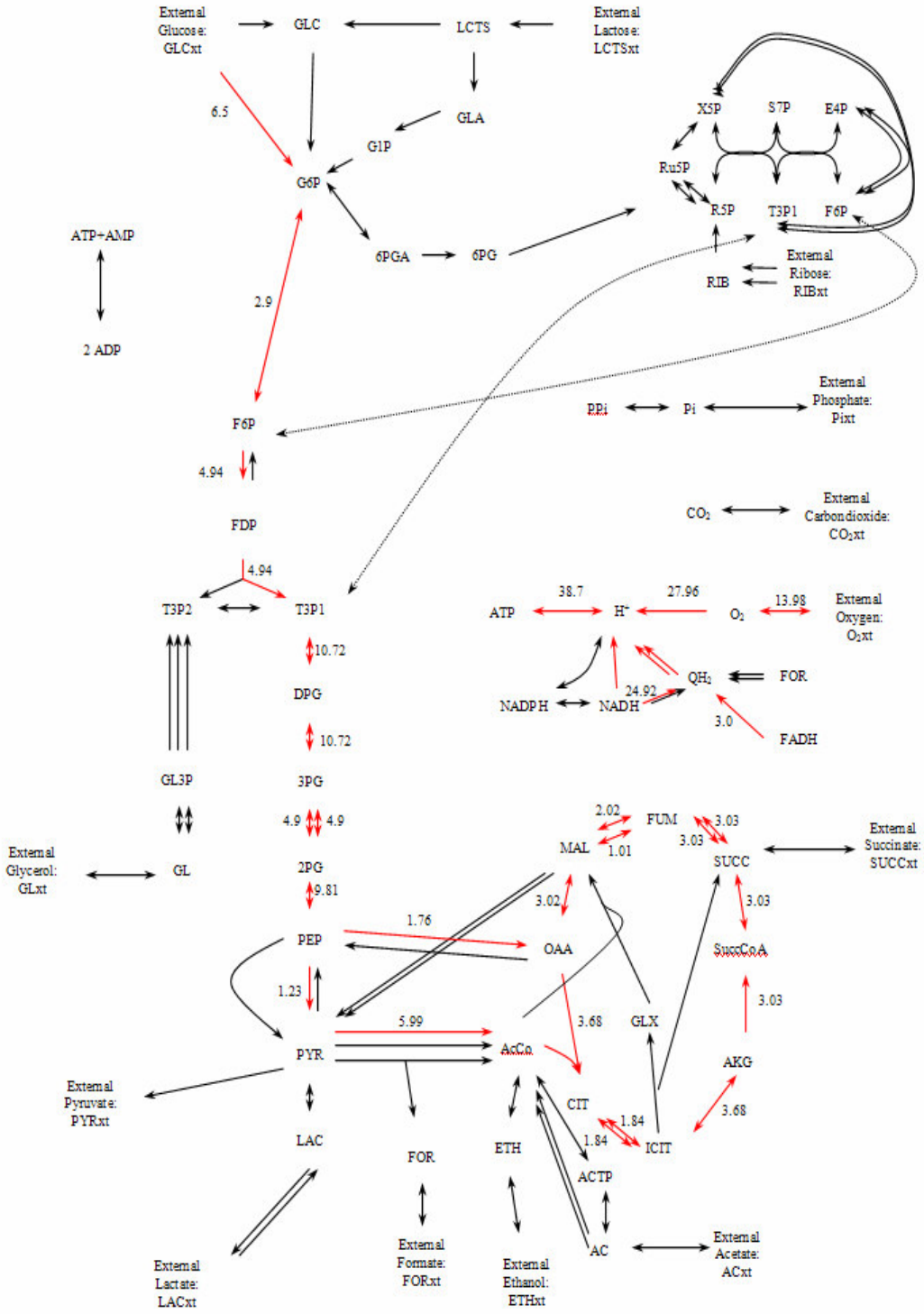

Figure 7.10. Flux distribution for aerobic metabolism of glucose by *Escherichia coli*

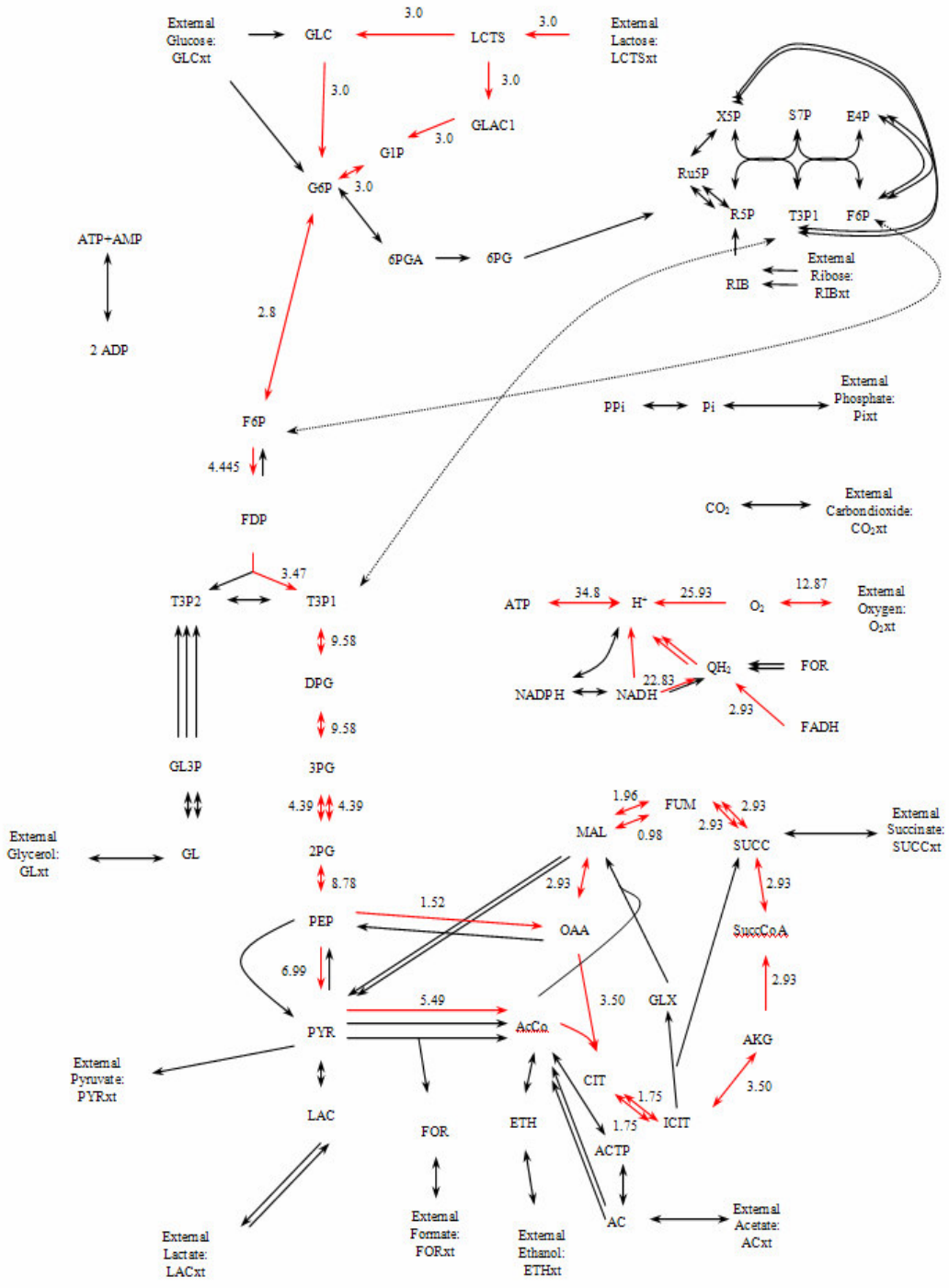

Figure 7.11. Flux distribution for aerobic metabolism of lactose by *Escherichia coli*

Flux distributions of glucose (PTS), and lactose (permease) aerobic metabolisms on metabolic network of *E. coli* are given in Figure 7.10 and 7.11. The red arrows show the

dominant fluxes, whereas the black ones are stagnant (zero) rates on the metabolism. When there is a shift from one substrate to another, flux distribution on the metabolism is more or less the same. But, the fluxes change a little bit. In general, fluxes are higher which give more biomass production on glucose than lactose. The only difference on flux distributions is the pathway of the substrate uptake.

7.3. Dynamics of Mixed Substrates Uptakes; Glucose and Lactose, Glucose Pulse in *Escherichia coli*

Mixed substrates of glucose and lactose are fed to the batch culture and a pulse of glucose (2.5 mmol/L) is injected to the medium at the 7th hour on the lactose growth. The aim is to see the immediate changes caused by the shift in substrate uptake.

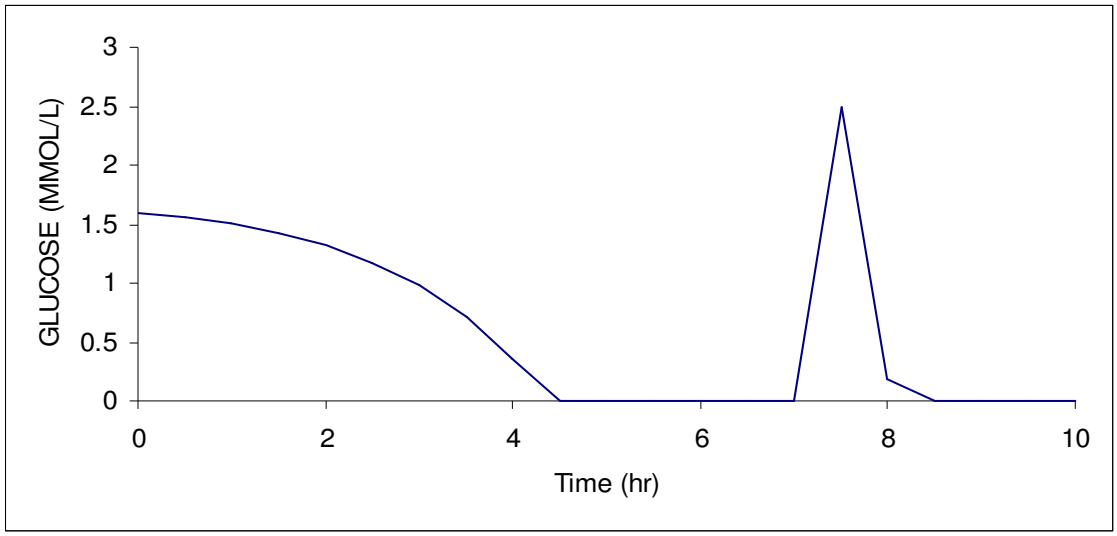

Figure 7.12. Glucose concentration profile for mixed substrates; glucose and lactose, and glucose pulse injection in *Escherichia coli*

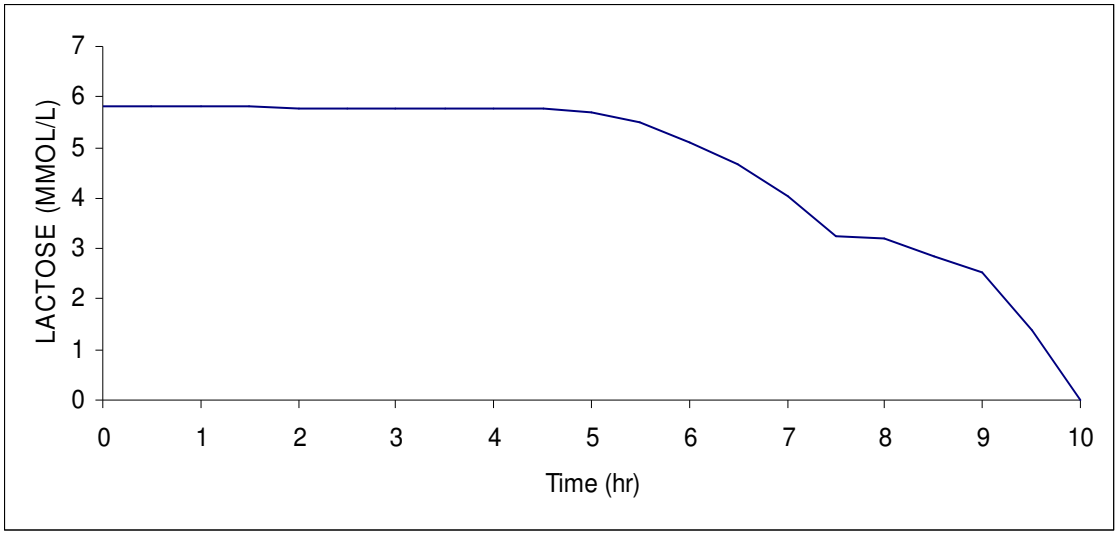

Figure 7.13. Lactose concentration profile for mixed substrates; glucose and lactose, and glucose pulse injection in *Escherichia coli*

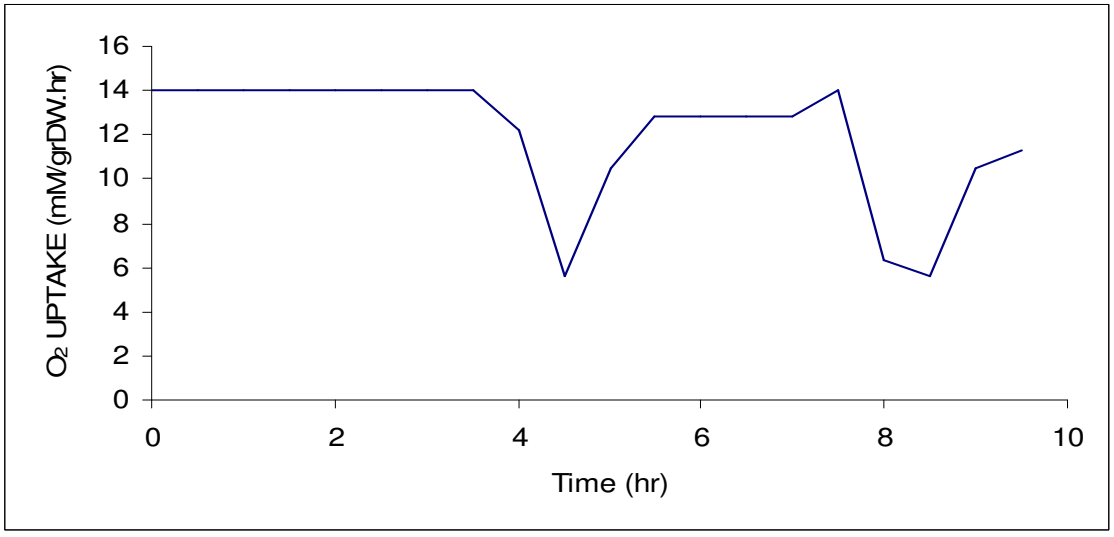

Figure 7.14. O_2 uptake rate for mixed substrates; glucose and lactose, and glucose pulse injection in *Escherichia coli*

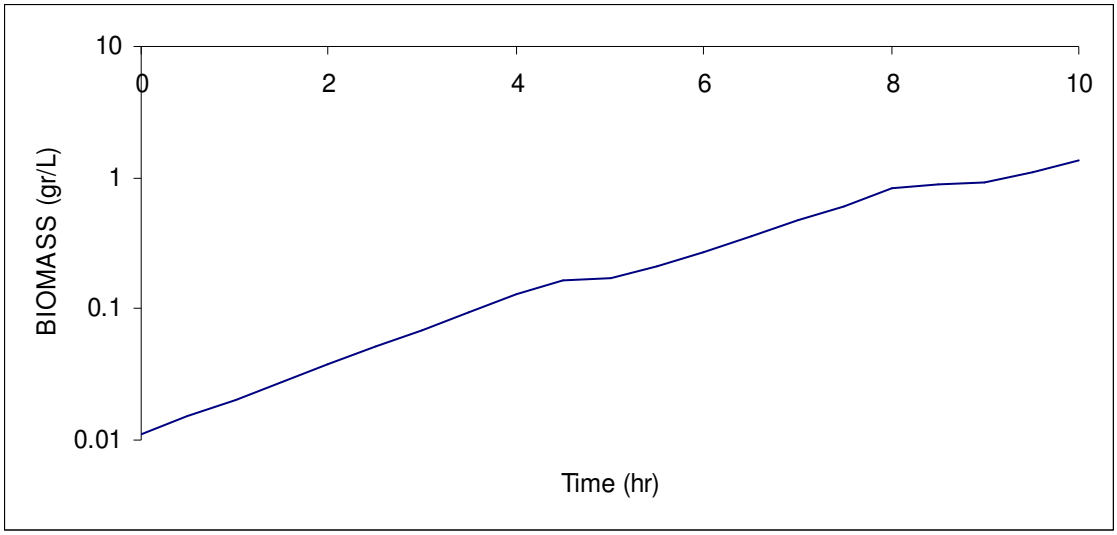

Figure 7.15. Biomass yield profile for mixed substrates; glucose and lactose, and glucose pulse injection in *Escherichia coli*

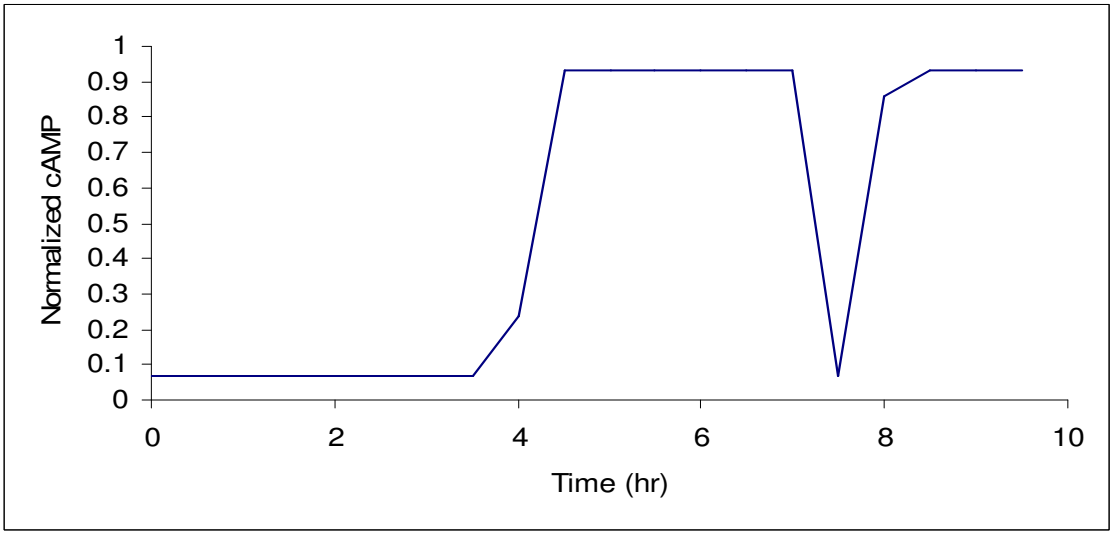

Figure 7.16. Normalized cAMP profile for mixed substrates; glucose and lactose, and glucose pulse injection in *Escherichia coli*

In Figure 7.12, it is clear that there is a glucose pulse injection on the lactose growth. The glucose pulse is delivered between the 7^{th} and 8^{th} hours. Again, glucose is the preferable

substrate over lactose in this system. Upon glucose injection, the consumption of lactose is reduced due to the catabolite repression, but lactose is being utilized in small amounts by the cell because of the presence of LacY (Permease) and lactose (allolactose) in the cell medium. As glucose becomes depleted at 8.5 hour, growth on lactose is slowly resumed and there is a decrease in the biomass. O_2 uptake rate level gives two minimums for the alteration of substrates. The first one is due to the shift from glucose to lactose, but the second is due to the repression of glucose on lactose. It is usual to observe a decrease in the normalized cAMP level. Glucose becomes dominant substrate, but the injected amount is small compared to the whole biomass present in the batch culture. Therefore, the depletion of glucose added is very quick. Then, lactose becomes the only substrate available.

7.4. Dynamics of Mixed Substrates Uptakes Including Membrane Transport System; Glucose and Lactose, Glucose Pulse in *Escherichia coli*

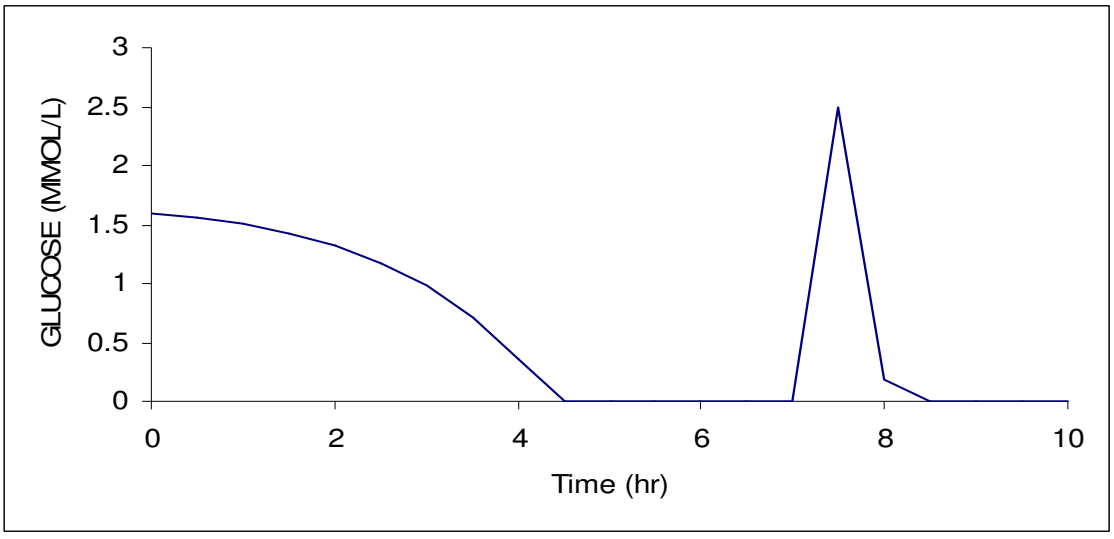

Figure 7.17. Glucose concentration profile for mixed substrates including membrane transport system; glucose and lactose, and glucose pulse injection in *Escherichia coli*

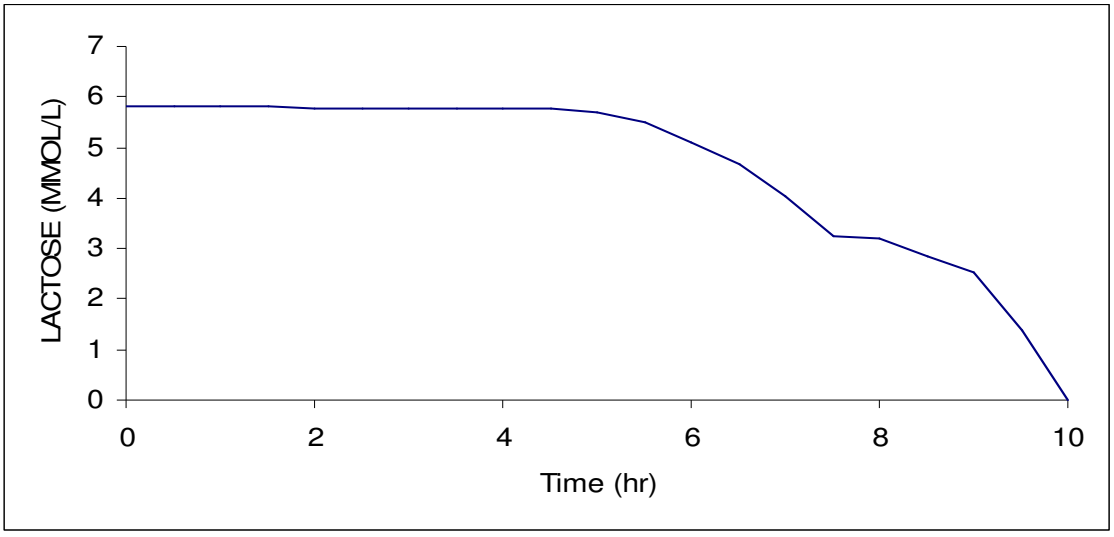

Figure 7.18. Lactose concentration profile for mixed substrates including membrane transport system; glucose and lactose, and glucose pulse injection in *Escherichia coli*

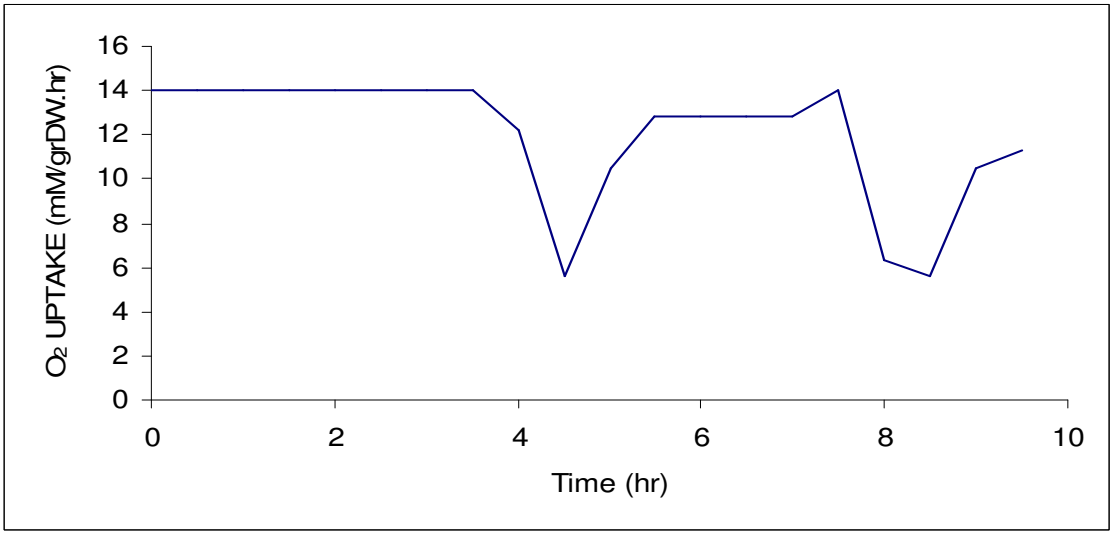

Figure 7.19. O_2 uptake rate for mixed substrates including membrane transport system; glucose and lactose, and glucose pulse injection in *Escherichia coli*

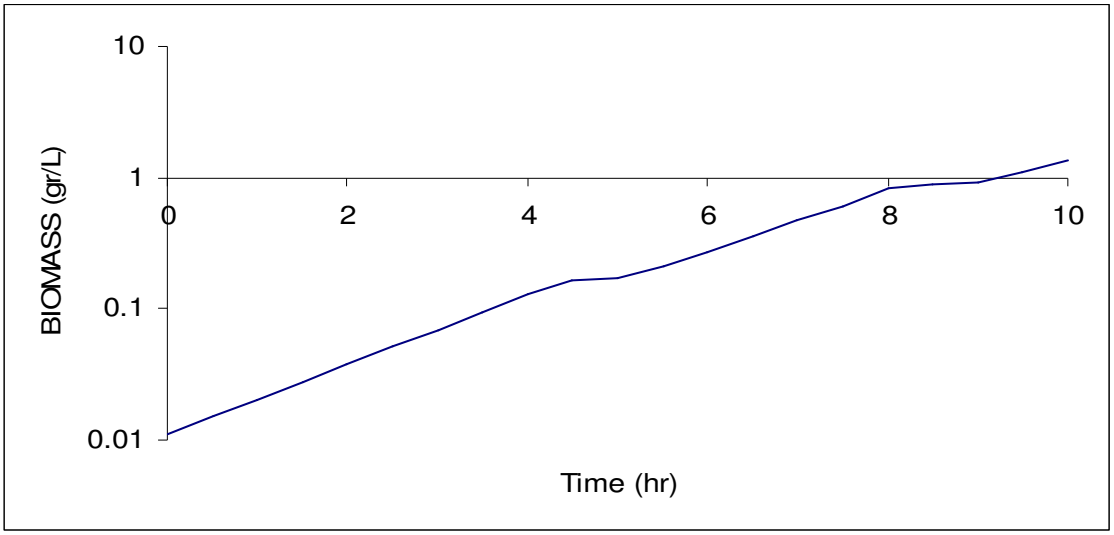

Figure 7.20. Biomass profile for mixed substrates including membrane transport system; glucose and lactose, and glucose pulse injection in *Escherichia coli*

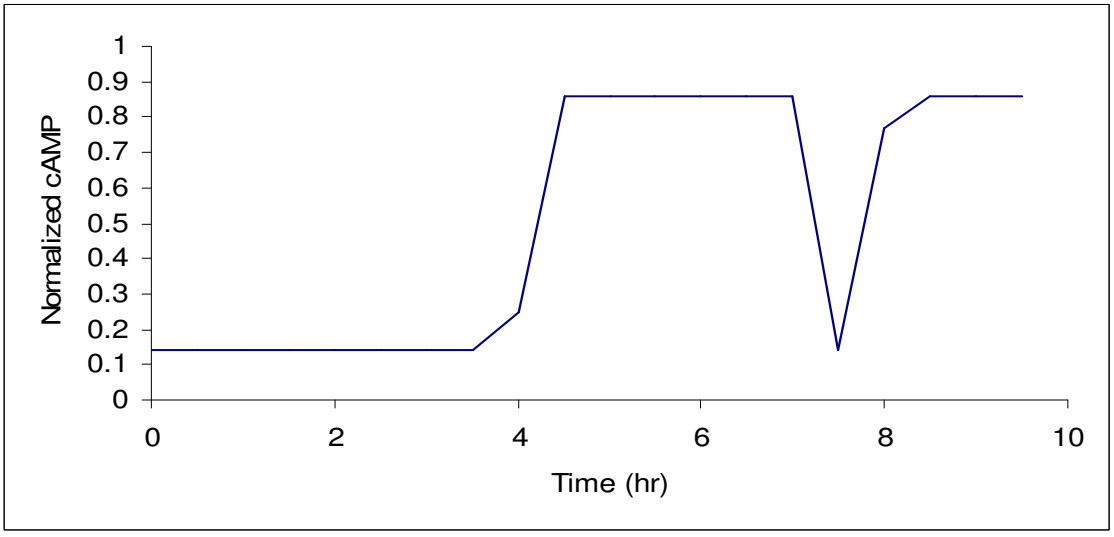

Figure 7.21. Normalized cAMP profile for mixed substrates including membrane transport system; glucose and lactose, and glucose pulse injection in *Escherichia coli*

A membrane transport system is added to the mixed substrate uptake; glucose and lactose and injection of glucose on lactose growth system. $EIIA^{Glc}$ only repress the production

of LacY permease which allows lactose transport through the cell membrane. Glucose is transported by the phosphotransferase system. $EIIA^{Glc}$ is phosphorylated as glucose is depleted. Phosphorylated $EIIA^{Glc}$ activates adenylate cyclase to result in the production of cAMP which effects the activation of the *lac* operon. Therefore, cAMP level and $EIIA^{Glc}$-P levels are all interrelated. When cAMP level increases, $EIIA^{Glc}$-P will increase in the same proportion. The result for the same system with the added membrane transport mechanism will will give identical outcomes. Therefore, Figures 7.12 – 7.16 are the same as with Figures 7.17 – 7.21.

7.5. Dynamics of Mixed Substrates Uptakes; Glucose and Lactose, Galactose Pulse in *Escherichia coli*

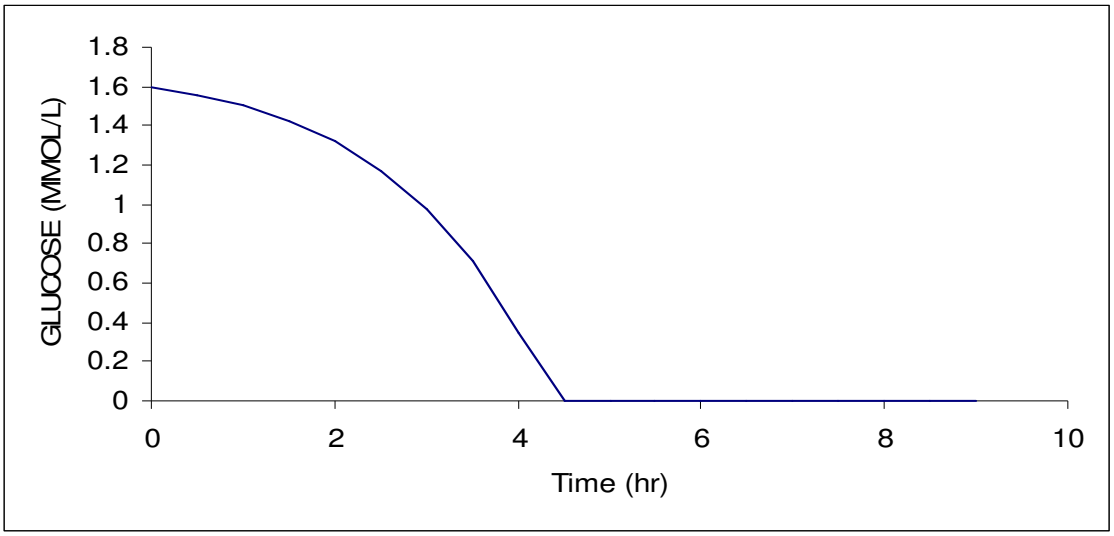

Figure 7.22. Glucose concentration profile for mixed substrates; glucose and lactose, and galactose pulse injection in *Escherichia coli*

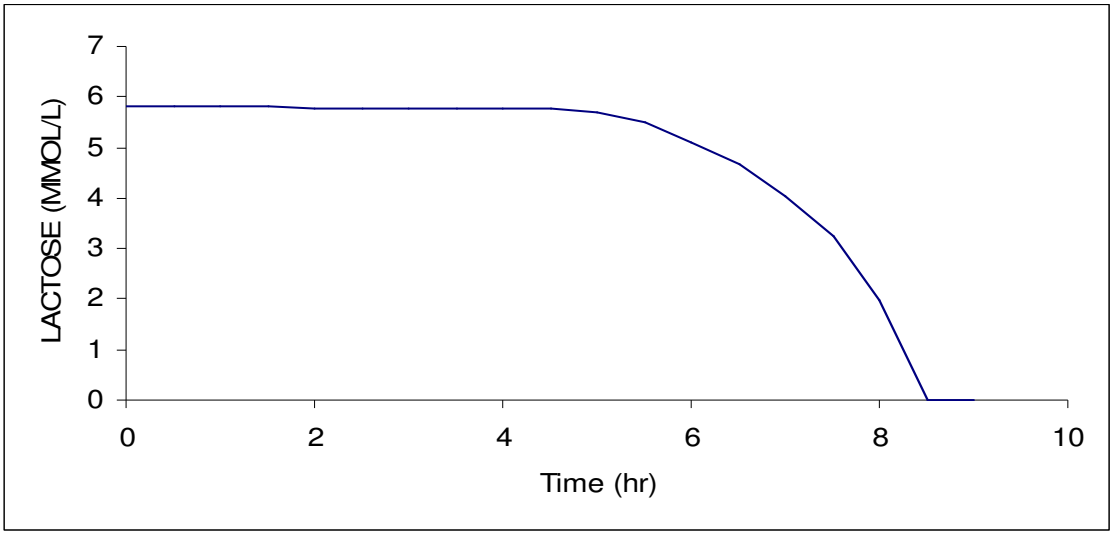

Figure 7.23. Lactose concentration profile for mixed substrates; glucose and lactose, and galactose pulse injection in *Escherichia coli*

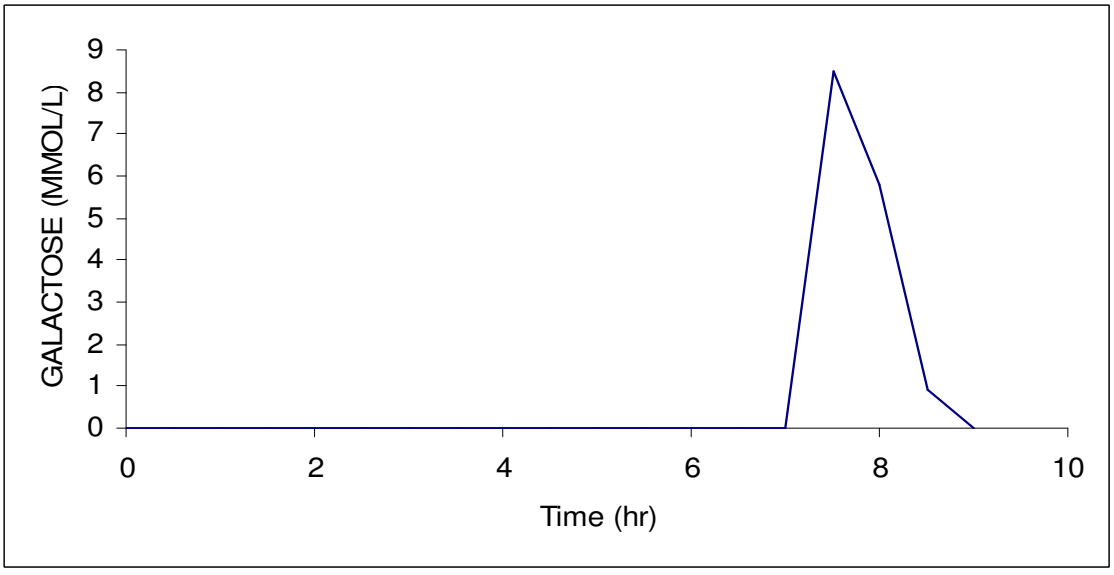

Figure 7.24. Galactose concentration profile for mixed substrates; glucose and lactose, and galactose pulse injection in *Escherichia coli*

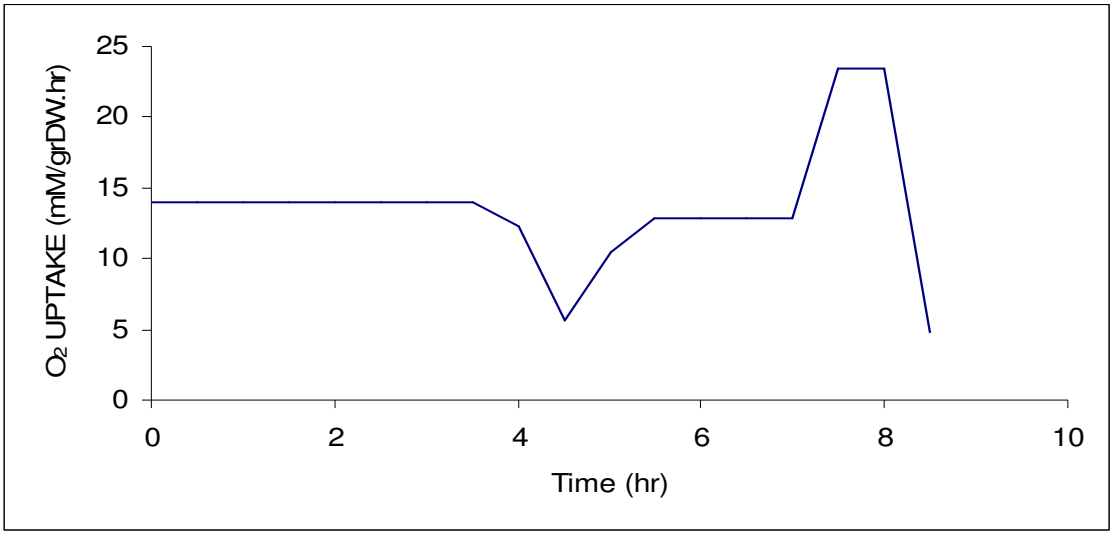

Figure 7.25. O_2 uptake rate for mixed substrates; glucose and lactose, and galactose pulse injection in *Escherichia coli*

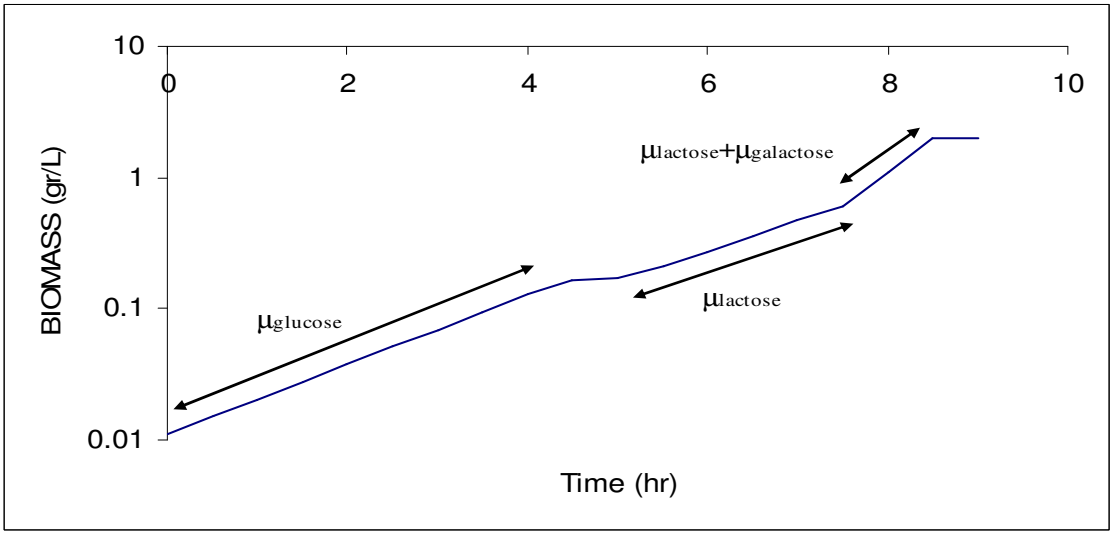

Figure 7.26. Biomass profile for mixed substrates; glucose and lactose, and galactose pulse injection in *Escherichia coli*

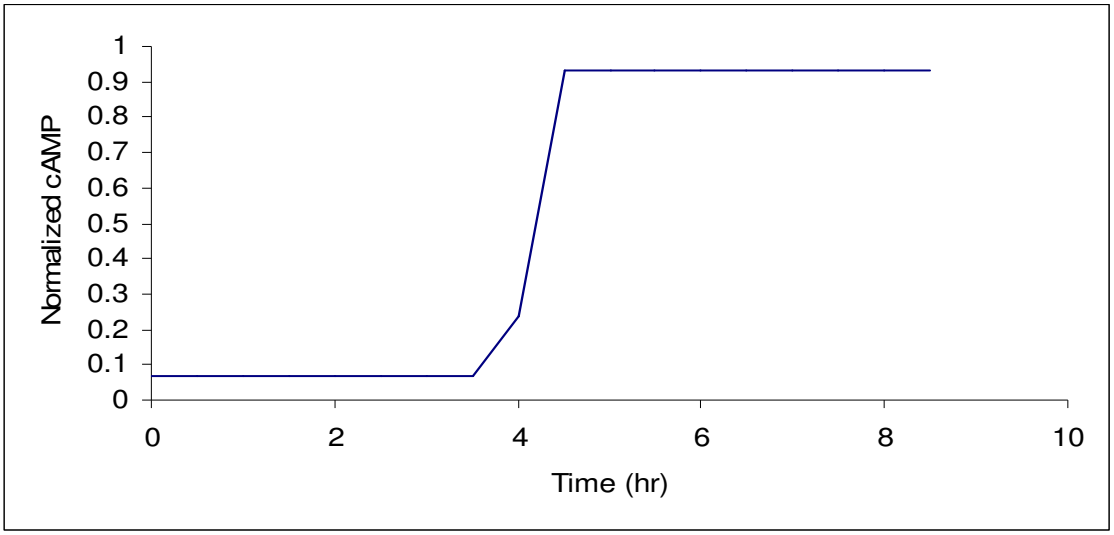

Figure 7.27. Normalized cAMP profile for mixed substrates; glucose and lactose, and galactose pulse injection in *Escherichia coli*

Galactose pulse injection is studied on growth of glucose and lactose substrates in order to illustrate the gal operon in *E. coli.* There is no difference on the glucose uptake part of growth. The difference comes as the galactose (8.5 mmol/L) is injected. The concentration of the galactose gives a peak and is consumed immediately due to high biomass yield in the medium. O_2 uptake rate level gives a rise as the injection occurs. In that time interval, lactose and galactose are taken up together and O_2 amount necessary for the aerobic growth is increased in that proportion. Galactose itself is the inducer of the REPRESSOR protein. Galactose is actually taken up by the permease system with an unknown mechanism and known *gal* operon interactions. The known operon operation was discussed in Chapter 5. Therefore, galactose must be present in the cell in order to permit the galactose transport. The injection is done during the lactose growth. Lactose is present in the medium and is hydrolyzed to glucose and galactose, so there is no problem for the uptake of galactose. The cAMP level is related neither with lactose, nor with galactose. So, there is only one shift in Figure 7.26 showing the change of substrates from glucose to lactose. The biomass growth on glucose was held upto 4.5 hour. Then, the biomass had been grown on lactose until the injection time of galactose. Galactose had been injected to the solution at 7.5 hour. Because

lactose was present and was converted to galactose and glucose in the metabolism, galactose was automatically taken up and utilized by the cell. However, the concentration of lactose is diminished at 8.5 hour. After that point on, there is only residual galactose in the culture and it gives a low growth rate of 0.019 hr^{-1}. The growth rate in the first period is 0.6165 hr^{-1} where the glucose is the dominant substrate over lactose. Then, in the second period lactose is taken up giving 0.5318 hr^{-1} growth rate. When galactose is injected, lactose and galactose are utilized simultaneously giving 1.184 hr^{-1} growth rate.

7.6. Dynamics of Mixed Substrates Uptakes; Glucose and Lactose, Mixture of Glucose and Galactose Pulse in *Escherichia coli*

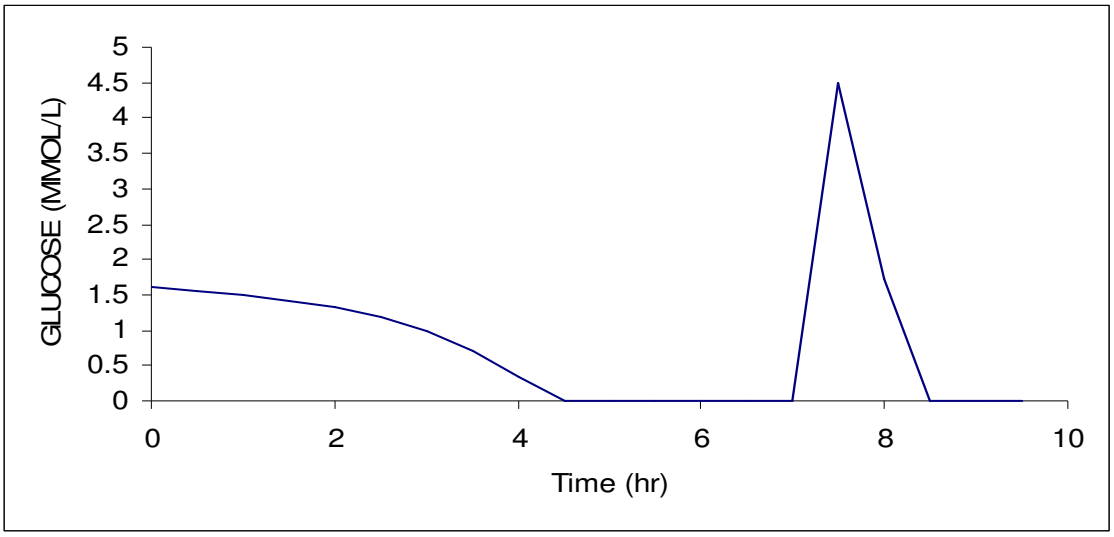

Figure 7.28. Glucose concentration profile for mixed substrates; glucose and lactose, and mixture of glucose and galactose pulse injection in *Escherichia coli*

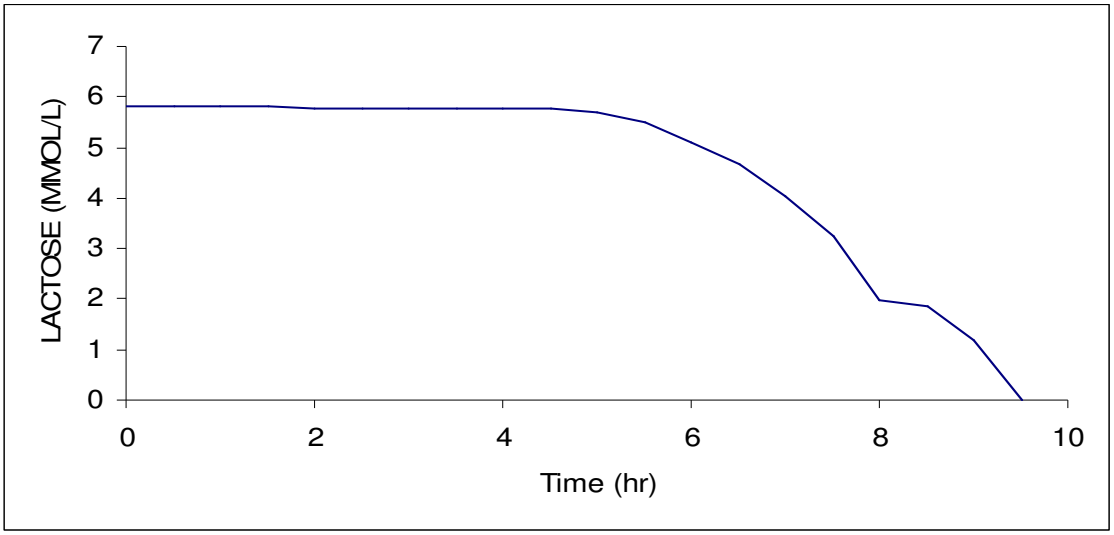

Figure 7.29. Lactose concentration profile for mixed substrates; glucose and lactose, and mixture of glucose and galactose pulse injection in *Escherichia coli*

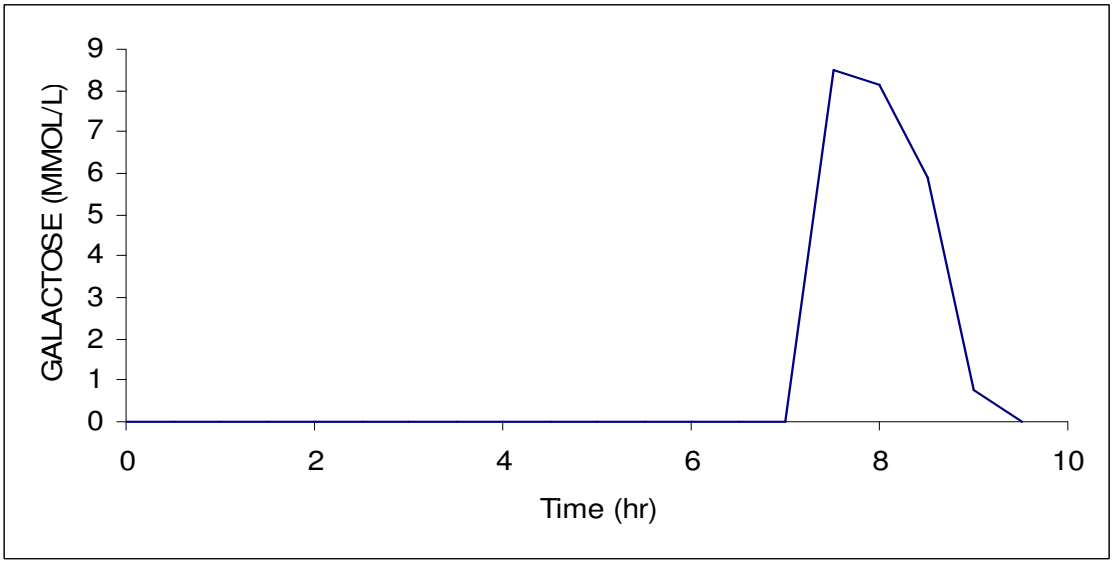

Figure 7.30. Galactose concentration profile for mixed substrates; glucose and lactose, and mixture of glucose and galactose pulse injection in *Escherichia coli*

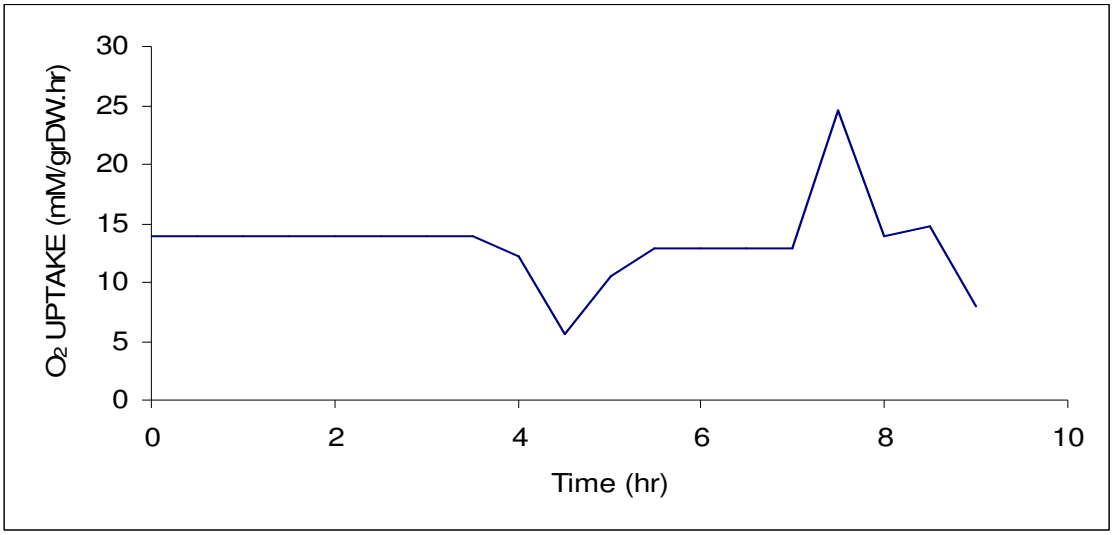

Figure 7.31. O_2 uptake rate for mixed substrates; glucose and lactose, and mixture of glucose and galactose pulse injection in *Escherichia coli*

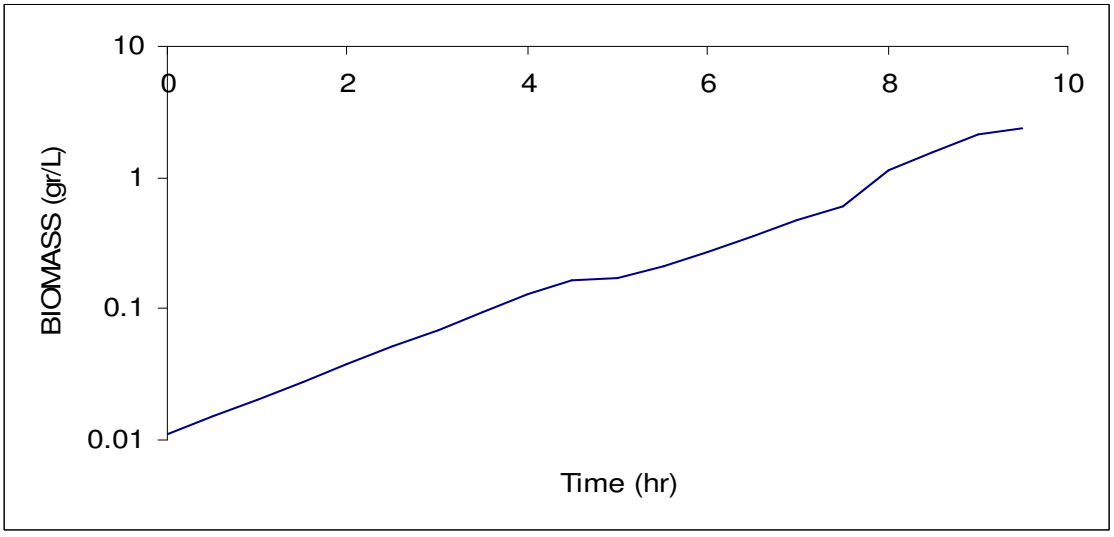

Figure 7.32. Biomass yield profile for mixed substrates; glucose and lactose, and mixture of glucose and galactose pulse injection in *Escherichia coli*

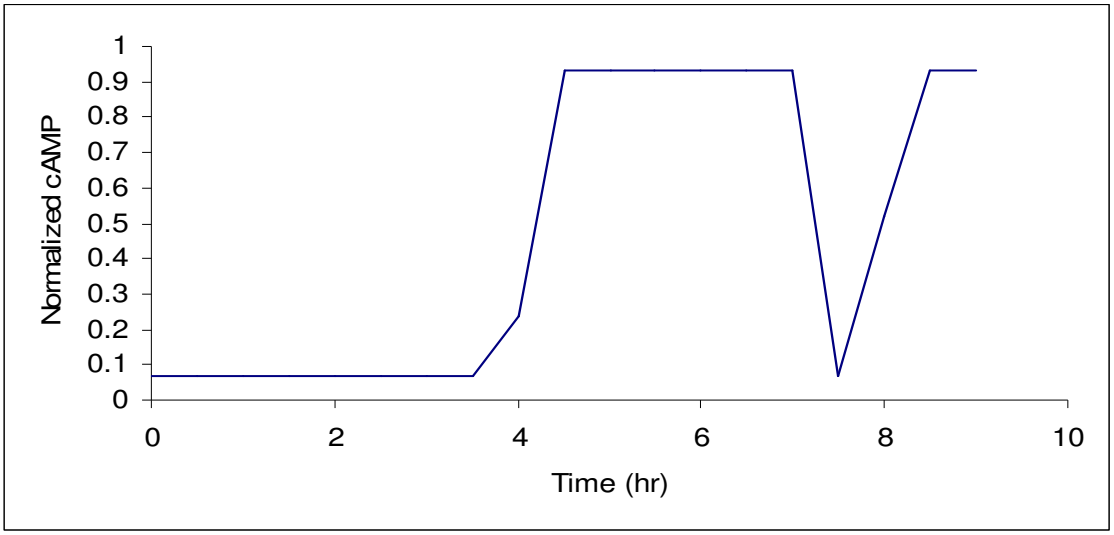

Figure 7.33. Normalized cAMP profile for mixed substrates; glucose and lactose, and mixture of glucose and galactose pulse injection in *Escherichia coli*

Mixture of glucose and galactose pulse injection is examined on the diauxic growth of glucose and lactose. It is aimed to decide and study the gal operon in terms of the glucose effect in *E. coli.* There is no difference on the glucose uptake part of growth. A mixture of glucose (4.5 mmol/L) and galactose (8.5 mmol/L) is added instantaneously on the lactose growth. Now, there are lactose, galactose and glucose all together in the cell. Glucose is taken up automatically. However, there are LacY (permease), allolactose and galactose present, and allow small lactose and galactose uptakes. Therefore, both O_2 uptake rate level and biomass yield will give a sharp rise. But, again glucose is the preferable sugar among the others. It will diminish the rise in the second step. From that time on, lactose and galactose uptakes are completely repressed until all injected glucose is consumed. Then, lactose and galactose are used simultaneously. Biomass yield will increase in an unstable manner during the injection period. It is sure that the cAMP level will decrease as the glucose is added to the medium.

7.7. Dynamics of Mixed Substrates Uptakes; Glucose, Sorbitol (Glucitol), and Glycerol in *Escherichia coli*

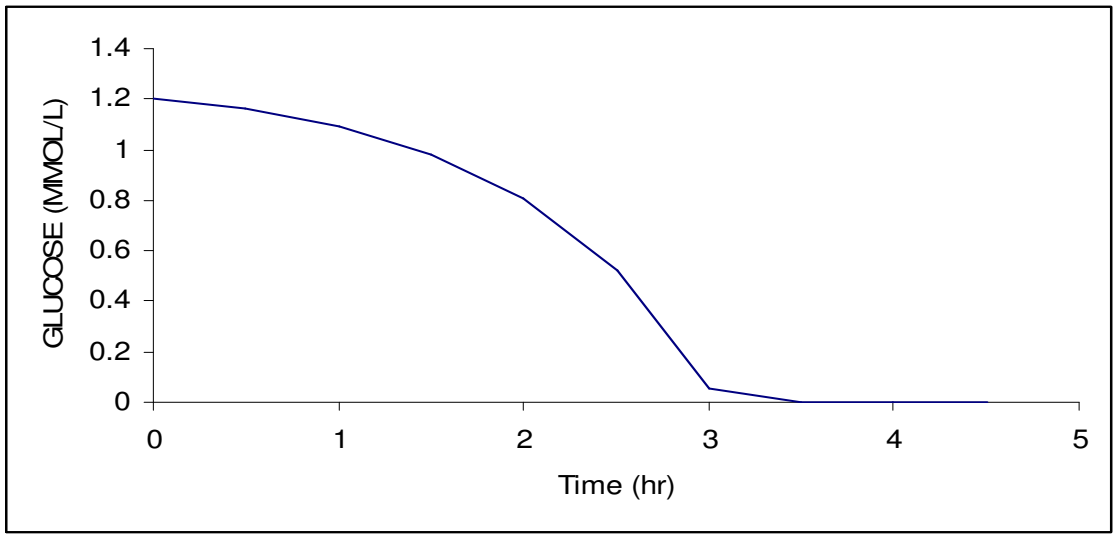

Figure 7.34. Glucose concentration profile for mixed substrates; glucose, sorbitol (glucitol) and glycerol in *Escherichia coli*

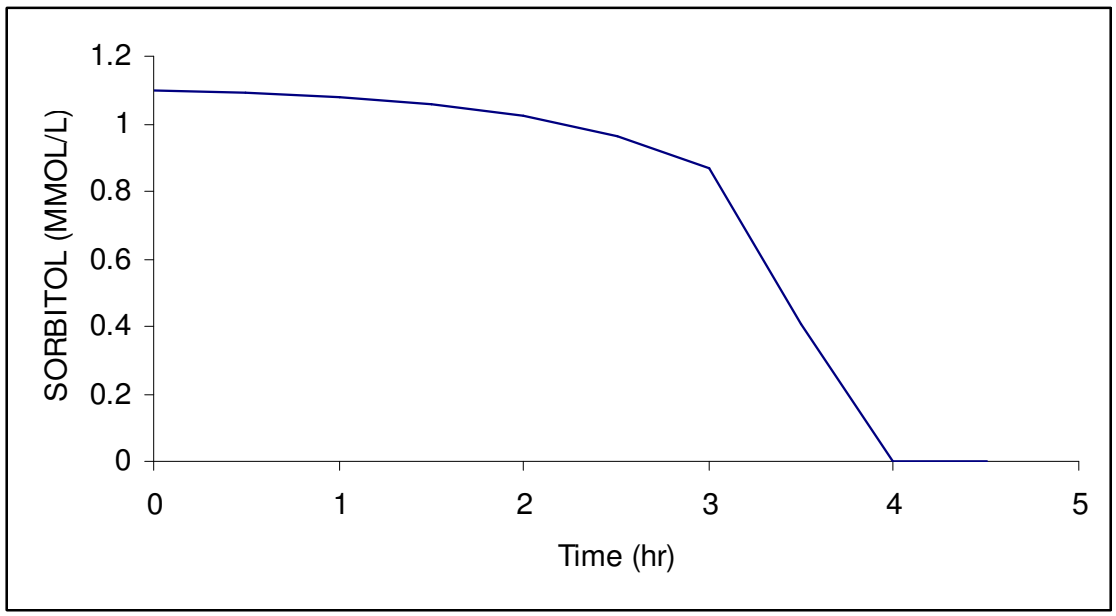

Figure 7.35. Sorbitol concentration profile for mixed substrates; glucose, sorbitol (glucitol) and glycerol in *Escherichia coli*

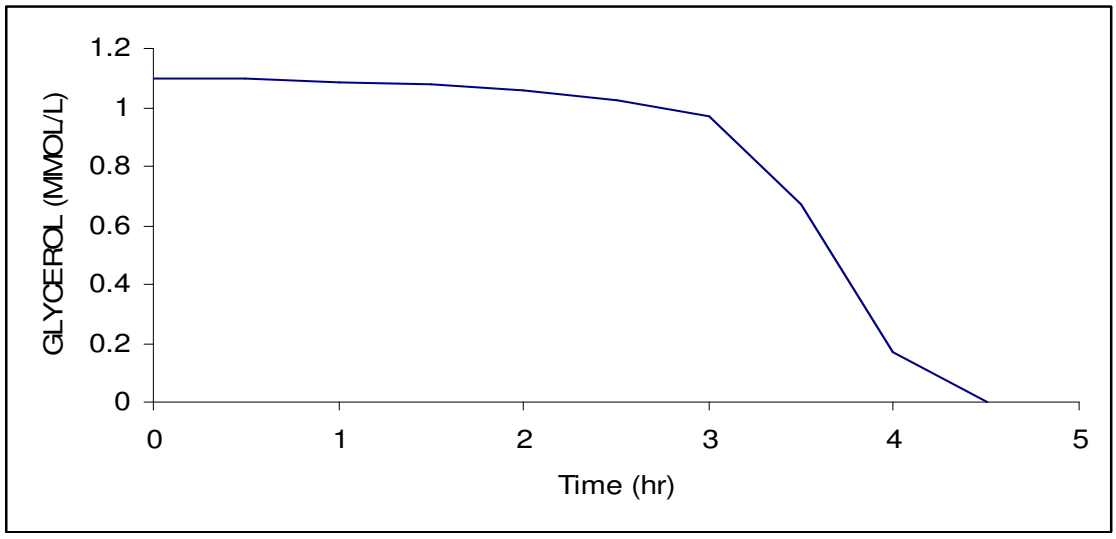

Figure 7.36. Glycerol concentration profile of mixed substrates; glucose, sorbitol (glucitol) and glycerol in *Escherichia coli*

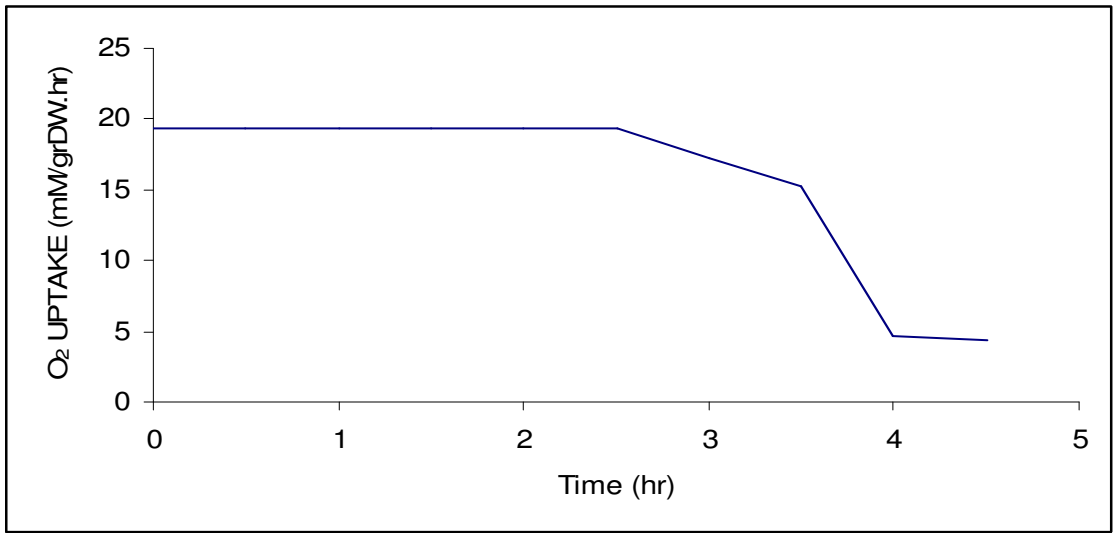

Figure 7.37. O_2 uptake rate of mixed substrates; glucose, sorbitol (glucitol), and glycerol in *Escherichia coli*

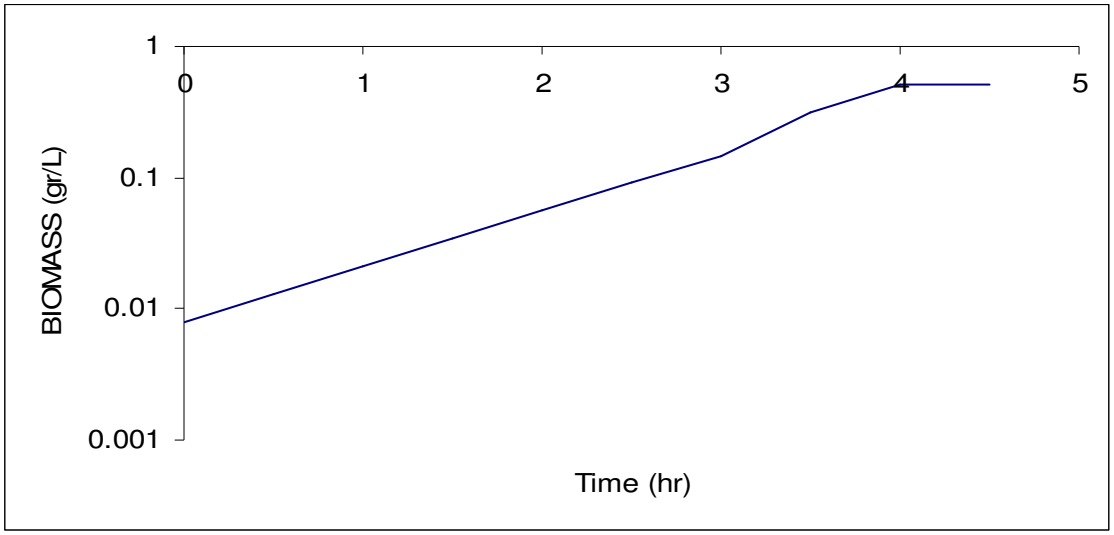

Figure 7.38. Biomass production profile for mixed substrates; glucose, sorbitol (glucitol) and glycerol in *Escherichia coli*

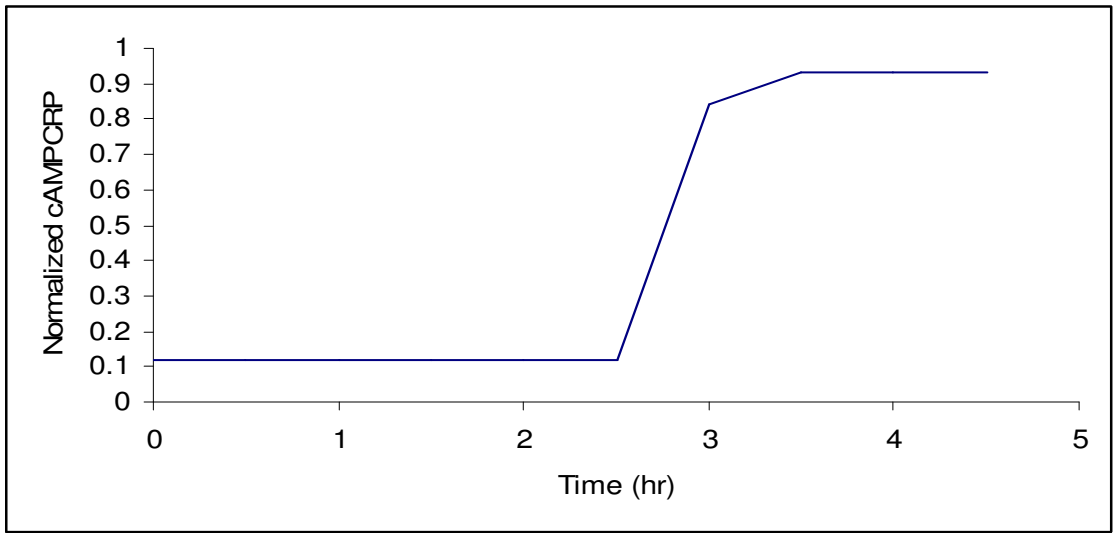

Figure 7.39. Normalized cAMPCRP profile for mixed substrates; glucose, sorbitol (glucitol), and glycerol in *Escherichia coli*

Another example of *E. coli* growth on mixed substrate is based on glucose, sorbitol (glucitol), and glycerol. Glucose and sorbitol are transported through the membrane by the phosphotransferase system (PTS). On the other hand, glycerol is transported by normal diffusion through the membrane. As it was explained in Chapter 5, there are two operons acting on the system; a gut operon and glp operon. Namely, the gut operon acting on sorbitol is repressed due to glucose in the medium and glp operon acting on glycerol metabolism is inhibited due to the presence of glucose and sorbitol. There are two shifts on biomass curve which gives a consistent result as given in the work of Kompala and Ramkrishna, (1984). However, the reported data of biomass concentration range was very small and these values cannot be obtained with the range of assumed initial conditions and substrate uptake rates. Figures from 7.34 to 7.39 give substrate concentrations, biomass yield, oxygen uptake and normalized cAMPCRP complex. The glucose is nearly depleted at 2.5 hr which is used simultaneously with sorbitol. However, as the glucose is depleted, glycerol starts being utilized in a small quantity. Sorbitol is all successively consumed at 4 hr and then glycerol at 4.5 hr. As a result, there are two refractions on the biomass concentrations indicating that one substrate is depleted and the other is started to be used. From the simulation results relying on the initial conditions, the growth rate of sorbitol is greater than both glucose and lactose and the growth rate of glucose is greater than the glycerol ($\mu_{SOR} > \mu_{GLC} > \mu_{GLY}$).

7.8. Dynamics of Mixed Substrates Uptakes; Glucose, Lactose, and Galactose in *Lactococcus lactis*

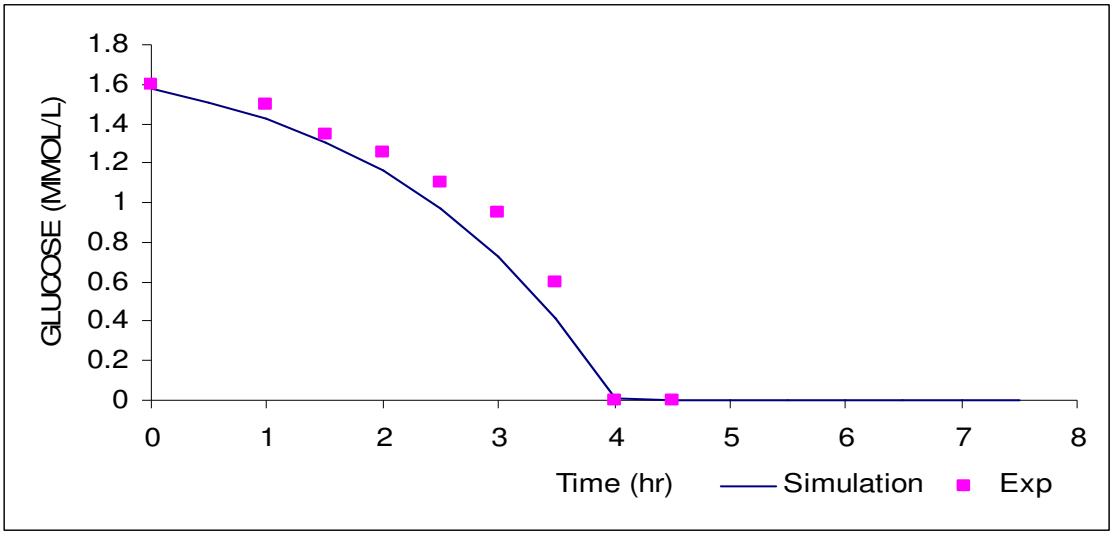

Figure 7.40. Glucose concentration profile for mixed substrates; glucose, lactose, and galactose in *Lactococcus lactis*

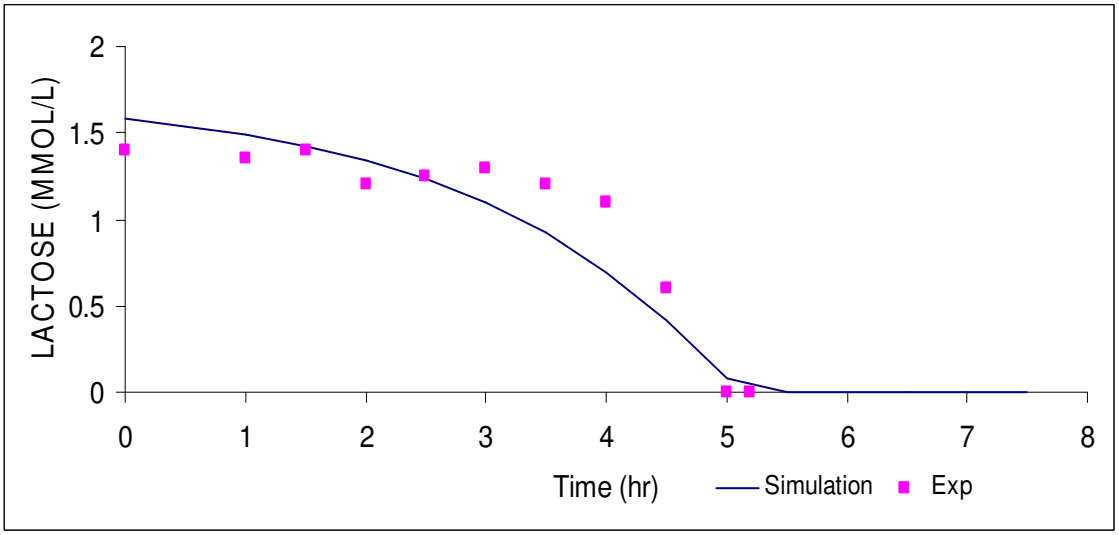

Figure 7.41. Lactose concentration profile for mixed substrates; glucose, lactose, and galactose in *Lactococcus lactis*

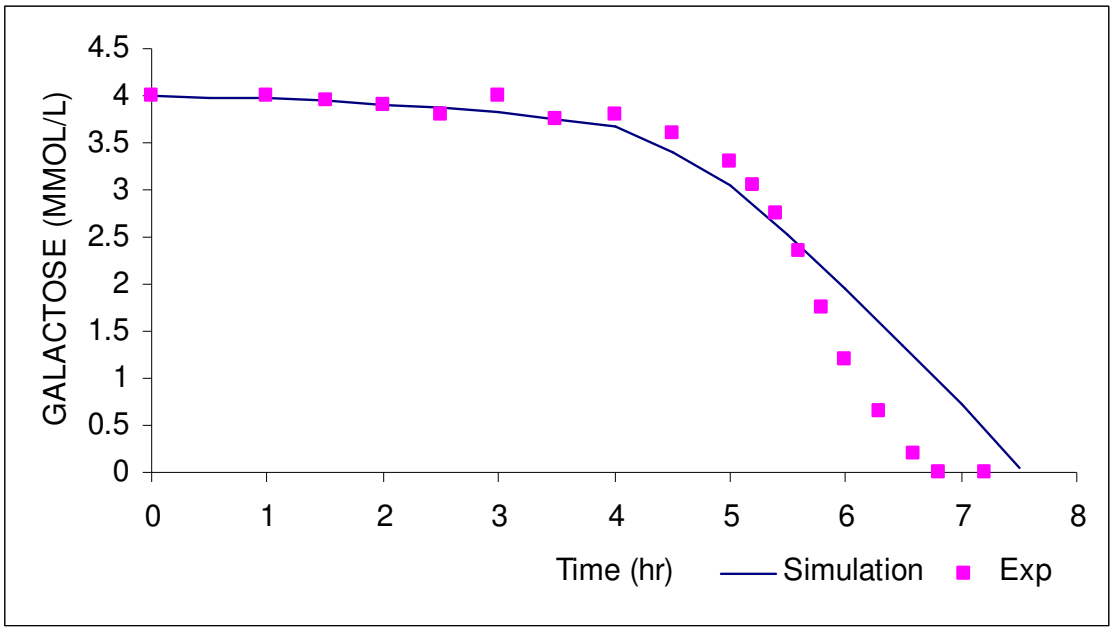

Figure 7.42. Galactose concentration profile for mixed substrates; glucose, lactose, and galactose in *Lactococcus lactis*

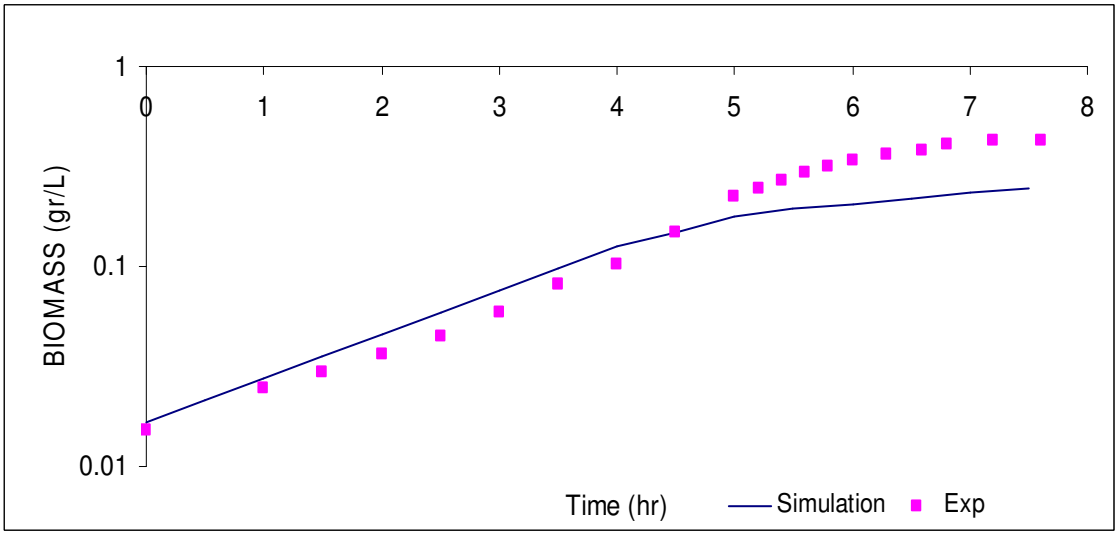

Figure 7.43. Biomass profile for mixed substrates; glucose, lactose, and galactose in *Lactococcus lactis*

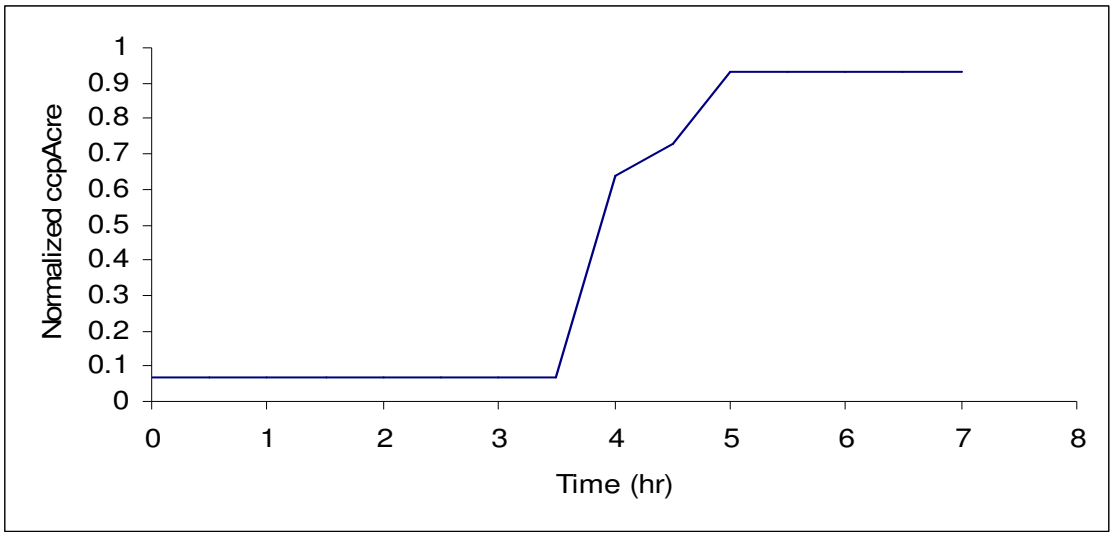

Figure 7.44. Normalized ccpAcre profile for mixed substrates; glucose, lactose, and galactose in *Lactococcus lactis*

The growth behaviour of *Lactococcus lactis* which is a gram positive bacterium, is examined glucose, lactose and galactose. First of all, this strain is different from *E. coli.* The membrane transport system and operon structure of *gal* operon are different in *L. lactis*. Glucose and lactose belong to the phosphotransferase system (PTS), whereas galactose belongs to permease transport system. It means that glucose and lactose will be used simultaneously at the beginning and galactose will be taken up sequentially. The same uptake rates and initial conditions on glucose and lactose are assumed in order to make a comparison between *L. lactis* and *E. coli*. *L. lactis* is a lactic acid bacteria. It is used for the production of lactic acid in fermented foods. Fermentation is anaerobic growth of biomass. It is clear that the biomass yield is lower than in *E. coli* which possesses aerobic growth. Due to the low growth rate for all substrates, they are consumed totally only after long of time periods. The inhibition of galactose transport is accomplished by both glucose and lactose. Since there is a high glucose uptake, glucose is depleted earlier than the others, like in *E. coli.* Finally, galactose is the only substrate in the medium. Catabolite Repression (CR) is mediated via a negative regulatory mechanism. Disruption of the *ccpA* gene reduces catabolite repression of several genes involved in the carbohydrate metabolism. A cis-acting sequence, termed catabolite-

responsive element (*cre*), present near the promoter of genes affected by CR, was found to be essential for mediating CR. A normalized *ccpAcre* is drawn Figure 7.44 to show the induction of galactose transport through the cell membrane. In Figure 7.43, there are two shifts in the growth level giving an allowance of uptake. The growth of biomass due to galactose is negligible. Moreover, growth on glucose is higher than the growth on lactose. Therefore, the same conclusion ($\mu_{GLC} > \mu_{LCTS} > \mu_{GLAC}$) on the growth rates can be made as was the case in *E. coli*. Experimental results are also given on the Figures 7.40 – 7.43 for the validation of simulation result. Simulated glucose and galactose concentrations fit the experimental data well. However, the simulated results of lactose utilization occur earlier than the experimental results. There is also a discrepancy between simulated and experimental results of biomass profile especially on galactose utilization. There are two noticeable slopes of the experimental data parts. In the simulation, there is no lag phase on the shift from one substrate to another, because glucose and lactose are transported through the membrane by phosphotransferase system and both have repression on the production of galactose permease. The substrates are always taken up by pairs. The pairs are glucose and lactose, lactose and galactose, and galactose itself. Therefore, the slope of biomass concentration curve (growth rate) is only slightly changed upon the substitution of one substrate to another in a pairwise manner.

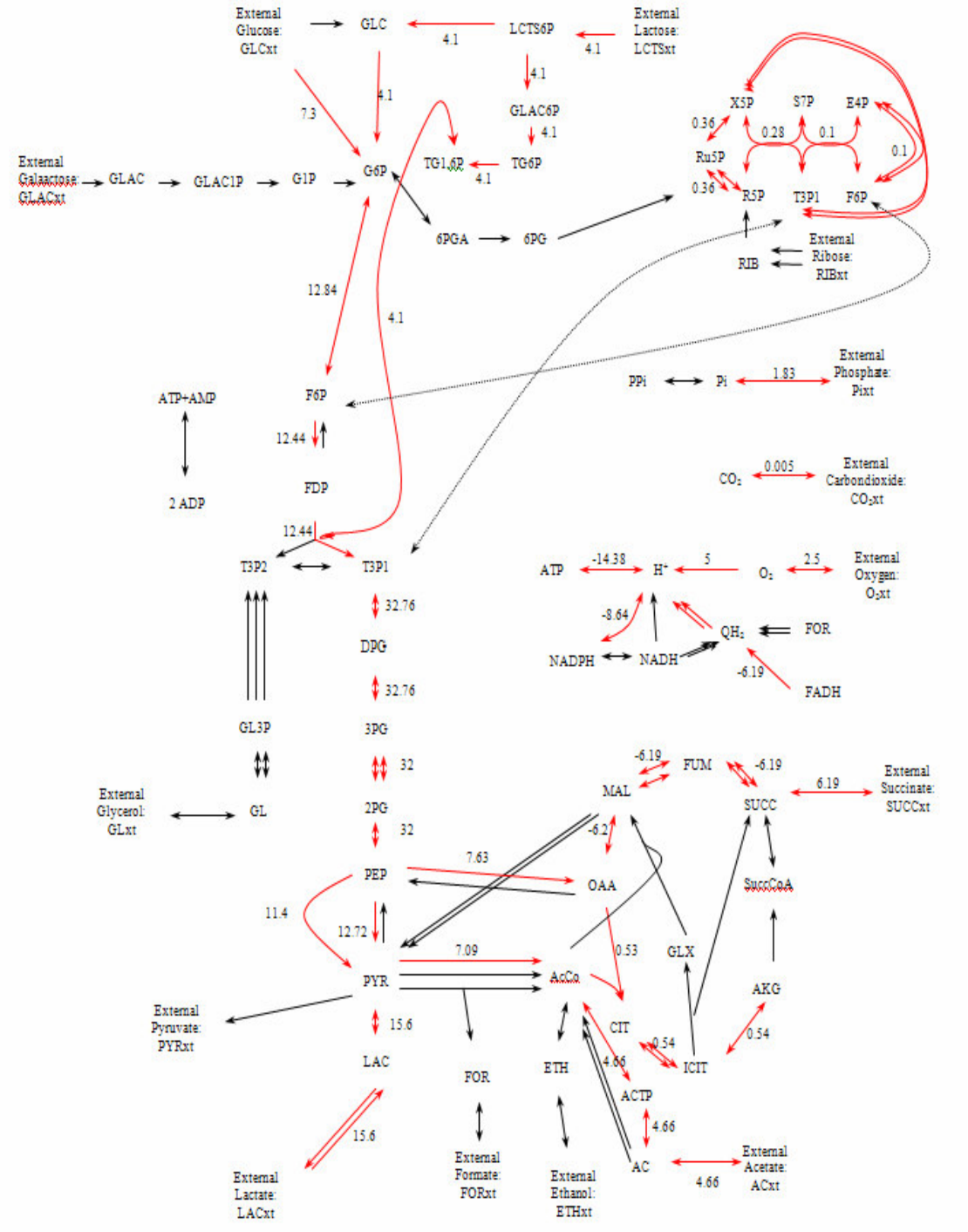

Figure 7.45. Flux distribution for anaerobic (microaerobic) metabolism of glucose and lactose by *Lactococcus lactis*

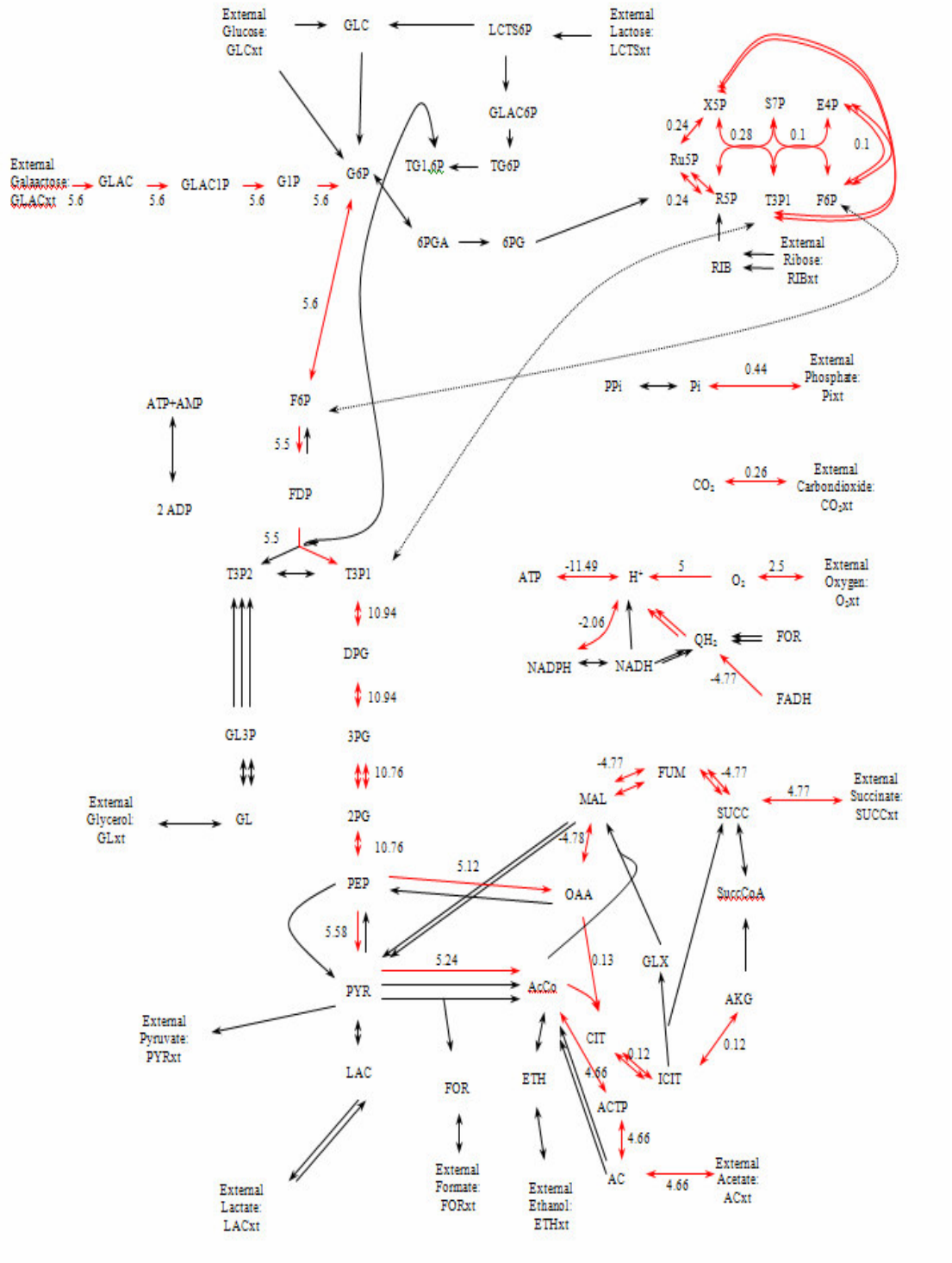

Figure 7.46. Flux distribution for anaerobic (microaerobic) metabolism of galactose by *Lactococcus lactis*

The flux distributions of glucose and lactose (PTS), and galactose (permease) anaerobic metabolisms of *L. lactis* are given in Figure 7.45 and 7.46. The red arrows show the dominant fluxes, whereas the black ones are stagnant rates on the metabolism. When there is a shift from one substrate to another, flux distribution on the metabolism is more or less the same. But, the fluxes change a little bit. In general, fluxes are higher which give more biomass production on glucose and lactose than galactose. The only difference on flux distributions is the pathway of the substrate uptake. The flux distribution on the TCA cycle is different than the aerobic growth in *E. coli*. Flux is not distributed all over the cycle completely and the dominant reactions, which give rise to entrance to the cycle, are different in anaerobic growth. External succinate, lactate and acetate are formed from the substrates in anaerobic growth which reduce the biomass yield.

8. CONCLUSION AND RECOMMENDATION

8.1. Conclusion

Aerobic growth of *Escherichia coli* and anaerobic growth of *Lactococcus lactis* in multiple carbon source of substrates are examined incorporating transcriptional regulation based on fuzzy logic. The computational method consists of dynamic flux balance analysis (FBA) and transcriptional regulation which are structured in MATLAB/SIMULINK.

Mainly, diauxic shift on glucose and lactose growth is studied in *E. coli*. In order to explain the regulatory shift, the operon structure controlling the environmental conditions must be known. *Lac* operon is responsible for the repression of glucose over lactose and the induction of lactose uptake. Glucose and lactose diauxic growth is modeled by *lac* operon structured in Fuzzy Logic. Aditionally, pulse injections of glucose, galactose and mixture of glucose and galactose are simulated over diauxic growth in *E. coli* in order to validate *lac* operon construction and to study *gal* operon which is responsible for the galactose uptake. The membrane transport system is also important in the sequence of sugar uptakes. Glucose, sorbitol (glucitol), and glycerol mixture growth is examined in *E. coli* both to analyze the responsible operons namely, *gut* operon and *glpKF* transcriptional unit and investigate the sugar uptake strategy which are either sequential or simultaneous. Anaerobic growth on glucose, lactose and galactose mixture is also simulated in *L. lactis,* which is lactic acid bacterium. All operon regulatory structure including *lac* operon are arranged in Fuzzy Logic.

Fuzzy Logic is introduced into regulatory flux balance analysis on the metabolic networks, where Boolean logic had been used earlier (Covert and Palsson, 2002). The results found in this study show that fuzzy logic can be better than Boolean logic. The structure of the operon, which controls the uptake of substrate or the rate of flux, is easily and quantitatively modeled by fuzzy controllers. The regulatory genes are considered either “on” or “off” in Boolean logic. Therefore, the adaptation of regulatory structure to changes in substrate concentration in the medium cannot be reflected as it happens. In the case of diauxic growth of

E. coli on glucose and lactose, the lag phase time period, which is formed due to catabolite repression and inducer exclusion, cannot be incorporated into the calculation of flux distributions when the regulatory structure is not modeled as when a Boolean formalism is preferred. Another result that can be deduced from fuzzy logic formalism, is the pulse injection of primarily preferred substrate to a medium when any other substrate uptake is being held. There will be an adaptation time to the uptake of preferred substrate that can easily be handled by this formalism. Fuzzy logic controlling action because of its gene expression model inside its inference, can deal with alteration from a higher level to a lower one, or vice versa. On simultaneous and sequential growth, fuzzy can be more effective than other logical structure. At any time, substrate that is repressed by other two substrates, cannot be modeled correctly in Boolean formalism. Partial substrate uptake rate is easily added in the metabolic network if fuzzy logic is used. The sugar can be utilized partially after the one of preferable sugars is totally consumed.

Fuzzy logic depends on human knowledge and experience on the system. Therefore, there is no unique way to map and implicate the solution. If the solution is estimated correctly, the logical structure can control the transcriptional regulation in an appropriate form.

Estimated initial conditions and substrate uptake rate constraints are taken either from the literature or that best fit to the flux distribution of growth. Therefore, there is no problem on the validation of experimental data if they exist. Fuzzy Inference System and Fuzzy Controller included in the model are easy to implement and insert into the calculations of Linear Programming.

8.2. Recommendation

The substrate uptake rates are held constant at each time step of calculations which is an undesirable assumption. However, uptake rate in each step cannot be predicted with the previous results. Actually, sugar uptake rate are different on initial, exponential, lag, stationary phases. Only an average of exponential phase uptake rate is used which is assumed to be constant. The uptake rate at each step must be estimated by a calculation method.

The fuzzy models are structured on one antecedent to one conclusion in our work. If more than one antecedent is used, the correlation of all in each other and effect on the conclusion must be well known. Fuzzy logic relies on the human knowledge and expertise on the system. Therefore, the gene expression and operon working principle must be examined very well which is coming from the experimental data. A more complicated operon model can be constructed relating two or more occasion to one or more conclusion.

Estimates of the initial conditions and substrate uptake rate constraints are chosen somewhat dependent on the range experimental data. That is, if the biomass concentration and substrate concentrations are increased in the medium, the behavior of biomass yield will be different. A quantity of bacteria (biomass) is always treated as one bacterium. The starvation on the substrate will be dominant if the biomass has been increased in excess amounts. Therefore, the study must be carried out in a range of experiments.

The reaction list contains mainly 113 reactions which were studied to determine the ability of the model to make accurate phenotypic predictions (Covert, 2002). These reactions and additional ones for different substrate membrane transport systems in *E. coli* and *L. lactis* are enough to model the regulation of the shift. Additional pathways can be included to the list. If a pathway is missed which affects the biomass growth, the simulated result will deviate from the experimental ones. Also, a better definition of biomass growth rate can be written to form more precise results.

APPENDIX A: SIMULATION RESULTS

A.1. Growth in Single Substrate of Glucose or Lactose of *Escherichia coli*

Table A.1. Growth in Single Substrate of Glucose of *Escherichia coli*

Time (hr)	GLUCOSE (mmol/L)	Biomass (g/L)
0.0	1.60	0.011
0.5	1.56	0.015
1.0	1.50	0.020
1.5	1.43	0.027
2.0	1.33	0.036
2.5	1.19	0.048
3.0	1.01	0.064
3.5	0.77	0.086
4.0	0.45	0.115
4.5	0.02	0.154
5.0	0.00	0.154

Table A.2. Growth in Single Substrate Lactose of *Escherichia coli*

Time (hr)	LACTOSE (mmol/L)	Biomass (g/L)
0.0	5.80	0.011
0.5	5.78	0.014
1.0	5.76	0.019
1.5	5.72	0.024
2.0	5.68	0.032
2.5	5.63	0.042
3.0	5.56	0.054
3.5	5.46	0.071
4.0	5.34	0.092
4.5	5.18	0.120
5.0	4.98	0.157
5.5	4.71	0.205
6.0	4.35	0.267
6.5	3.89	0.349
7.0	3.29	0.455
7.5	2.51	0.594
8.0	1.49	0.775
8.5	0.16	1.011
9.0	0.00	1.011

A.2. Growth in Mixed Substrates of Glucose and Lactose of *Escherichia coli*

Table A.3. Growth in Mixed Substrates of Glucose and Lactose of *Escherichia coli*

Time (hr)	GLUCOSE (MMOL/L)	LACTOSE (MMOL/L)	O_2 UPTAKE (mM/g DW.hr)	Biomass (g/L)	cAMP	GROWTH RATE: μ (1/hr)
0	1.60	5.80	13.98	0.011	0.07	0.6166
0.5	1.56	5.80	13.98	0.015	0.07	0.6166
1	1.50	5.80	13.98	0.020	0.07	0.6166
1.5	1.42	5.80	13.98	0.028	0.07	0.6166
2	1.32	5.79	13.98	0.038	0.07	0.6166
2.5	1.17	5.79	13.98	0.051	0.07	0.6166
3	0.98	5.79	13.98	0.070	0.07	0.6166
3.5	0.71	5.78	13.98	0.095	0.07	0.6166
4	0.35	5.77	12.25	0.130	0.24	0.5053
4.5	0.00	5.76	5.64	0.167	0.93	0.0772
5	0.00	5.70	10.45	0.173	0.93	0.3805
5.5	0.00	5.48	12.87	0.210	0.93	0.5319
6	0.00	5.12	12.87	0.274	0.93	0.5319
6.5	0.00	4.65	12.87	0.357	0.93	0.5319
7	0.00	4.04	12.87	0.466	0.93	0.5319
7.5	0.00	3.24	12.87	0.608	0.93	0.5319
8	0.00	2.19	12.87	0.793	0.93	0.5319
8.5	0.00	0.83	8.38	1.034	0.93	0.2510
9	0.00	0.00		1.172		

A.3. Growth in Mixed Substrates of Glucose and Lactose and a Pulse Injection of Glucose of *Escherichia coli*

Table A.4. Growth in Mixed Substrates of Glucose and Lactose and a Pulse Injection of Glucose of *Escherichia coli*

Time (hr)	GLUCOSE (MMOL/L)	LACTOSE (MMOL/L)	O2 UPTAKE (mM/g DW.hr)	Biomass (g/L)	cAMP	GROWTH RATE: μ (1/hr)
0	1.60	5.80	13.982	0.011	0.07	0.617
0.5	1.56	5.80	13.982	0.015	0.07	0.617
1	1.50	5.80	13.982	0.020	0.07	0.617
1.5	1.42	5.80	13.982	0.028	0.07	0.617
2	1.32	5.79	13.982	0.038	0.07	0.617
2.5	1.17	5.79	13.982	0.051	0.07	0.617
3	0.98	5.79	13.982	0.070	0.07	0.617
3.5	0.71	5.78	13.982	0.095	0.07	0.617
4	0.35	5.77	12.246	0.130	0.24	0.505
4.5	0.00	5.76	5.641	0.167	0.93	0.077
5	0.00	5.70	10.450	0.173	0.93	0.381
5.5	0.00	5.48	12.867	0.210	0.93	0.532
6	0.00	5.12	12.867	0.274	0.93	0.532
6.5	0.00	4.65	12.867	0.357	0.93	0.532
7	0.00	4.04	12.867	0.466	0.93	0.532
7.5	2.50	3.24	13.982	0.608	0.07	0.617
8	0.19	3.18	6.334	0.827	0.86	0.124
8.5	0.00	2.86	5.641	0.880	0.93	0.077
9	0.00	2.53	10.450	0.914	0.93	0.381
9.5	0.00	1.39	11.328	1.106	0.93	0.436
10	0.00	0.00		1.375		0.039

A.4. Growth in Mixed Substrates of Glucose and Lactose and a Pulse Injection of Glucose with Membrane Transport System of *Escherichia coli*

Table A.5. Growth in Mixed Substrates of Glucose and Lactose and a Pulse Injection of Glucose with Membrane Transport System of *Escherichia coli*

Time (hr)	GLUCOSE (MMOL/L)	LACTOSE (MMOL/L)	O2 UPTAKE (mM/g DW.hr)	Biomass (g/L)	cAMP	GROWTH RATE: μ (1/hr)
0.0	1.60	5.80	13.98	0.011	0.14	0.6166
0.5	1.56	5.80	13.98	0.015	0.14	0.6166
1.0	1.50	5.80	13.98	0.020	0.14	0.6166
1.5	1.42	5.80	13.98	0.028	0.14	0.6166
2.0	1.32	5.79	13.98	0.038	0.14	0.6166
2.5	1.17	5.79	13.98	0.051	0.14	0.6166
3.0	0.98	5.79	13.98	0.070	0.14	0.6166
3.5	0.71	5.78	13.98	0.095	0.14	0.6166
4.0	0.35	5.77	12.25	0.130	0.25	0.5053
4.5	0.00	5.76	5.64	0.167	0.86	0.0772
5.0	0.00	5.70	10.45	0.173	0.86	0.3805
5.5	0.00	5.48	12.87	0.210	0.86	0.5319
6.0	0.00	5.12	12.87	0.274	0.86	0.5319
6.5	0.00	4.65	12.87	0.357	0.86	0.5319
7.0	0.00	4.04	12.87	0.466	0.86	0.5319
7.5	2.50	3.24	13.98	0.608	0.14	0.6166
8.0	0.19	3.18	6.33	0.827	0.77	0.1238
8.5	0.00	2.86	5.64	0.880	0.86	0.0772
9.0	0.00	2.53	10.45	0.914	0.86	0.3805
9.5	0.00	1.39	11.33	1.106	0.86	0.4355
10.0	0.00	0.00		1.375		0.0386

A.4. Growth in Mixed Substrates of Glucose and Lactose with a Pulse Injection of Galactose of *Escherichia coli*

Table A.6. Growth in Mixed Substrates of Glucose and Lactose with a Pulse Injection of Galactose of *Escherichia coli*

Time (hr)	GLUCOSE (MMOL/L)	LACTOSE (MMOL/L)	O_2 UPTAKE (mM/g DW.hr)	Biomass (g/L)	cAMP	GROWTH RATE: μ (1/hr)
0.0	1.60	5.80	13.98	0.011	0.14	0.6166
0.5	1.56	5.80	13.98	0.015	0.14	0.6166
1.0	1.50	5.80	13.98	0.020	0.14	0.6166
1.5	1.42	5.80	13.98	0.028	0.14	0.6166
2.0	1.32	5.79	13.98	0.038	0.14	0.6166
2.5	1.17	5.79	13.98	0.051	0.14	0.6166
3.0	0.98	5.79	13.98	0.070	0.14	0.6166
3.5	0.71	5.78	13.98	0.095	0.14	0.6166
4.0	0.35	5.77	12.25	0.130	0.25	0.5053
4.5	0.00	5.76	5.64	0.167	0.86	0.0772
5.0	0.00	5.70	10.45	0.173	0.86	0.3805
5.5	0.00	5.48	12.87	0.210	0.86	0.5319
6.0	0.00	5.12	12.87	0.274	0.86	0.5319
6.5	0.00	4.65	12.87	0.357	0.86	0.5319
7.0	0.00	4.04	12.87	0.466	0.86	0.5319
7.5	2.50	3.24	13.98	0.608	0.14	0.6166
8.0	0.19	3.18	6.33	0.827	0.77	0.1238
8.5	0.00	2.86	5.64	0.880	0.86	0.0772
9.0	0.00	2.53	10.45	0.914	0.86	0.3805
9.5	0.00	1.39	11.33	1.106	0.86	0.4355
10.0	0.00	0.00		1.375		0.0386

A.5. Growth in Mixed Substrates of Glucose and Lactose and a Pulse Injection of Glucose and Galactose Mixture of *Escherichia coli*.

Table A.7. Growth in Mixed Substrates of Glucose and Lactose and a Pulse Injection of Glucose and Galactose Mixture of *Escherichia coli*

Time (hr)	GLUCOSE (MMOL/L)	LACTOSE (MMOL/L)	GALACTOSE (MMOL/L)	O_2 UPTAKE (mM/g DW.hr)	Biomass (g/L)	cAMP	GROWTH RATE: μ (1/hr)
0.0	1.60	5.80	0.00	13.982	0.011	0.07	0.6166
0.5	1.56	5.80	0.00	13.982	0.015	0.07	0.6166
1.0	1.50	5.80	0.00	13.982	0.020	0.07	0.6166
1.5	1.42	5.80	0.00	13.982	0.028	0.07	0.6166
2.0	1.32	5.79	0.00	13.982	0.038	0.07	0.6166
2.5	1.17	5.79	0.00	13.982	0.051	0.07	0.6166
3.0	0.98	5.79	0.00	13.982	0.070	0.07	0.6166
3.5	0.71	5.78	0.00	13.982	0.095	0.07	0.6166
4.0	0.35	5.77	0.00	12.246	0.130	0.24	0.5053
4.5	0.00	5.76	0.00	5.6408	0.167	0.93	0.0772
5.0	0.00	5.70	0.00	10.45	0.173	0.93	0.3805
5.5	0.00	5.48	0.00	12.867	0.210	0.93	0.5319
6.0	0.00	5.12	0.00	12.867	0.274	0.93	0.5319
6.5	0.00	4.65	0.00	12.867	0.357	0.93	0.5319
7.0	0.00	4.04	0.00	12.867	0.466	0.93	0.5319
7.5	0.00	3.24	8.50	23.513	0.608	0.93	1.1838
8.0	0.00	1.99	5.81	23.513	1.098	0.93	1.1838
8.5	0.00	0.00	0.94	4.8088	1.985	0.93	0.0199
9.0	0.00	0.00	0.00		2.005		

A.6. Growth in Mixed Substrates of Glucose, Sorbitol (Glucitol) and Glycerol of *Escherichia coli*

Table A.8. Growth in Mixed Substrates of Glucose, Sorbitol (Glucitol) and Glycerol of *Escherichia coli*

Time (hr)	GLUCOSE (MMOL/L)	SORBITOL (MMOL/L)	GLYCEROL (MMOL/L)	O_2 UPTAKE (mM/g DW.hr)	Biomass (g/L)	cAMP CRP	GROWTH RATE: μ (1/hr)
0.0	1.20	1.10	1.10	19.379	0.0080	0.12	0.9712
0.5	1.16	1.09	1.10	19.379	0.0130	0.12	0.9712
1.0	1.09	1.08	1.09	19.379	0.0211	0.12	0.9712
1.5	0.98	1.06	1.08	19.379	0.0343	0.12	0.9712
2.0	0.81	1.02	1.05	19.379	0.0558	0.12	0.9712
2.5	0.52	0.96	1.02	19.379	0.0907	0.12	0.9712
3.0	0.05	0.87	0.97	17.271	0.1474	0.84	1.5387
3.5	0.00	0.41	0.67	15.269	0.3181	0.93	0.9749
4.0	0.00	0.00	0.17	4.702	0.5179	0.93	0.0001
4.5	0.00	0.00	0.00	4.320	0.5179	0.93	0.0684

A.7. Growth in Mixed substrates of Glucose, Lactose and Galactose of *Lactococcus lactis*

Table A.9. Growth in Mixed substrates of Glucose, Lactose and Galactose of *Lactococcus lactis*

Time (hr)	GLUCOSE (MMOL/L)	LACTOSE (MMOL/L)	GALACTOSE (MMOL/L)	Biomass (g/L)	ccpA-Cre	GROWTH RATE: μ (1/hr)
0.0	1.58	1.58	4.00	0.017	0.07	0.5039
0.5	1.51	1.54	3.99	0.021	0.07	0.5039
1.0	1.42	1.49	3.97	0.028	0.07	0.5039
1.5	1.31	1.43	3.94	0.036	0.07	0.5039
2.0	1.16	1.34	3.91	0.046	0.07	0.5039
2.5	0.97	1.24	3.87	0.059	0.07	0.5039
3.0	0.72	1.10	3.82	0.076	0.07	0.5039
3.5	0.41	0.92	3.75	0.097	0.07	0.5039
4.0	0.01	0.70	3.67	0.125	0.64	0.3457
4.5	0.00	0.42	3.39	0.149	0.73	0.3464
5.0	0.00	0.08	3.04	0.177	0.93	0.1828
5.5	0.00	0.00	2.52	0.194	0.93	0.1205
6.0	0.00	0.00	1.96	0.206	0.93	0.1205
6.5	0.00	0.00	1.36	0.219	0.93	0.1205
7.0	0.00	0.00	0.73	0.233	0.93	0.1205
7.5	0.00	0.00	0.05	0.247		

APPENDIX B: COMPUTATIONAL CODE STRUCTURED IN MATLAB

The computational codes for growth in mixed substrates of *Esherichia coli* and *Lactococcus lactis* are given in the successive sections as a hardcopy. The computational work was performed in *Matlab*. The developed programs were also given in a separate CD as a softcopy which is attached to the end of this Thesis. In addition to these programs, Fuzzy Controller Blocks, structured in *Simulink Matlab*, were also included in the CD. The structure variables describing their Fuzzy Inference System were entered to a Fuzzy Controller Blocks. The variables must be located in the MATLAB workspace when the program is executed.

B.1. Matlab Code for Growth in Mixed Substrates of Glucose and Lactose of *Escherichia coli*

```
clc
clear all
close all
GlucosecAMP=readfis('GlucosecAMP'); cAMPLacZYA=readfis('cAMPLacZYA');
LacYLactoseUptakeGlucose=readfis('LacYLactoseUptakeGlucose');
LactoseUptakeAllolactoseRepressor=readfis('LactoseUptakeAllolactoseRepressor');
AllolactoseLacZYA=readfis('AllolactoseLacZYA');
LacYLactoseUptakeLactose=readfis('LacYLactoseUptakeLactose');
%Initial concentration of External Biomass (XMe)(g/L) & External Glucose (GluMe)(mmol/L)
LacMe=5.8; GluMe=1.6; XMe=0.011;
%Time step 0.5 hr
dt=0.5;
```

```
%Initial Values of Substrate Glucose Concentration (mmol/L)
LACTOSE(1)=LacMe; GLUCOSE(1)=GluMe; XBio(1)=XMe; t(1)=0;
Scavlactose=LACTOSE(1)/XBio(1)/dt; Scavglucose=GLUCOSE(1)/XBio(1)/dt;
Supinitiallactose=3.0; Supinitialglucose=6.5; Suplactose=0.15; Supglucose=6.5;
Slacup=Suplactose/Supinitiallactose; Sglup=Supglucose/Supinitialglucose;
GlucoseUptake=[0 Sglup]; LactoseUptake=[0 Slacup];
    for i=1:19
%Time
t(i+1)=t(i)+dt;
%Linear Programming for the maximization of Biomass
%Stoichiometric matrix for MFA - E-COLI
A=xlsread('DENEMEECOLI', 'Matrix');
B=A';
Ib=zeros(167,1); ub=inf*ones(167,1);
%Upper&Lower Boundaries of ATP non-growth associated maintenance flux
Ib(151,1)=15; ub(151,1)=15;
%Upper&Lower Boundaries of Biomass Production fluxes
Ib(152,1)=0; ub(152,1)=inf;
%When the glucose concentration becomes considerable diluted level
%Upper&Lower Boundaries of Glucose Transport fluxes
  Ib(154,1)=min(Supglucose,Scavglucose); ub(154,1)=min(Supglucose,Scavglucose);
de=Ib(154,1)/Supinitialglucose;
GlucoseUptake=[0 de];
%Upper&Lower Boundaries of Transport fluxes
sim('GlucoseUptake')
cAMPList(i,1)=cAMP;
```

```
if cAMP<=0.70
    Suplactose=0.15;
    Slacup=Suplactose/Supinitiallactose;
    LactoseUptake=[0 Slacup]

elseif    cAMP>0.70

    if cAMP>=0.90
       if i==x
    sim('LactoseUptake')
    Suplactose=LactoseUptakeResult*Supinitiallactose;
    LactoseUptake=[0 LactoseUptakeResult];
       else
    sim('LactoseUptake')
    LUR=LactoseUptakeResult+GLactoseUptakeResult;
    Suplactose=LUR*Supinitiallactose;
    LactoseUptake=[0 LUR];
end

    else
    sim('LactoseUptake')
    Suplactose=LactoseUptakeResult*Supinitiallactose
    LactoseUptake=[0 LactoseUptakeResult];

end
end
```

```
%Lac Operon regulation structured in Fuzzy Logic Controller in Simulink
Ib(155,1)=min(Suplactose,Scavlactose); ub(155,1)=min(Suplactose,Scavlactose);
%GLup
Ib(156,1)=0; ub(156,1)=0;
%PYRup
Ib(157,1)=-inf; ub(157,1)=0;
%LACup
Ib(158,1)=-inf; ub(158,1)=0;
%FORup
Ib(159,1)=-inf; ub(159,1)=0;
%ETHup
Ib(160,1)=-inf; ub(160,1)=0;
%Acup
Ib(161,1)=-inf; ub(161,1)=0;
%SUCCup
Ib(162,1)=-inf; ub(162,1)=0;
%RIBup
Ib(163,1)=0; ub(163,1)=0;
%Piup
Ib(164,1)=0; ub(164,1)=inf;
%CO2up
Ib(165,1)=-inf; ub(165,1)=0;
%O2up
Ib(166,1)=0; ub(166,1)=inf;
%HEup
Ib(167,1)=0; ub(167,1)=0;
```

```
f=zeros(167,1);
f(152,1)=-1;
b=zeros(77,1);
X=linprog(f,[],[],B,b,Ib,ub);
SON(:,i)=X;
O2up(i,1)=X(166,1);
LACTOSE(i+1)=LACTOSE(i)+X(155,1)/X(152,1)*XBio(i)*(1-exp(X(152,1)*dt));
GLUCOSE(i+1)=GLUCOSE(i)+X(154,1)/X(152,1)*XBio(i)*(1-exp(X(152,1)*dt));
if LACTOSE(i+1)<=0
  LACTOSE(i+1)=0;
end
if GLUCOSE(i+1)<=0
   GLUCOSE(i+1)=0;
   if GLUCOSE(i)-GLUCOSE(i+1)>0
     x=i+1
  end
end
XBio(i+1)=XBio(i)*exp(X(152,1)*dt); Scavlactose=LACTOSE(i+1)/XBio(i+1)/dt
Scavglucose=GLUCOSE(i+1)/XBio(i+1)/dt
VGRO(i,1)=X(152,1); UPG(i,1)=Ib(154,1); UPL(i,1)=Ib(155,1);
a(i)=t(i);
end
figure(1)
plot(t,XBio)
xlabel('Time (hr)')
title('Biomass Concentration (g/L)  vs Time ')
```

```
figure(2)
plot(t,GLUCOSE)
xlabel('Time (hr)')
title('GLUCOSE (mM)')
figure(3)
plot(t,LACTOSE)
xlabel('Time (hr)')
title('LACTOSE (mM)')
figure(4)
plot(a,cAMPList)
xlabel('Time (hr)')
title('cAMPList')
figure(5)
plot(a,O2up)
xlabel('Time (hr)')
title('O2up (mM/grDW.hr)')
```

B.2. Matlab Code for Growth in Mixed Substrates of Glucose and Lactose with Membrane Transport System of *Escherichia coli*

```
clc
clear all
close all
GlucoseEIIAP=readfis('GlucoseEIIAP'); EIIAPcAMP=readfis('EIIAPcAMP');
cAMPLacZYA2=readfis('cAMPLacZYA2');
LacYLactoseUptakeGlucose=readfis('LacYLactoseUptakeGlucose');
LactoseUptakeAllolactoseRepressor=readfis('LactoseUptakeAllolactoseRepressor');
AllolactoseLacZYA=readfis('AllolactoseLacZYA');
LacYLactoseUptakeLactose=readfis('LacYLactoseUptakeLactose');
%Initial concentration of External Biomass (XMe)(g/L) & External Glucose (GluMe)(mmol/L)
LacMe=5.8; GluMe=1.6; XMe=0.011;
%Time step 0.5 hr
dt=0.5;
%Initial Values of Substrate Glucose Concentration (mmol/L)
LACTOSE(1)=LacMe; GLUCOSE(1)=GluMe; XBio(1)=XMe; t(1)=0;
Scavlactose=LACTOSE(1)/XBio(1)/dt; Scavglucose=GLUCOSE(1)/XBio(1)/dt;
Supinitiallactose=3.0; Supinitialglucose=6.5; Suplactose=0.15; Supglucose=6.5;
Slacup=Suplactose/Supinitiallactose; Sglup=Supglucose/Supinitialglucose;
GlucoseUptake=[0 Sglup]; LactoseUptake=[0 Slacup];
   for i=1:21
%Time
t(i+1)=t(i)+dt;
%Linear Programming for the maximization of Biomass
```

```
%Stoichiometric matrix for MFA - E-COLI
A=xlsread('DENEMEECOLI', 'Matrix');
B=A';
Ib=zeros(167,1);
ub=inf*ones(167,1);
%Upper&Lower Boundaries of ATP non-growth associated maintenance flux
Ib(151,1)=15; ub(151,1)=15;
%Upper&Lower Boundaries of Biomass Production fluxes
Ib(152,1)=0; ub(152,1)=inf;
%When the glucose concentration becomes considerable diluted level
%Upper&Lower Boundaries of Glucose Transport fluxes
  Ib(154,1)=min(Supglucose,Scavglucose);   ub(154,1)=min(Supglucose,Scavglucose);
de=Ib(154,1)/Supinitialglucose;
GlucoseUptake=[0 de];
%Upper&Lower Boundaries of Transport fluxes
if i==16
% Pulse 2.5mmol/L glucose is added to the medium.
Glupulse=2.5;
GLUCOSE(i)=Glupulse;
Scavglucose=Glupulse/XBio(i)/dt;
Supglucose=6.5; Supinitialglucose=6.5;
Ib(154,1)=min(Supglucose,Scavglucose); ub(154,1)=min(Supglucose,Scavglucose);
de=Ib(154,1)/Supinitialglucose;
GlucoseUptake=[0 de];
end
sim('GlucoseEIIAPUptake')
```

```
cAMPList(i,1)=cAMP;
if cAMP<=0.70
   Suplactose=0.15;
   Slacup=Suplactose/Supinitiallactose;
   LactoseUptake=[0 Slacup]
elseif    cAMP>0.70
   if cAMP>=0.84
      if i==x
   sim('LactoseUptake')
   Suplactose=LactoseUptakeResult*Supinitiallactose;
   LactoseUptake=[0 LactoseUptakeResult];
      else
   sim('LactoseUptake')
   LUR=LactoseUptakeResult+GLactoseUptakeResult;
   Suplactose=LUR*Supinitiallactose;
   LactoseUptake=[0 LUR];
end
   else
   sim('LactoseUptake')
   Suplactose=LactoseUptakeResult*Supinitiallactose
   LactoseUptake=[0 LactoseUptakeResult];
end
end
%Lac Operon regulation structured in Fuzzy Logic Controller in Simulink
Ib(155,1)=min(Suplactose,Scavlactose); ub(155,1)=min(Suplactose,Scavlactose);
%GLup
```

```
Ib(156,1)=0; ub(156,1)=0;
%PYRup
Ib(157,1)=-inf; ub(157,1)=0;
%LACup
Ib(158,1)=-inf; ub(158,1)=0;
%FORup
Ib(159,1)=-inf; ub(159,1)=0;
%ETHup
Ib(160,1)=-inf; ub(160,1)=0;
%Acup
Ib(161,1)=-inf; ub(161,1)=0;
%SUCCup
Ib(162,1)=-inf; ub(162,1)=0;
%RIBup
Ib(163,1)=0; ub(163,1)=0;
%Piup
Ib(164,1)=0; ub(164,1)=inf;
%CO2up
Ib(165,1)=-inf; ub(165,1)=0;
%O2up
Ib(166,1)=0; ub(166,1)=inf;
%HEup
Ib(167,1)=0; ub(167,1)=0;
f=zeros(167,1);
f(152,1)=-1;
b=zeros(77,1);
```

```
X=linprog(f,[],[],B,b,Ib,ub);
SON(:,i)=X;
O2up(i,1)=X(166,1);
LACTOSE(i+1)=LACTOSE(i)+X(155,1)/X(152,1)*XBio(i)*(1-exp(X(152,1)*dt));
GLUCOSE(i+1)=GLUCOSE(i)+X(154,1)/X(152,1)*XBio(i)*(1-exp(X(152,1)*dt));
if LACTOSE(i+1)<=0
  LACTOSE(i+1)=0;
end
if GLUCOSE(i+1)<=0
   GLUCOSE(i+1)=0;
   if GLUCOSE(i)-GLUCOSE(i+1)>0
      x=i+1
  end
end
XBio(i+1)=XBio(i)*exp(X(152,1)*dt); Scavlactose=LACTOSE(i+1)/XBio(i+1)/dt
Scavglucose=GLUCOSE(i+1)/XBio(i+1)/dt
VGRO(i,1)=X(152,1); UPG(i,1)=Ib(154,1); UPL(i,1)=Ib(155,1); a(i)=t(i);
end
figure(1)
plot(t,XBio)
xlabel('Time (hr)')
title('Biomass Concentration (g/L)  vs Time ')
figure(2)
plot(t,GLUCOSE)
xlabel('Time (hr)')
title('GLUCOSE (mM)')
```

```
figure(3)
plot(t,LACTOSE)
xlabel('Time (hr)')
title('LACTOSE (mM)')
figure(4)
plot(a,cAMPList)
xlabel('Time (hr)')
title('cAMPList')
figure(5)
plot(a,O2up)
xlabel('Time (hr)')
title('O2up (mM/grDW.hr)')
```

B.3. Growth in Mixed Substrates of Glucose and Lactose and a Pulse Injection of Glucose on Lactose of *Escherichia coli*

```
clc
clear all
close all
GlucosecAMP=readfis('GlucosecAMP'); cAMPLacZYA=readfis('cAMPLacZYA');
LacYLactoseUptakeGlucose=readfis('LacYLactoseUptakeGlucose');
LactoseUptakeAllolactoseRepressor=readfis('LactoseUptakeAllolactoseRepressor');
AllolactoseLacZYA=readfis('AllolactoseLacZYA');
LacYLactoseUptakeLactose=readfis('LacYLactoseUptakeLactose');
%Initial concentration of External Biomass (XMe)(g/L) & External Glucose (GluMe)(mmol/L)
LacMe=5.8; GluMe=1.6; XMe=0.011;
%Time step 0.5 hr
dt=0.5;
%Initial Values of Substrate Glucose Concentration (mmol/L)
LACTOSE(1)=LacMe; GLUCOSE(1)=GluMe; XBio(1)=XMe; t(1)=0;
Scavlactose=LACTOSE(1)/XBio(1)/dt; Scavglucose=GLUCOSE(1)/XBio(1)/dt;
Supinitiallactose=3.0; Supinitialglucose=6.5; Suplactose=0.15; Supglucose=6.5;
Slacup=Suplactose/Supinitiallactose; Sglup=Supglucose/Supinitialglucose;
GlucoseUptake=[0 Sglup]; LactoseUptake=[0 Slacup];
   for i=1:21
%Time
t(i+1)=t(i)+dt;
%Linear Programming for the maximization of Biomass
%Stoichiometric matrix for MFA - E-COLI
```

```
A=xlsread('DENEMEECOLI', 'Matrix'); B=A';
Ib=zeros(167,1);
ub=inf*ones(167,1);
%Upper&Lower Boundaries of ATP non-growth associated maintenance flux
Ib(151,1)=15; ub(151,1)=15;
%Upper&Lower Boundaries of Biomass Production fluxes
Ib(152,1)=0; ub(152,1)=inf;
%When the glucose concentration becomes considerable diluted level
%Upper&Lower Boundaries of Glucose Transport fluxes
  Ib(154,1)=min(Supglucose,Scavglucose); ub(154,1)=min(Supglucose,Scavglucose);
de=Ib(154,1)/Supinitialglucose;
GlucoseUptake=[0 de];
%Upper&Lower Boundaries of Transport fluxes
if i==16
% Pulse 2.5mmol/L glucose is added to the medium.
Glupulse=2.5; GLUCOSE(i)=Glupulse;
Scavglucose=Glupulse/XBio(i)/dt;
Supglucose=6.5; Supinitialglucose=6.5;
Ib(154,1)=min(Supglucose,Scavglucose); ub(154,1)=min(Supglucose,Scavglucose);
de=Ib(154,1)/Supinitialglucose;
GlucoseUptake=[0 de];
end
sim('GlucoseUptake')
cAMPList(i,1)=cAMP;
if cAMP<=0.70
    Suplactose=0.15;
```

```
    Slacup=Suplactose/Supinitiallactose;
    LactoseUptake=[0 Slacup]
elseif    cAMP>0.70
    if cAMP>=0.90
        if i==x
    sim('LactoseUptake')
    Suplactose=LactoseUptakeResult*Supinitiallactose;
    LactoseUptake=[0 LactoseUptakeResult];
        else
    sim('LactoseUptake')
    LUR=LactoseUptakeResult+GLactoseUptakeResult;
    Suplactose=LUR*Supinitiallactose;
    LactoseUptake=[0 LUR];
end
    else
    sim('LactoseUptake')
    Suplactose=LactoseUptakeResult*Supinitiallactose
    LactoseUptake=[0 LactoseUptakeResult];
end
end
%Lac Operon regulation structured in Fuzzy Logic Controller in Simulink
Ib(155,1)=min(Suplactose,Scavlactose); ub(155,1)=min(Suplactose,Scavlactose);
%GLup
Ib(156,1)=0; ub(156,1)=0;
%PYRup
Ib(157,1)=-inf; ub(157,1)=0;
```

```
%LACup
Ib(158,1)=-inf; ub(158,1)=0;
%FORup
Ib(159,1)=-inf; ub(159,1)=0;
%ETHup
Ib(160,1)=-inf; ub(160,1)=0;
%Acup
Ib(161,1)=-inf; ub(161,1)=0;
%SUCCup
Ib(162,1)=-inf; ub(162,1)=0;
%RIBup
Ib(163,1)=0; ub(163,1)=0;
%Piup
Ib(164,1)=0; ub(164,1)=inf;
%CO2up
Ib(165,1)=-inf; ub(165,1)=0;
%O2up
Ib(166,1)=0; ub(166,1)=inf;
%HEup
Ib(167,1)=0; ub(167,1)=0;
f=zeros(167,1);
f(152,1)=-1;
b=zeros(77,1);
X=linprog(f,[],[],B,b,Ib,ub);
SON(:,i)=X; O2up(i,1)=X(166,1);
LACTOSE(i+1)=LACTOSE(i)+X(155,1)/X(152,1)*XBio(i)*(1-exp(X(152,1)*dt));
```

```
GLUCOSE(i+1)=GLUCOSE(i)+X(154,1)/X(152,1)*XBio(i)*(1-exp(X(152,1)*dt));
if LACTOSE(i+1)<=0
  LACTOSE(i+1)=0;
end
if GLUCOSE(i+1)<=0
   GLUCOSE(i+1)=0;
   if GLUCOSE(i)-GLUCOSE(i+1)>0
     x=i+1
  end
end
XBio(i+1)=XBio(i)*exp(X(152,1)*dt); Scavlactose=LACTOSE(i+1)/XBio(i+1)/dt
Scavglucose=GLUCOSE(i+1)/XBio(i+1)/dt
VGRO(i,1)=X(152,1); UPG(i,1)=Ib(154,1); UPL(i,1)=Ib(155,1); a(i)=t(i);
end
figure(1)
plot(t,XBio)
xlabel('Time (hr)')
title('Biomass Concentration (g/L)  vs Time ')
figure(2)
plot(t,GLUCOSE)
xlabel('Time (hr)')
title('GLUCOSE (mM)')
figure(3)
plot(t,LACTOSE)
xlabel('Time (hr)')
title('LACTOSE (mM)')
```

```
figure(4)
plot(a,cAMPList)
xlabel('Time (hr)')
title('cAMPList')
figure(5)
plot(a,O2up)
xlabel('Time (hr)')
title('O2up (mM/grDW.hr)')
```

B.4. Growth in Mixed Substrates of Glucose and Lactose and a Pulse Injection of Galactose on Lactose of *Escherichia coli*

```
clc
clear all
close all
GlucosecAMP=readfis('GlucosecAMP');
cAMPLacZYA=readfis('cAMPLacZYA');
LacYLactoseUptakeGlucose=readfis('LacYLactoseUptakeGlucose');
LactoseUptakeAllolactoseRepressor=readfis('LactoseUptakeAllolactoseRepressor');
AllolactoseLacZYA=readfis('AllolactoseLacZYA');
LacYLactoseUptakeLactose=readfis('LacYLactoseUptakeLactose');
%Initial concentration of External Biomass (XMe)(g/L) & External Glucose (GluMe)(mmol/L)
LacMe=5.8; GluMe=1.6; XMe=0.011;
%Time step 0.5 hr
dt=0.5;
%Initial Values of Substrate Glucose Concentration (mmol/L)
LACTOSE(1)=LacMe; GLUCOSE(1)=GluMe; XBio(1)=XMe;
t(1)=0;
Scavlactose=LACTOSE(1)/XBio(1)/dt; Scavglucose=GLUCOSE(1)/XBio(1)/dt;
Supinitiallactose=3.0; Supinitialglucose=6.5; Suplactose=0.15; Supglucose=6.5;
Slacup=Suplactose/Supinitiallactose; Sglup=Supglucose/Supinitialglucose;
GlucoseUptake=[0 Sglup]; LactoseUptake=[0 Slacup];
   for i=1:21
%Time
t(i+1)=t(i)+dt;
```

```
%Linear Programming for the maximization of Biomass
%Stoichiometric matrix for MFA - E-COLI
A=xlsread('DENEMEECOLI', 'Matrix'); B=A';
Ib=zeros(167,1);
ub=inf*ones(167,1);
%Upper&Lower Boundaries of ATP non-growth associated maintenance flux
Ib(151,1)=15; ub(151,1)=15;
%Upper&Lower Boundaries of Biomass Production fluxes
Ib(152,1)=0; ub(152,1)=inf;
%When the glucose concentration becomes considerable diluted level
%Upper&Lower Boundaries of Glucose Transport fluxes
  Ib(154,1)=min(Supglucose,Scavglucose); ub(154,1)=min(Supglucose,Scavglucose);
de=Ib(154,1)/Supinitialglucose;
GlucoseUptake=[0 de];
%Upper&Lower Boundaries of Transport fluxes
if i==16
% Pulse 2.5mmol/L glucose is added to the medium.
Glupulse=2.5;
GLUCOSE(i)=Glupulse;
Scavglucose=Glupulse/XBio(i)/dt;
Supglucose=6.5; Supinitialglucose=6.5;
Ib(154,1)=min(Supglucose,Scavglucose); ub(154,1)=min(Supglucose,Scavglucose);
de=Ib(154,1)/Supinitialglucose;
GlucoseUptake=[0 de];
end
sim('GlucoseUptake')
```

```
cAMPList(i,1)=cAMP;
if cAMP<=0.70
   Suplactose=0.15;
   Slacup=Suplactose/Supinitiallactose;
   LactoseUptake=[0 Slacup]
elseif    cAMP>0.70
   if cAMP>=0.90
      if i==x
   sim('LactoseUptake')
   Suplactose=LactoseUptakeResult*Supinitiallactose;
   LactoseUptake=[0 LactoseUptakeResult];
      else
   sim('LactoseUptake')
   LUR=LactoseUptakeResult+GLactoseUptakeResult;
   Suplactose=LUR*Supinitiallactose;
   LactoseUptake=[0 LUR];
end
   else
   sim('LactoseUptake')
   Suplactose=LactoseUptakeResult*Supinitiallactose
   LactoseUptake=[0 LactoseUptakeResult];
end
end
%Lac Operon regulation structured in Fuzzy Logic Controller in Simulink
Ib(155,1)=min(Suplactose,Scavlactose); ub(155,1)=min(Suplactose,Scavlactose);
%GLup
```

```
Ib(156,1)=0; ub(156,1)=0;
%PYRup
Ib(157,1)=-inf; ub(157,1)=0;
%LACup
Ib(158,1)=-inf; ub(158,1)=0;
%FORup
Ib(159,1)=-inf; ub(159,1)=0;
%ETHup
Ib(160,1)=-inf; ub(160,1)=0;
%Acup
Ib(161,1)=-inf; ub(161,1)=0;
%SUCCup
Ib(162,1)=-inf; ub(162,1)=0;
%RIBup
Ib(163,1)=0; ub(163,1)=0;
%Piup
Ib(164,1)=0; ub(164,1)=inf;
%CO2up
Ib(165,1)=-inf; ub(165,1)=0;
%O2up
Ib(166,1)=0; ub(166,1)=inf;
%HEup
Ib(167,1)=0; ub(167,1)=0;
f=zeros(167,1);
f(152,1)=-1;
b=zeros(77,1);
```

```
X=linprog(f,[],[],B,b,Ib,ub);
SON(:,i)=X;
O2up(i,1)=X(166,1);
LACTOSE(i+1)=LACTOSE(i)+X(155,1)/X(152,1)*XBio(i)*(1-exp(X(152,1)*dt));
GLUCOSE(i+1)=GLUCOSE(i)+X(154,1)/X(152,1)*XBio(i)*(1-exp(X(152,1)*dt));
if LACTOSE(i+1)<=0
  LACTOSE(i+1)=0;
end
if GLUCOSE(i+1)<=0
   GLUCOSE(i+1)=0;
   if GLUCOSE(i)-GLUCOSE(i+1)>0
      x=i+1
  end
end
XBio(i+1)=XBio(i)*exp(X(152,1)*dt);
Scavlactose=LACTOSE(i+1)/XBio(i+1)/dt
Scavglucose=GLUCOSE(i+1)/XBio(i+1)/dt
VGRO(i,1)=X(152,1); UPG(i,1)=Ib(154,1); UPL(i,1)=Ib(155,1); a(i)=t(i);
end
figure(1)
plot(t,XBio)
xlabel('Time (hr)')
title('Biomass Concentration (g/L)  vs Time ')
figure(2)
plot(t,GLUCOSE)
xlabel('Time (hr)')
```

```
title('GLUCOSE (mM)')
figure(3)
plot(t,LACTOSE)
xlabel('Time (hr)')
title('LACTOSE (mM)')
figure(4)
plot(a,cAMPList)
xlabel('Time (hr)')
title('cAMPList')
figure(5)
plot(a,O2up)
xlabel('Time (hr)')
title('O2up (mM/grDW.hr)')
```

B.5. Growth in Mixed Substrates of Glucose and Lactose and a Pulse Injection of Mixture of Glucose and Galactose on Lactose of *Escherichia coli*

```
clc
clear all
close all
GlucosecAMP=readfis('GlucosecAMP'); cAMPLacZYA=readfis('cAMPLacZYA');
LacYLactoseUptakeGlucose=readfis('LacYLactoseUptakeGlucose');
LactoseUptakeAllolactoseRepressor=readfis('LactoseUptakeAllolactoseRepressor');
AllolactoseLacZYA=readfis('AllolactoseLacZYA');
LacYLactoseUptakeLactose=readfis('LacYLactoseUptakeLactose');
cAMPGalactose=readfis('cAMPGalactose');
%Initial concentration of External Biomass (XMe)(g/L) & External Glucose (GluMe)(mmol/L)
LacMe=5.8; GluMe=1.6; XMe=0.011;
%Time step 0.5 hr
dt=0.5;
%Initial Values of Substrate Glucose Concentration (mmol/L)
LACTOSE(1)=LacMe; GLUCOSE(1)=GluMe; GLACTOSE(1)=0; XBio(1)=XMe; t(1)=0;
Scavlactose=LACTOSE(1)/XBio(1)/dt; Scavglucose=GLUCOSE(1)/XBio(1)/dt;
Supinitiallactose=3.0; Supinitialglucose=6.5; Suplactose=0.15; Supglucose=6.5;
Slacup=Suplactose/Supinitiallactose;
Sglup=Supglucose/Supinitialglucose;
GlucoseUptake=[0 Sglup]; LactoseUptake=[0 Slacup];
   for i=1:19
%Time
t(i+1)=t(i)+dt;
```

```
%Linear Programming for the maximization of Biomass
%Stoichiometric matrix for MFA - E-COLI
A=xlsread('DENEMEECOLIGALACTOSE', 'Matrix'); B=A';
Ib=zeros(170,1);
ub=inf*ones(170,1);
%Upper&Lower Boundaries of ATP non-growth associated maintenance flux
Ib(153,1)=15; ub(153,1)=15;
%Upper&Lower Boundaries of Biomass Production fluxes
Ib(154,1)=0; ub(154,1)=inf;
%When the glucose concentration becomes considerable diluted level
%Upper&Lower Boundaries of Glucose Transport fluxes
Ib(156,1)=min(Supglucose,Scavglucose); ub(156,1)=min(Supglucose,Scavglucose);
de=Ib(156,1)/Supinitialglucose;
GlucoseUptake=[0 de];
%Upper&Lower Boundaries of Transport fluxes
sim('GlucoseUptake')
cAMPList(i,1)=cAMP;
if cAMP<=0.70
   Suplactose=0.15;
   Slacup=Suplactose/Supinitiallactose;
   LactoseUptake=[0 Slacup]
elseif    cAMP>0.70
   if cAMP>=0.90
      if i==x
   sim('LactoseUptake')
   Suplactose=LactoseUptakeResult*Supinitiallactose;
```

```
    LactoseUptake=[0 LactoseUptakeResult];
       else
    sim('LactoseUptake')
    LUR=LactoseUptakeResult+GLactoseUptakeResult;
    Suplactose=LUR*Supinitiallactose;
    LactoseUptake=[0 LUR];
end
    else
    sim('LactoseUptake')
    Suplactose=LactoseUptakeResult*Supinitiallactose
    LactoseUptake=[0 LactoseUptakeResult];
end
end
%Lac Operon regulation structured in Fuzzy Logic Controller in Simulink
Ib(157,1)=min(Suplactose,Scavlactose); ub(157,1)=min(Suplactose,Scavlactose);
%GALACup
Ib(158,1)=0; ub(158,1)=0;
if GLACTOSE(i)>0
sim('GalactosevsGlucoseUptake')
Scavglactose=GLACTOSE(i)/XBio(i)/dt
Supglactose=GalactoseUptake*6.5;
Ib(158,1)=min(Supglactose,Scavglactose); ub(158,1)=min(Supglactose,Scavglactose);
end
if i==16
% Pulse 2.5mmol/L glucose is added to the medium.
Glupulse=4.5;
```

```
GLUCOSE(i)=Glupulse;
Scavglucose=Glupulse/XBio(i)/dt
Supglucose=6.5; Supinitialglucose=6.5;
Ib(156,1)=min(Supglucose,Scavglucose); ub(156,1)=min(Supglucose,Scavglucose);
de=Ib(156,1)/Supinitialglucose;
GlucoseUptake=[0 de];
sim('GlucoseUptake')
cAMPList(i,1)=cAMP;
% Pulse 8.5mmol/L galactose is added to the medium.
if X(10,1)-X(11,1)>0
sim('GalactosevsGlucoseUptake')
Glacpulse=8.5;
GLACTOSE(i)=Glacpulse;
Scavglactose=GLACTOSE(i)/XBio(i)/dt; Supglactose=GalactoseUptake*6.5;
Ib(158,1)=min(Supglactose,Scavglactose); ub(158,1)=min(Supglactose,Scavglactose);
else
Ib(158,1)=0; ub(158,1)=0;
end
end
%GLup
Ib(159,1)=0; ub(159,1)=0;
%PYRup
Ib(160,1)=-inf; ub(160,1)=0;
%LACup
Ib(161,1)=-inf; ub(161,1)=0;
%FORup
```

```
Ib(162,1)=-inf; ub(162,1)=0;
%ETHup
Ib(163,1)=-inf; ub(163,1)=0;
%Acup
Ib(164,1)=-inf; ub(164,1)=0;
%SUCCup
Ib(165,1)=-inf; ub(165,1)=0;
%RIBup
Ib(166,1)=0; ub(166,1)=0;
%Piup
Ib(167,1)=0; ub(167,1)=inf;
%CO2up
Ib(168,1)=-inf; ub(168,1)=0;
%O2up
Ib(169,1)=0; ub(169,1)=inf;
%HEup
Ib(170,1)=0; ub(170,1)=0;
f=zeros(170,1);
f(154,1)=-1;
b=zeros(78,1);
X=linprog(f,[],[],B,b,Ib,ub);
SON(:,i)=X;
O2up(i,1)=X(169,1);
LACTOSE(i+1)=LACTOSE(i)+X(157,1)/X(154,1)*XBio(i)*(1-exp(X(154,1)*dt));
GLUCOSE(i+1)=GLUCOSE(i)+X(156,1)/X(154,1)*XBio(i)*(1-exp(X(154,1)*dt))
GLACTOSE(i+1)=GLACTOSE(i)+X(158,1)/X(154,1)*XBio(i)*(1-exp(X(154,1)*dt));
```

```
if GLACTOSE(i+1)<=0
  GLACTOSE(i+1)=0;
end
if LACTOSE(i+1)<=0
  LACTOSE(i+1)=0;
end
if GLUCOSE(i+1)<=0
   GLUCOSE(i+1)=0;
   if GLUCOSE(i)-GLUCOSE(i+1)>0
      x=i+1
  end
end
XBio(i+1)=XBio(i)*exp(X(154,1)*dt); Scavlactose=LACTOSE(i+1)/XBio(i+1)/dt
Scavglucose=GLUCOSE(i+1)/XBio(i+1)/dt
VGRO(i,1)=X(154,1); UPG(i,1)=Ib(156,1); UPL(i,1)=Ib(157,1);a(i)=t(i);
end
figure(1)
plot(t,XBio)
xlabel('Time (hr)')
title('Biomass Concentration (g/L)  vs Time ')
figure(2)
plot(t,GLUCOSE)
xlabel('Time (hr)')
title('GLUCOSE (mM)')
figure(3)
plot(t,LACTOSE)
```

```
xlabel('Time (hr)')

title('LACTOSE (mM)')

figure(5)

plot(t,GLACTOSE)

xlabel('Time (hr)')

title('GLACTOSE (mM)')

figure(4)

plot(a,cAMPList)

xlabel('Time (hr)')

title('cAMPList')

figure(6)

plot(a,O2up)

xlabel('Time (hr)')

title('O2up (mM/grDW.hr)')
```

B.6. Growth in Mixed Substrates of Glucose, Sorbitol (Glucitol) and Glycerol of *Escherichia coli*

```
clc
clear all
close all
GlucosecAMPCRP=readfis('GlucosecAMPCRP');
cAMPCRPSorbitolUptake=readfis('cAMPCRPSorbitolUptake');
GlucoseSorbitolEIIA=readfis('GlucoseSorbitolEIIA');
EIIAGlpK=readfis('EIIAGlpK'); GlpKG3PFormation=readfis('GlpKG3PFormation');
%Initial concentration of External Biomass (XMe)(g/L) & External Glucose
%(GluMe)(mmol/L) External Sorbitol (GluMe)(mmol/L) External Glycerol
GluMe=1.2; SorMe=1.1; GlyMe=1.1; XMe=0.008;
%Time step 0.5 hr
dt=0.5;
%Initial Values of Substrate Glucose Concentration (mmol/L)
SORBITOL(1)=SorMe; GLUCOSE(1)=GluMe; GLYCEROL(1)=GlyMe; XBio(1)=XMe; t(1)=0;
Scavsorbitol=SORBITOL(1)/XBio(1)/dt; Scavglucose=GLUCOSE(1)/XBio(1)/dt;
Scavglycerol=GLYCEROL(1)/XBio(1)/dt;
Supinitialsorbitol=4.5; Supinitialglucose=8.5; Supinitialglycerol=4; Supsorbitol=1.6;
Supglucose=8; Supglycerol=4.0;
Ssorup=Supsorbitol/Supinitialsorbitol; Sglup=Supglucose/Supinitialglucose;
Sglyup=Supglycerol/Supinitialglycerol; Ssorglup=Supsorbitol+Supglucose;
GlucoseUptake=[0 Sglup];
   for i=1:10
%Time
```

```
t(i+1)=t(i)+dt;
%Linear Programming for the maximization of Biomass
%Stoichiometric matrix for MFA - E-COLI
A=xlsread('DENEMEECOLIGLUCOSESORBITOL', 'Matrix'); B=A';
Ib=zeros(171,1); ub=inf*ones(171,1);
%Upper&Lower Boundaries of ATP non-growth associated maintenance flux
Ib(154,1)=15; ub(154,1)=15;
%Upper&Lower Boundaries of Biomass Production fluxes
Ib(155,1)=0; ub(155,1)=inf;
%When the glucose concentration becomes considerable diluted level
%Upper&Lower Boundaries of Glucose Transport fluxes
Ib(157,1)=min(Supglucose,Scavglucose); ub(157,1)=min(Supglucose,Scavglucose);
de=Ib(157,1)/Supinitialglucose;
GlucoseUptake=[0 de];
%Upper&Lower Boundaries of Transport fluxes
sim('SorbitolUptake')
cAMPList(i,1)=cAMPCRP;
%Gut Operon regulation structured in Fuzzy Logic Controller in Simulink
Ib(160,1)=min(GSorbitolUptake*Supinitialsorbitol+Supsorbitol,Scavsorbitol);
ub(160,1)=min(GSorbitolUptake*Supinitialsorbitol+Supsorbitol,Scavsorbitol);
if cAMPCRP<=0.15
   Ib(160,1)=Supsorbitol;  ub(160,1)=Supsorbitol;
end
SUM=Ib(160,1)+Ib(157,1)
GlucoseSorbitolUptake=[0 SUM/Ssorglup]
sim('GlucoseSorbitolEIIAG3PFormation')
```

```
%Glycerol Operon regulation structured in Fuzzy Logic Controller in Simulink
Ib(107,1)=min(G3PFormation*Supinitialglycerol,Scavglycerol);
ub(107,1)=min(G3PFormation*Supinitialglycerol,Scavglycerol);
%LCTSup
Ib(158,1)=0; ub(158,1)=0;
%GLup
Ib(159,1)=0; ub(159,1)=inf;
%PYRup
Ib(161,1)=-inf; ub(161,1)=0;
%LACup
Ib(162,1)=-inf; ub(162,1)=0;
%FORup
Ib(163,1)=-inf; ub(163,1)=0;
%ETHup
Ib(164,1)=-inf; ub(164,1)=0;
%Acup
Ib(165,1)=-inf; ub(165,1)=0;
%SUCCup
Ib(166,1)=-inf; ub(166,1)=0;
%RIBup
Ib(167,1)=0; ub(167,1)=0;
%Piup
Ib(168,1)=0; ub(168,1)=inf;
%CO2up
Ib(169,1)=-inf; ub(169,1)=0;
%O2up
```

```
Ib(170,1)=0; ub(170,1)=inf;
%HEup
Ib(171,1)=0; ub(171,1)=0;
f=zeros(171,1); f(155,1)=-1; b=zeros(79,1);
X=linprog(f,[],[],B,b,Ib,ub);
SON(:,i)=X; O2up(i,1)=X(170,1);
SORBITOL(i+1)=SORBITOL(i)+X(160,1)/X(155,1)*XBio(i)*(1-exp(X(155,1)*dt));
GLUCOSE(i+1)=GLUCOSE(i)+X(157,1)/X(155,1)*XBio(i)*(1-exp(X(155,1)*dt));
GLYCEROL(i+1)=GLYCEROL(i)+X(159,1)/X(155,1)*XBio(i)*(1-exp(X(155,1)*dt));
if SORBITOL(i+1)<=0
  SORBITOL(i+1)=0;
end
if GLUCOSE(i+1)<=0
   GLUCOSE(i+1)=0;
end
XBio(i+1)=XBio(i)*exp(X(155,1)*dt); Scavsorbitol=SORBITOL(i+1)/XBio(i+1)/dt
Scavglucose=GLUCOSE(i+1)/XBio(i+1)/dt; Scavglycerol=GLYCEROL(i+1)/XBio(i+1)/dt
VGRO(i,1)=X(155,1); UPG(i,1)=Ib(157,1); UPS(i,1)=Ib(160,1); UPGLY(i,1)=X(159,1);
UPGL3P(i,1)=Ib(107,1); a(i)=t(i);
end
figure(1)
plot(t,XBio)
xlabel('Time (hr)')
title('Biomass Concentration (g/L)  vs Time ')
figure(2)
plot(t,GLUCOSE)
```

```
xlabel('Time (hr)')
title('GLUCOSE (mM)')
figure(3)
plot(t,SORBITOL)
xlabel('Time (hr)')
title('SORBITOL (mM)')
figure(4)
plot(a,cAMPList)
xlabel('Time (hr)')
title('cAMPList')
figure(5)
plot(a,O2up)
xlabel('Time (hr)')
title('O2up (mM/grDW.hr)')
figure(6)
plot(t,GLYCEROL)
xlabel('Time (hr)')
title('GLYCEROL (mM)')
```

B.7. Growth in Mixed Substrates of Glucose, Lactose and Galactose of *Lactococcus lactis*

```
clc
clear all
close all
LGlucoseccpAcre=readfis('LGlucoseccpAcre'); ccpAcreGalK=readfis('ccpAcreGalK');
GalKGalactoseUptake=readfis('GalKGalactoseUptake');
%Initial concentration of External Biomass (XMe)(g/L) & External Glucose (GluMe)(mmol/L)
LacMe=1.58; GlacMe=4.0; GluMe=1.58; XMe=0.0167;
%Time step 0.5 hr
dt=0.5;
%Initial Values of Substrate Glucose Concentration (mmol/L)
LACTOSE(1)=LacMe; GLUCOSE(1)=GluMe; GLACTOSE(1)=GlacMe; XBio(1)=XMe; t(1)=0;
Scavlactose=LACTOSE(1)/XBio(1)/dt; Scavglucose=GLUCOSE(1)/XBio(1)/dt;
Scavglactose=GLACTOSE(1)/XBio(1)/dt;
Supinitiallactose=4.1; Supinitialglucose=7.3; Supinitialglactose=6.7; Supglucose=7.3; Suplactose=4.1;
Sglup=Supglucose/Supinitialglucose;
LGlucoseUptake=[0 Sglup];
   for i=1:15
%Time
t(i+1)=t(i)+dt;
%Linear Programming for the maximization of Biomass
%Stoichiometric matrix for MFA - E-COLI
A=xlsread('DENEMEECOLILCTSGLCGLAC', 'Matrix'); B=A';
Ib=zeros(178,1);
ub=inf*ones(178,1);
```

```
%Upper&Lower Boundaries of ATP non-growth associated maintenance flux
Ib(161,1)=15; ub(161,1)=15;
%Upper&Lower Boundaries of Biomass Production fluxes
Ib(162,1)=0; ub(162,1)=inf;
%When the glucose concentration becomes considerable diluted level
%Upper & Lower Boundaries of Glucose and Lactose Transport fluxes
  Ib(164,1)=min(Supglucose,Scavglucose); ub(164,1)=min(Supglucose,Scavglucose);
  Ib(165,1)=min(Suplactose,Scavlactose); ub(165,1)=min(Suplactose,Scavlactose);
de=(Ib(164,1)+Ib(165,1))/(Supinitialglucose+Supinitiallactose);
TOTAL(i)=de;
GlucoseLactoseUptake=[0 de];
%Upper & Lower Boundaries of Galactose Transport fluxes by Simulink
sim('LLactisgalactoseuptake')
ccpAcreList(i,1)=ccpAcre;
Ib(166,1)=GalactoseUptake*Supinitialglactose; ub(166,1)=GalactoseUptake*Supinitialglactose;
Glact=GalactoseUptake*Supinitialglactose
%GLup
Ib(167,1)=0; ub(167,1)=0;
%PYRup
Ib(168,1)=-inf; ub(168,1)=0;
%LACup
Ib(169,1)=-inf; ub(169,1)=0;
%FORup
Ib(170,1)=0; ub(170,1)=0;
%ETHup
Ib(171,1)=0; ub(171,1)=0;
```

```
%Acup
Ib(172,1)=-inf; ub(172,1)=0;
%SUCCup
Ib(173,1)=-inf; ub(173,1)=0;
%RIBup
Ib(174,1)=0; ub(174,1)=0;
%Piup
Ib(175,1)=0; ub(175,1)=inf;
%CO2up
Ib(176,1)=-inf; ub(176,1)=0;
%O2up
Ib(177,1)=0; ub(177,1)=2.5;
%HEup
Ib(178,1)=0; ub(178,1)=0;
f=zeros(178,1); f(162,1)=-1; b=zeros(82,1);
X=linprog(f,[],[],B,b,Ib,ub);
SON(:,i)=X; O2up(i,1)=X(177,1);
LACTOSE(i+1)=LACTOSE(i)+X(165,1)/X(162,1)*XBio(i)*(1-exp(X(162,1)*dt));
GLUCOSE(i+1)=GLUCOSE(i)+X(164,1)/X(162,1)*XBio(i)*(1-exp(X(162,1)*dt));
GLACTOSE(i+1)=GLACTOSE(i)+X(166,1)/X(162,1)*XBio(i)*(1-exp(X(162,1)*dt));
if LACTOSE(i+1)<=0
   LACTOSE(i+1)=0;
end
if GLUCOSE(i+1)<=0
  GLUCOSE(i+1)=0;
end
```

```
XBio(i+1)=XBio(i)*exp(X(162,1)*dt);
Scavlactose=LACTOSE(i+1)/XBio(i+1)/dt; Scavglucose=GLUCOSE(i+1)/XBio(i+1)/dt;
Scavglactose=GLACTOSE(i+1)/XBio(i+1)/dt;
VGRO(i,1)=X(162,1); UPG(i,1)=Ib(164,1); UPL(i,1)=Ib(165,1); UPGL(i,1)=Ib(166,1); a(i)=t(i);
end
%plot(t,LACTOSE,t,GLUCOSE,t,XBio)
figure(1)
plot(t,XBio)
xlabel('Time (hr)')
title('Biomass Concentration (g/L)  vs Time ')
figure(2)
plot(t,GLUCOSE)
xlabel('Time (hr)')
title('GLUCOSE (mM)')
figure(3)
plot(t,LACTOSE)
xlabel('Time (hr)')
title('LACTOSE (mM)')
figure(5)
plot(t,GLACTOSE)
xlabel('Time (hr)')
title('GALACTOSE (mM)')
```

APPENDIX C: LIST OF METABOLIC REACTIONS IN *Escherichia coli* AND *Lactococcus lactis*

Table C.1. List of Reactions Used in *Escherichia coli* and *Lactococcus lactis*

	GLYCOLYSIS				
		Reaction	Protein	Reaction	
1	GLCPTS	Glucose transport		GLCxt + PEP -> G6P + PYR	
2	GLCUP	Glucose transport (low affinity)		GLCxt + HEXT -> GLC	
3	GLACUP	Galactose (low affinity)		GLACxt + HEXT → GLAC	
4	GLACUP	Galactose (low affinity)		GLCxt + HEXT → GLC	
5	GLACUP	Galactose (high affinity)		GLACxt + ATP → GLAC + ADP + PI	
6	LACYR	Lactose permease		LCTSxt + HEXT -> LCTS	
7	LACYR	Lactose permease		LCTS -> LCTSxt + HEXT	
8	LACUP	Lactate uptake		LACxt + HEXT -> LAC	
9	LACDN	Lactate secretion		LAC -> LACxt + HEXT	
10	LACZ	Beta-galactosidase (LACTase)		LCTS -> GLC + bDGLAC	
11	GALKR	Galactokinase		GLAC + ATP -> GAL1P + ADP	
12	GALKR	Galactokinase		GAL1P + ADP -> GLAC + ATP	
13	GALTR	Galactose-1-phosphate uridylyltransferase		GAL1P + UTP -> PPI + UDPGAL	
14	GALTR	Galactose-1-phosphate uridylyltransferase		PPI + UDPGAL -> GAL1P + UTP	
15	GALER	UDP-glucose 4-epimerase		UDPGAL -> UDPG	
16	GALER	UDP-glucose 4-epimerase		UDPG -> UDPGAL	
17	GALUR	UDP-glucose-1-phosphate uridylyltransferase		G1P + UTP -> UDPG + PPI	
18	GALUR	UDP-glucose-1-phosphate uridylyltransferase		UDPG + PPI -> G1P + UTP	
19	GLK	Glucokinase		GLC + ATP -> G6P + ADP	
20	LACGI	D-galactose 6-phosphate		LCTS6P -> GLC + GLAC6P	
21	UNK10	D-tagatose 6-phosphate		GLAC6P -> TG6P	

22	UNK10	D-tagatose 6-phosphate	TG6P -> GLAC6P
23	UNK11	D-tagatose 1,6-bisphosphate	TG1,6P -> GLYP + GLY3P
24	UNK11	D-tagatose 1,6-bisphosphate	GLYP + GLY3P -> TG1,6P
25	PGIR	Phosphoglucose isomerase	G6P -> F6P
26	PGIR	Phosphoglucose isomerase	F6P -> G6P
27	PGMR	Phosphoglucomutase	G1P -> G6P
28	PGMR	Phosphoglucomutase	G6P -> G1P
29	PFKA	Phosphofructokinase	F6P + ATP -> FDP + ADP
30	PFKB	Phosphofructokinase B	F6P + ATP -> FDP + ADP
31	FBP	Fructose-1,6-bisphosphatase	FDP -> F6P + PI
32	FBAR	Fructose-1,6-bisphosphatate aldolase	FDP -> T3P1 + T3P2
33	FBAR	Fructose-1,6-bisphosphatate aldolase	T3P1 + T3P2 -> FDP
34	TPIAR	Triosphosphate Isomerase	T3P1 -> T3P2
35	TPIAR	Triosphosphate Isomerase	T3P2 -> T3P1
36	GAPAR	Glyceraldehyde-3-phosphate dehydrogenase-A complex	T3P1 + PI + NAD -> NADH + 13PDG
37	GAPAR	Glyceraldehyde-3-phosphate dehydrogenase-A complex	NADH + 13PDG -> T3P1 + PI + NAD
38	PGKR	Phosphoglycerate kinase	13PDG + ADP -> 3PG + ATP
39	PGKR	Phosphoglycerate kinase	3PG + ATP -> 13PDG + ADP
40	GPMAR	Phosphoglycerate mutase 1	3PG -> 2PG
41	GPMAR	Phosphoglycerate mutase 1	2PG -> 3PG
42	GPMBR	Phosphoglycerate mutase 2	3PG -> 2PG
43	GPMBR	Phosphoglycerate mutase 2	2PG -> 3PG
44	ENOR	Enolase	2PG -> PEP
45	ENOR	Enolase	PEP -> 2PG
46	PYKA	Pyruvate Kinase II	PEP + ADP -> PYR + ATP
47	PYKF	Pyruvate Kinase I	PEP + ADP -> PYR + ATP

48	PPSA	Phosphoenolpyruvate synthase	PYR + ATP -> PEP + AMP + PI
	TCA Cycle		
	Reaction	**Protein**	**Reaction**
49	PYRUPR	Pyruvate transport	PYRxt + HEXT -> PYR
50	PYRUPR	Pyruvate transport	PYR -> PYRxt + HEXT
51	PFLA	Pyruvate formate lyase 1	PYR + COA -> ACCOA + FOR
52	PFLC	Pyruvate formate lyase 2	PYR + COA -> ACCOA + FOR
53	ACEE	Pyruvate dehydrogenase	PYR + COA + NAD -> NADH + CO2 + ACCOA
54	GLTA	Citrate synthase	ACCOA + OA -> COA + CIT
55	ACNAR	Aconitase A	CIT -> ICIT
56	ACNAR	Aconitase A	ICIT -> CIT
57	ACNBR	Aconitase B	CIT -> ICIT
58	ACNBR	Aconitase B	ICIT -> CIT
59	ICDAR	Isocitrate dehydrogenase	ICIT + NADP -> CO2 + NADPH + AKG
60	ICDAR	Isocitrate dehydrogenase	CO2 + NADPH + AKG -> ICIT + NADP
61	SUCA	2-Ketoglutarate dehyrogenase	AKG + NAD + COA -> CO2 + NADH + SUCCOA
62	SUCCR	Succinyl-CoA synthetase	SUCCOA + ADP + PI -> ATP + COA + SUCC
63	SUCCR	Succinyl-CoA synthetase	ATP + COA + SUCC -> SUCCOA + ADP + PI
64	SDHA1	Succinate dehydrogenase	SUCC + FAD -> FADH + FUM
65	FRDA	Fumarate reductase	FUM + FADH -> SUCC + FAD
66	FUMAR	Fumarase A	FUM -> MAL

67	FUMAR	Fumarase A	MAL -> FUM
68	FUMBR	Fumarase B	FUM -> MAL
69	FUMBR	Fumarase B	MAL -> FUM
70	FUMCR	Fumarase C	FUM -> MAL
71	FUMCR	Fumarase C	MAL -> FUM
72	MDHR	Malate dehydrogenase	MAL + NAD -> NADH + OA
73	MDHR	Malate dehydrogenase	NADH + OA -> MAL + NAD
74	MAEB	Malic enzyme (NADP)	MAL + NADP -> CO2 + NADPH + PYR
75	SFCA	Malic enzyme (NAD)	MAL + NAD -> CO2 + NADH + PYR
76	PPC	Phosphoenolpyruvate carboxylase	PEP + CO2 -> OA + PI
77	PCKA	Phosphoenolpyruvate carboxykinase	OA + ATP -> PEP + CO2 + ADP
78	ACEA	Isocitrate lyase	ICIT -> GLX + SUCC
79	ACEB	Malate synthase A	ACCOA + GLX -> COA + MAL
	Pentose phosphate		
	Reaction	**Protein**	**Reaction**
80	ZWFR	Glucose 6-phosphate-1-dehydrogenase	G6P + NADP -> D6PGL + NADPH
81	ZWFR	Glucose 6-phosphate-1-dehydrogenase	D6PGL + NADPH -> G6P + NADP
82	PGL	6-Phosphogluconolactonase	D6PGL -> D6PGC
83	GND	6-Phosphogluconate dehydrogenase (decarboxylating)	D6PGC + NADP -> NADPH + CO2 + RL5P
84	RPER	Ribulose phosphate 3-epimerase	RL5P -> X5P
85	RPER	Ribulose phosphate 3-epimerase	X5P -> RL5P
86	RPIAR	Ribose-5-phosphate isomerase A	RL5P -> R5P
87	RPIAR	Ribose-5-phosphate isomerase A	R5P -> RL5P
88	RPIBR	Ribose-5-phosphate isomerase B	RL5P -> R5P
89	RPIBR	Ribose-5-phosphate isomerase B	R5P -> RL5P

90	TKTA1R	Transketolase I	R5P + X5P -> T3P1 + S7P
91	TKTA1R	Transketolase I	T3P1 + S7P -> R5P + X5P
92	TKTB1R	Transketolase II	R5P + X5P -> T3P1 + S7P
93	TKTB1R	Transketolase II	T3P1 + S7P -> R5P + X5P
94	TALAR	Transaldolase A	T3P1 + S7P -> E4P + F6P
95	TALAR	Transaldolase A	E4P + F6P -> T3P1 + S7P
96	TALBR	Transaldolase B	T3P1 + S7P -> E4P + F6P
97	TALBR	Transaldolase B	E4P + F6P -> T3P1 + S7P
98	TKTA2R	Transketolase I	X5P + E4P -> F6P + T3P1
99	TKTA2R	Transketolase I	F6P + T3P1 -> X5P + E4P
100	TKTB2R	Transketolase II	X5P + E4P -> F6P + T3P1
101	TKTB2R	Transketolase II	F6P + T3P1 -> X5P + E4P
	Ribose		
	Reaction	**Protein**	**Reaction**
102	RIBUPR	Ribose transport	RIBxt + ATP -> RIB + ADP + PI
103	RBSK	Ribokinase	RIB + ATP -> R5P + ADP
	Glycerol		
	Reaction	**Protein**	**Reaction**
104	GLUPR	Glycerol transporter	GLxt -> GL
105	GLUPR	Glycerol transporter	GL -> GLxt
106	GLPK	Glycerol kinase	GL + ATP -> GL3P + ADP
107	GLPA	Glycerol-3-phosphate dehydroganase (anaerobic)	GL3P + Q -> T3P2 + QH2
108	GLPD	Glycerol-3-phosphate dehydroganase (aerobic)	GL3P + Q -> T3P2 + QH2

	Lactate		
	Reaction	**Protein**	**Reaction**
109	DLD1R	D-Lactate dehydrogenase 1	PYR + NADH -> NAD + LAC
110	DLD1R	D-Lactate dehydrogenase 1	NAD + LAC -> PYR + NADH
111	DLD2	D-Lactate dehydrogenase (cyctochrome)	LAC + Q -> PYR + QH2
	Fermentation Ethanol		
	Reaction	**Protein**	**Reaction**
112	ETHUPR	Ethanol transport	ETHxt + HEXT -> ETH
113	ETHUPR	Ethanol transport	ETH -> ETHxt + HEXT
114	ADHER	Acetaldehyde dehydrogenase	ACCOA +2 NADH -> ETH +2 NAD + COA
115	ADHER	Acetaldehyde dehydrogenase	ETH +2 NAD + COA -> ACCOA +2 NADH
	Acetate		
	Reaction	**Protein**	**Reaction**
116	ACUPR	Acetate transport	ACxt + HEXT -> AC
117	ACUPR	Acetate transport	AC -> ACxt + HEXT
118	ACS	Acetyl-CoA synthetase	ATP + AC + COA -> AMP + PPI + ACCOA
119	ACKAR	Acetate kinase A	ACTP + ADP -> ATP + AC
120	ACKAR	Acetate kinase A	ATP + AC -> ACTP + ADP
121	PTAR	Phosphotransacetylase	ACCOA + PI -> ACTP + COA
122	PTAR	Phosphotransacetylase	ACTP + COA -> ACCOA + PI
	Energy		

	Reaction	**Protein**	**Reaction**
123	ADK	Adenylate kinase	ATP + AMP -> 2 ADP
124	ADK	Adenylate kinase	2 ADP -> ATP + AMP
	Respiration		
	Reaction	**Protein**	**Reaction**
125	CO2TXR	Carbon dioxide transport	CO2xt -> CO2
126	CO2TXR	Carbon dioxide transport	CO2 -> CO2xt
127	O2TXR	Oxygen transport	O2xt -> O2
128	O2TXR	Oxygen transport	O2 -> O2xt
129	CYDA	Cytochrome oxidase bd	QH2 +.5 O2 -> Q +2 HEXT
130	CYOA	Cytochrome oxidase bo3	QH2 +.5 O2 -> Q +2.5 HEXT
131	FDNG	Formate dehydrogenase-N	FOR + Q -> QH2 + CO2 +2 HEXT
132	FDOH	Formate dehydrogenase-O	FOR + Q -> QH2 + CO2 +2 HEXT
133	FORUPR	Formate transport	FORxt -> FOR
134	FORUPR	Formate transport	FOR -> FORxt
135	ATPAR	F0F1-ATPase	ATP + AMPATP -> ADP + PI +4 HEXT
136	ATPAR	F0F1-ATPase	ADP + PI +4 HEXT -> ATP + AMPATP
137	PNTA1	Pyridine nucleotide transhydrogenase	NADPH + NAD -> NADP + NADH
138	PNTA2	Pyridine nucleotide transhydrogenase	NADP + NADH +2 HEXT -> NADPH + NAD
139	NDH	NADH dehydrogenase II	NADH + Q -> NAD + QH2
140	NUOA	NADH dehydrogenase I	NADH + Q -> NAD + QH2 +3.5 HEXT
141	SDHA2	Succinate dehydrogenase complex	FADH + Q -> FAD + QH2
142	SDHA2	Succinate dehydrogenase complex	FAD + QH2 -> FADH + Q
143	DCTAR	Succinate transport	SUCCxt + HEXT -> SUCC

144	DCTAR	Succinate transport	SUCC -> SUCCxt + HEXT
145	DCUAR	Succinate transport	SUCCxt + HEXT -> SUCC
146	DCUAR	Succinate transport	SUCC -> SUCCxt + HEXT
147	DCUBR	Succinate transport	SUCCxt + HEXT -> SUCC
148	DCUBR	Succinate transport	SUCC -> SUCCxt + HEXT
149	DCUC	Succinate efflux	SUCC -> SUCCxt +HEXT
	Phosphate		
	Reaction	**Protein**	**Reaction**
150	PIUP2R	Phosphate transport	PIxt + HEXT -> PI
151	PIUP2R	Phosphate transport	PI -> PIxt + HEXT
152	PPA	Inorganic pyrophosphatase	PPI -> 2 PI
	Biomass Production Flux		
	Reaction	**Protein**	**Reaction**
153	ATPM	ATP non-growth associated maintenance flux	ATP -> ADP + PI
154	VGRO	Biomass production flux	41.25 ATP + 3.54 NAD + 18.22 NADPH + 0.2 G6P + 0.07 F6P + 0.89 R5P + 0.36 E4P + 0.12 T3PI + 1.493PG + 0.51 PEP + 2.83 PYR + 3.74 ACCOA + 1.78 OA + 1.07 AKG -> 3.74 COA + 41.25 ADP + 41.25PI + 3.54 NADH + 18.22 NADP +1 Biomass
155	Growth	Biomass exchange (growth)	Biomass + 13 ATP -> 13 ADP + 13 PI

	Exchange Fluxes		
	Acex	Acetate exchange	
	CO2ex	Carbon dioxide exchange	
	ETHex	Ethanol exchange	
	FORex	Formate exchange	
	GLCex	Glucose exchange	
	GLACex	Galactose exchange	
	Glex	Glycerol exchange	
	Growth	Biomass exchange (growth)	
	LACex	Lactate exchange	
	LCTSex	Lactose exchange	
	O2ex	Oxygen exchange	
	Piex	Phosphate exchange	
	PYRex	Pyruvate exchange	
	RIBex	Ribose exchange	
	SUCCex	Succinate exchange	

Abbreviation	Metabolites	Abbreviation	Metabolites
13PDG	1,3-bis-Phosphoglucerate	FADH	Flavin adenine dinucleotide reduced
2PG	2-Phosphoglycerate	FDP	Fructose 1,6-diphosphate
3PG	3-Phosphoglycerate	FOR	Formate
AC	Acetate	FORxt	External formate
ACCOA	Acetyl-CoA	FUM	Fumarate
ACTP	Acetyl-phosphate	G1P	Glucose 1-phosphate
ACxt	External Acetate	G6P	Glucose 6-phosphate
ADP	Adenosine diphosphate	GAL1P	Galactose 1-phosphate
AKG	a-Ketoglutarate	GL	Glycerol
AMP	Adenosine monophosphate	GL3P	Glycerol 3-phosphate
ATP	Adenosine triphosphate	GLAC	Galactose
bDGLAC	b-D-Galactose	GLACxt	External Galactose
bDGLC	b-D-Glucose	GLC	a-D-Glucose

Abbreviation	Metabolites	Abbreviation	Metabolites
Biomass	Cell biomass	NADP	Nicotinamide adenine dinucleotide phosphate
CIT	Citrate	NADPH	Nicotinamide adenine dinucleotide phosphate reduced
CO2	Carbondioxide	O2	Oxygen
CO2xt	External carbondioxide	O2xt	External Oxygen
COA	Coenzyme A	OA	Oxaloacetate
D6PC	D-6-Phosphate- gluconate	PEP	Phosphoenolpyruvate
D6PGL	D-6-Phosphate- glucono-delta-lactone	PG	Phospatidyl glycerol
E4P	Erthrose 4-phosphate	PI	Phosphate (inorganic)
ETH	Ethanol	PIxt	External phosphate
ETHxt	External ethanol	PPI	Pyrophosphate
F6P	Fructose 6-phosphate	PYR	Pyruvate
FAD	Flavin adenine dinucleotide	PYRxt	External pyruvate
GLCxt	External glucose	Q	Ubiquinone
GLX	Glyoxylate	QH2	Ubiquinol
GLxt	External glycerol	RIB	Ribose
HEXT	External H+	RIBxt	External ribose
ICIT	Isocitrate	RL5P	Ribulose 5-phosphate
LAC	D-Lactate	S7P	Sedo-Heptulose
LACxt	External lactate	SUCC	Succinate
LCTS	Lactose	SUCCOA	Succinate CoA
LCTSxt	External lactose	SUCCxt	External succinate
MAL	Malate	T3PI	Glyceraldehyde 3-phosphate
NAD	Nicotinamide adenine dinucleotide	T3P2	Dihydroxyacetone phosphate
NADH	Nicotinamide adenine dinucleotide reduced	UDPG	UDP Glucose
PYRxt	External pyruvate	UDPGAL	UDP Galactose
Q	Ubiquinone	UTP	Uridine triphosphate
QH2	Ubiquinol	X5P	Xylulose 5-phosphate

REFERENCES

Adhya, S. and M. Geanacopoulos, 1997, "Functional Characterization of Roles of *GalR* and *GalS* as regulators of the gal Regulon", *J. Bacteriology*, pp. 228-234.

Adhya, S., 1996, "Regulation of Gene Expression in *Escherichia coli*", (Lin, E. C. C. and A. S. Lynch, eds), pp. 181–200, R. G. Landes Company, Austin, TX

Bonarius, H. P. J., G. Schmid and J. Tramper, 1997, "Flux Analysis of Underdetermined Metabolic Networks: the Quest for the Missing Constraints", *Trends Biotechnol.*, 15, pp. 308-314.

Covert, M. W. and B. Palsson, 2002, "Transcriptional Regulation in Constraints-based Metabolic Models of *Escherichia coli*" *J. Biological Chemistry*, 277, 31, pp. 28058-28064.

Covert, M. W., C. H. Schilling and B. Palsson, 2001, "Regulation of Gene Expression in Flux Balance Models of Metabolism", *J. Theoretical Biology*, 213, pp. 73-88.

Cox, S. J., S. S. Levanon, G. N. Bennett and K. Y. San, 2005, "Genetically Constrained Metabolic Flux Analysis", *Metabolic Engineering*, Article in Press, pp. 1-12.

Edwards, J. and B. Palsson, 1999, "Properties of the *Haemophilus influenzae* Rd Metabolic Genotype", *J. Biol. Chem.*, 274, pp. 17410-17416.

Edwards, J. S. and B. O. Palsson, 2000, "The *Escherichia coli* MG1655 in Silico Metabolic Genotype: its Definition, Characteristics, and Capabilities", *Proceedings of the National Academy of Sciences*, 97, pp. 5528-5533.

Edwards, J. S., R. U. Ibarra and B. O. Palsson, 2001, "In Silico Predictions of *Escherichia coli* Metabolic Capabilities are Consistent with Experimental Data", *Natural Biotechnology*, 19, pp. 125-130.

Edwards, J. S., R. Ramakrishna, C. H. Schilling and B. O. Palsson, 1999, "Metabolic Flux Balance Analysis", In Lee S. Y., and E. T. Papoutsakis (ed.), *Metabolic engineering*, Marcel Dekker, New York, N.Y., pp. 13–57.

Frey, P. A., 1996, "The Leloir Pathway: a Mechanistic Imperative for Three Enzymes to Change the Stereochemical Configuration of a Single Carbon in Galactose." *J. FASEB*, 10(4), pp. 461-70.

Goodwin, B. C., 1969, "Control Dynamics of β-galactosidase in Relation to the Bacterial Cell Cycle", *Eur. J. Biochem.*, 10, pp. 515–522.

Gulik, W. M., W. T. Laat, J. L. Vinke and J. J. Heijnen, 2000, "Application of Metabolic Flux Analysis for the Identification of Metabolic Bottlenecks in the Biosynthesis of Penicillin-G", *Biotechnol. Bioeng*, 68, 6, pp. 602-618.

Hong Bum Kim, H. B., C. P. Smith, J. Micklefield and F. Mavituna, 2004, "Metabolic Flux Analysis for Calcium Dependent Antibiotic (CDA) Production in *Streptomyces coelicolor*", *Metabolic Engineering*, 6, pp. 313–325

Hueck, C. J. and Hillen, W., 1995, "Catabolite Repression in *Bacillus subtilis*: a Global Regulatory Mechanism for the Gram-positive Bacteria", *Molecular Microbiology*, 15, pp. 395–401.

Kompala, D. S., D. Ramkrishna and T. T. Tsao, 1984, "Cybernetic Modeling of Microbial Growth on Multiple Substrates", *Biotechnology and Bioengineering*, 26, pp. 1272-1281.

Kremling, A., K. Bettenbrock, B. Laube, K. Jahreis, J. W. Lengeler and E. D. Gilles, 2001, "The Organization of Metabolic Reaction Networks: III. Application for Diauxic Growth on Glucose and Lactose", *Metabolic Engineering*, 3, pp. 362-379.

Kuipers, O. P., E. J. Luesink, R. E. Herpen, B. P. Grossiord, O. P. Kuipers and W. M. Vos, 1998, "Transcriptional Activation of the Glycolytic *Las* Operon and Catabolite

Repression of the *Gal* Operon in *Lactococcus lactis* are Mediated by the Catabolite Control Protein *CcpA*", *Molecular Microbiology*, 30(4), pp. 789-798.

Lee, B., J. C. Liao, L. Yang and J. Yen, 1999, "Incorporating Qualitative Knowledge in Enzyme Kinetic Models Using Fuzzy Logic", *Biotechnol., Bioeng.*, 62, pp. 722-729.

Lee, S. B. and J. E. Bailey, 1984a,b "Genetically Structured Models for *Lac* Promoter-Operator Function in the *Esherichia coli* Chromosome and in Multicopy Plasmids: *Lac* Operator Function", *Biotechnology Bioengineering*, 26, pp. 1372-1389.

Lengeler, J. and H.Steinberger, 1978, *Mol. Gen. Genet.*, 164, pp. 163-169.

Luesink, E. J., R. van Herpen, B. P. Grossiord, O. P. Kuipers and W. M. deVos, 1998, "Transcriptional Activation of the Glycolytic *las* Operon and Catabolite Repression of the *gal* Operon in *Lactococcus lactis* are Mediated by the Catabolite Control Protein *ccpA*", *Mol. Microbiol.*, 30, pp. 789–798.

Mackey, M. C., M. Santillan and N. Yildirim, 2004, "Modeling Operon Dynamics: the *Tryptophan* and *Lactose* Operons as Paradigms", *C. R. Biologies*, 327, pp. 211-224.

Majewski, R. A. and M. M. Domach, 1990, "Simple Constrained Optimization View of Acetate Overflow in *E. coli*", *Biotechnol. Bioeng.*, 35, pp. 732–738.

Neidhardt, F. C., R. Curtiss III, J. L. Ingraham, E. C. C. Lin, K. B. Low Jr, B. Magasanik, W.S. Reznikoff, M. Riley, M. Schaechter, and H. E. Umbarger, 1996, "*Escherichia coli* and *Salmonella*, Cellular and Molecular Biology", Second Edition, *American Society for Microbiology*, Washington, D.C.

Neidhardt, F. C., J. L. Ingraham and M. Schaechter, 1990, "Physiology of the Bacterial Cell", *Sinauer Associates*, Inc., Sunderland, Mass.

Neidhardt, F. C., J. L. Ingraham, K. B. Low, B. Magasanik, M. Schaechter and H. E. Umbarger, 1987, "*Escherichia coli* and *Salmonella typhimurium*: Cellular and Molecular Biology", *American Society for Microbiology*, Washington, D.C.

Palsson, B., 2002, "Flux Balance Analysis: Basic Concepts", *Class Notes*, BE160C/203 topic II.10.

Pestka, S., B. L. Daugherty, V. Jung, K. Hotta and R. K. Pestka, 1984, "Anti-*mRNA*: Specific Inhibition of Translation of Single *mRNA* Molecules", *Proc. Natl. Acad. Sci.*, USA, 81, pp. 7525–7528.

Postma, P. W., J. W. Lengeler and G. R. Jacobson, 1993, "Phosphoenolpyruvate: Carbohydratephosphotransferase Systems of Bacteria" *Microbiol. rev.*, 57, pp. 543-594.

Pramanik, J. and J. D. Keasling, 1997, "Stoichiometric Model of *Escherichia coli* Metabolism: Incorporation of Growth-Rate Dependent Biomass Composition and Mechanistic Energy Requirements", *Biotechnol. Bioeng.*, 56, pp. 398–421.

Pramanik, J. and J. D. Keasling, 1998. "Effect of *Escherichia coli* Biomass Composition on Central Metabolic Fluxes Predicted by a Stoichiometric Model", *Biotechnol. Bioeng.*, 60, pp. 230–238.

Provost, A. and G. Bastin, 2004, "Dynamic Metabolic Modelling Under the Balanced Growth Condition"*, J. Process Control*, 14, pp. 717-728.

Ramkrishna, D., S. J. Parulekar and N. B. Jansen, 1989, "Bacterial Growth on Lactose: An Experimental Investigation"*, Biotech. Bioeng.*, 34, pp. 705-716.

Ruppin, E., O. Berkman and T. Shlomi*,* 2004 "Constraint-Based modeling of perturbed Organisms: A Room for improvement", *School of Computer Science*, Tel-Aviv University, pp. 1-3.

Ruppin, E., O. Berkman and T. Shomi, 2005, "Regulatory On/Off Minimization Of Metabolic Flux Changes Following Genetic Perturbations", *Biological Sciences:Microbiology,* pp. 1-14.

San, K. Y., S. Cox, S. Shalel Levanon and G. N. Bennett, 2003, "Metabolic Flux Analysis Based on Dynamic Genomic Information", *In: 225th American Chemical Society National Meeting*, New Orleans, LA.

Segre, D., G. M. Church and D. Vitkup, 2002, "Analysis of Optimality in Natural and Perturbed Metabolic Networks", *PNAS*, 99, 23, pp. 15112-15117.

Snyder, D., A. Larry and E. E. Wendy Champness, 1997, "Molecular Genetics of Bacteria", *Washington DC: ASM Press*, pp. 275.

Sokhansanj, B. A., J. P. Fitch, J. N. Quong and A. A. Quong, 2004, "Linear Fuzzy Gene Network Models Obtained from Microarray Data by Exhaustive Search", *BMC Bioinformatics,* 5, 108, pp. 1-12.

Sokhansanj, B. A. and J. P. Fitch, 2001, "URC Fuzzy Modeling and Simulation of Gene Regulation", *23rd Annual EMBS International Conference*, pp. 2918-2021.

Stelling, J. and S. Klamt, 2003, "Stoichiometric Analysis of Metabolic Network", *4th International Conference on Systems Biology*, pp. 18-24.

Thomas, R., 1973, "Boolean Formalization of Genetic Control Circuits", *J. Theor. Biol.*, 42, pp. 563-585.

Thompson, J., K. W. Turner and T. D. Thomas, 1978, "Catabolite Inhibition and Sequential Metabolism of Sugars by *Streptococcus lactis*", *J. Bacteriology*, pp. 1163-1174.

Varma, A. and B. O. Palsson, 1994a, "Metabolic Flux Balancing: Basic Concepts, Scientific and Practical Use", *Bio. Technology*, pp. 994-998.

Varma, A. and B. O. Palsson, 1994b, "Stoichiometric Flux Balance Models Quantitatively Predict Growth and Metabolic By-Product Secretion in Wild-Type *Escherichia coli* W3110", *A. Environ. Micro.*, pp. 3724-3731.

Wong, P., S. Gladney and J. D. Keasling, 1997, "Mathematical Model of the *lac* Operon: Inducer Exclusion, Catabolite Repression, and Diauxic Growth on Glucose and Lactose"*, Biotechnological Progress*, 13, pp. 132-143.

Woolf, P. J. and Y. Wang, 2000 "A Fuzzy Logic Approach to Analyzing Gene Expression Data", *Physiol. Genomics*, 3, pp. 9-15.

Yagil, G. and E. Yagil, 1971, "On the Relation Between Effector Concentration and the Rate of Induced Enzyme Synthesis", *J. Biophys.,* 11, pp. 11-29.

Yamada, M. and M. H. Jr Saier, 1988, "Positive and Negative Regulators for Glucitol (*gut*) Operon Expression in *Escherichia coli", J. Molecular Biol.*, 203, pp. 569-583.

Yamada, T., 1987, "Regulation of Glycolysis in *Streptococcus lactis*. Sugar Transport and Metabolism in Gram Positive Bacteria", *Ellis Howood Series in Biochemistry and Biotechnology*, In: J. Reizer and A. Peterkofsky (eds), Chichester, UK, pp. 69–93.

Yanofsky, C. and V. Horn, 1994, "Role of Regulatory Features of the *trp* Operons of *E. coli* in Mediating a Response to a Nutritional Shift", *J. Bacteriol.*, 176, pp. 6245–6254.

Yen, J. and Langari R., 1999, "Fuzzy Logic: Intelligence, Control, and Information", *Penntice Hall*, ch. 1-5, pp. 1-140.

Yildirim, N. and M. C. Mackey, 2003, "Feedback Regulation in the *Lactose* Operon: A Mathematical Modeling Study and Comparison with Experimental Data", *Biophysical Journal*, 84, pp. 2841-2851.

Ying H., 2000, "Fuzzy Control and Modeling: Analytical Foundations and Applications", *IEEE Press*, ch. 1, pp. 1-13.